CZECH TECHNICAL UNIVERSITY IN PRAGUE

FACULTY OF CIVIL ENGINEERING

DEPARTMENT OF HYDRAULIC STRUCTURES

MAZOUROV WEIR – LAYOUT AND DESIGN OF THE SMALL HPP

MASTER THESIS

MARIE PECHAROVÁ

Master thesis supervisor: Ing. Miroslav Brouček, Ph.D.

Assoc. Prof. Dipl.-Ing. Pavel Borisovich Ryzhakov, PhD

January 2024

ČESKÉ VYSOKÉ UČENÍ TECHNICKÉ V PRAZE
Fakulta stavební
Thákurova 7, 166 29 Praha 6

ZADÁNÍ DIPLOMOVÉ PRÁCE

I. OSOBNÍ A STUDIJNÍ ÚDAJE

Příjmení: Pecharová Jméno: Marie Osobní číslo: 484498

Zadávající katedra: K142 - Katedra hydrotechniky

Studijní program: Stavební inženýrství

Studijní obor: Vodní hospodářství a vodní stavby

II. ÚDAJE K DIPLOMOVÉ PRÁCI

Název diplomové práce: Jez Mazourov - dispoziční řešení a návrh MVE

Název diplomové práce anglicky: Mazourov Weir - layout and design of the small HPP

Pokyny pro vypracování:
S pomocí 2D numerického modelu ustáleného proudění vypracujte dispoziční řešení rekonstrukce jezu Mazurov, tj. umístěte objekty MVE, rybího přechodu a sportovní propusti pro turistickou plavbu tak, aby byla zajištěna jejich optimální funkce s maximální pravděpodobností. Při řešení repsektujte omezení vyplývající z kóty přelivné hrany jezu a stávajícího uspořádání profilu jezu. Kapacity jednotlivých objektů stanovte v návaznosti na hydrologické podklady lokality. Numerický 2 D model vypracujte v softwaru HEC-RAS.
Dále proveďte hydrotechnický návrh MVE na lokalitě do úrovně detailu výkresové a výpočtové části odpovídající stupni DSP.
Práci vypracujte v anglickém jazyce a při jejím zpracování využijte možností konzultací na UPC.

Seznam doporučené literatury:
Medřický V., Valenta P.: Hydrotechnické stavby 1, Navrhování jezů, ČVUT, 2009, ISBN 978-80-01-04309-7;
Gabriel P. a kol., Jezy, SNTL, 1989;
Malé vodní elektrárny, Gabriel, P., Čihák, F. Kalandra, P., ISBN: 80-01-01812-1;
Skriptum Navrhování vodních elektráren, Gabriel, P., Kučerová, J., ISBN 80-01-01304-9;
HEC-RAS 2D User's Manual
další odborná literatura z oblasti numercikého modelování, jezů, rybích přechodů, sportovních propustí a malých vodních elektráren se vztahem k tématu diplomové práce;
relevantní technické normy, zejména ČSN 75 2601 Malé vodní elektrárny - základní požadavky, TNV 75 2303 Jezy a stupně, TNV 75 2321 Zprůchodňování migračních bariér rybími přechody, ČSN 73 1208 Navrhování betonových konstrukcí vodohospodářských objektů, příslušné EC a legislativní přepisy.

Jméno vedoucího diplomové práce: Ing. Miroslav Brouček, Ph.D.

Datum zadání diplomové práce: 19.9.2023 Termín odevzdání diplomové práce: 8.1.2024
Údaj uveďte v souladu s datem v časovém plánu příslušného ak. roku

Podpis vedoucího práce Podpis vedoucího katedry

III. PŘEVZETÍ ZADÁNÍ

Beru na vědomí, že jsem povinen vypracovat diplomovou práci samostatně, bez cizí pomoci, s výjimkou poskytnutých konzultací. Seznam použité literatury, jiných pramenů a jmen konzultantů je nutné uvést v diplomové práci a při citování postupovat v souladu s metodickou příručkou ČVUT „Jak psát vysokoškolské závěrečné práce“ a metodickým pokynem ČVUT „O dodržování etických principů při přípravě vysokoškolských závěrečných prací“.

Datum převzetí zadání Podpis studenta(ky)

I declare that I have prepared my master thesis independently using the literature and materials provided.

In Prague on _____ _____

Marie Pecharová

Acknowledgements

I thank the thesis supervisor Ing. Miroslav Brouček, Ph.D., for his expert advice, time, and patience during consultations. I would also like to thank my tutor at the Polytechnic University of Catalonia Assoc. Prof. Dipl.-Ing. Pavel Borisovich Ryzhakov PhD and my employer Ing. Karel Kraml for their insightful feedback.

My great thanks also go to the Povodí Vltavy, State Enterprise, which provided me with useful materials that enabled me to complete the thesis successfully.

Furthermore, I'm very grateful to my family who have supported me throughout my studies and who have provided me with excellent conditions for its completion.

Finally, I would like to thank the professors at the Czech Technical University in Prague. Thank you for how you approached teaching and thank you for the inspiration you instilled in your students.

Abstract

The Master thesis focuses on mathematical modelling and simulation of the river flow of a layout solution for reconstruction of the Mazourov weir on the Sázava River. Within the layout design, the main objective is the placement of a small hydropower plant, a fish passage, and a sports sluice for tourist navigation. The suitability of the layout proposal of the hydraulic structures is verified by 2D numerical modelling. For numerical simulation, HEC-RAS software is used. The thesis also deals with the hydraulic design of the small hydropower plant up to the level of drawing and calculation appropriate to the corresponding stage of the documentation for the building permit.

Keywords

2D numerical modelling, HEC-RAS 2D, HPP design, fish passage design, sports sluice design

Content

INTRODUCTION AND THESIS OBJECTIVES

The thesis focuses mainly on numerical modelling of river flow, then on hydraulic calculations of individual hydraulic structures and lastly on drawing documentation of individual hydraulic structures. 2D numerical modelling of the flow is performed in the HEC-RAS software. Hydraulic calculations are carried out by the author of the work as well as the drawing documentation.

The thesis also includes a proposal for the reconstruction of the Mazourov weir on the Sázava River, which is now in poor condition. The designed parts of the weir are subsequently used in the 2D modelling of the flow in the Mazourov weir upstream area.

SUMMARY OF RECEIVED DOCUMENTS

Majority of materials provided to the author of this work were obtained in the process of preparing the Documentation for the building permit for the project of a small hydropower plant on the Mazourov weir. The author of the present master thesis has been working on the design proposal of a small hydropower plant for the company Stream Hydropower s.r.o. under the direct supervision of Ing. Karel Kraml. Other materials were provided to the author directly by Povodí Vltavy, State Enterprise.

All materials received for the preparation of the thesis are:

- Longitudinal profile of the Sázava River between the river kilometres 70.05 and 90.14 provided by the Povodí Vltavy, State Enterprise
- Cross sections of both the riverbed and the weir structure between the river kilometres 70.05 and 90.14 provided by the Povodí Vltavy, State Enterprise
- Layouts of the weir structure provided by the Povodí Vltavy, State Enterprise
- Cross sections through the weir structure provided by Geodesy České Budějovice
- Biological survey of the area of interest by the Czech Union for Nature Conservation (ČSOP)
- Hydrology data provided by the Czech Hydrometeorological Institute (CHMI)
- Information from geological boreholes in the vicinity provided by Czech Geological Survey
- Personal photo documentation from the field survey in March 2023 and January 2024
- Statement on the existence of a power grid
- Digital Terrain Model (DTM) of Sázava River provided by Povodí Vltavy, State Enterprise
- Capacity curve of Mazourov weir structure provided by Povodí Vltavy, State Enterprise

1 MODELLING THEORY

1.1 Hydraulic Engineering Research

Factors such as extremely high cost and unreproducible nature of water structures are the main drivers for the use of hydraulic research methods. Therefore, hydraulic research has become an important part of the pre-design phase of any major water project. The cost of the research is usually lower than the costs induced by any additional construction work, rebuilding or higher operating costs. Currently, there is an increase in demand for hydraulic research in connection with increased investment in the implementation of flood control measures, and the use of hydropower [4].

The current needs of water management practice require the investigation of increasingly complex hydrodynamic phenomena and the solution of more complex problems. The most important basic tools of hydraulic research are:

- physical modelling,
- numerical modelling,
- combination of mathematical and physical modelling [3, 4].

1.2 Physical Modelling

The main purpose of physical modelling is to represent and observe complex hydrodynamic phenomena occurring in reality using a scaled model. This way, actual physical phenomena that are difficult to study in real conditions are analysed on a similar, but much smaller “replica”. Another purpose of physical modelling is to extrapolate model observations to a prototype. Prototype is an actual hydraulic structure that is being modelled [10].

Physical modelling is based on the similarity between the prototype representing reality and the scaled model. Physical modelling is based on the theory of similarity of hydrodynamic phenomena, based either on its mathematical description or on a dimensional analysis of physical quantities. The main objective of the research on the hydraulic model is to investigate the laws of water flow, its effect on the environment and its interaction with the bypassed structures. The model also helps to design optimal hydraulic design and size of hydraulic structures [3, 10].

Research of hydraulic structures on physical models is most often implemented through so-called hydraulic models, which are based on the mechanical similarity of water flow on a scale model

in the laboratory and in reality. Other types of physical models use the analogy of water flow research with other media, such as air. Such models are called aerodynamic models [4].

The advantages of physical modelling on scaled hydraulic models include its relatively small size, which allows for quick and easy modifications, low cost, fast, accurate and systematic measurement of hydraulic and physical quantities by laboratory instruments, independence from external influences and accessibility [3].

1.3 Numerical Modelling

In general, mathematical modelling of hydraulic systems has been an essential tool for the effective assessment of structures and measures in both river engineering and water and sewerage networks for many years. By analysing the hydraulic and qualitative results of the simulations, system weaknesses can be identified [16].

The development of computer technology has enabled the emergence of mathematical modelling. Mathematical modelling allows us to solve problems and simulate such hydrodynamic phenomena, whose mathematical formulation is extremely complex, efficiently and with higher accuracy. Mathematical modelling is based on the similarity between real and abstract systems and allows the investigation of real systems using abstract systems by using mathematical models. If it is possible to describe a phenomenon sufficiently mathematically, it is then possible to use mathematical modelling to investigate very complex physical phenomena in large-scale systems. These complex physical phenomena are most often described by partial differential equations or their systems. Usually, these equations are solved numerically, hence the term numerical modelling [3].

Numerical modelling has exploded in recent years and is increasingly being used instead of physical modelling for several reasons. Advantages of a numerical model include, for example, lower financial requirements compared to a physical model, lower space requirements in the laboratory, less labour-intensive model building, and greater flexibility in exploring alternative solutions [12].

However, it is imperative to mention that the physical model still has an irreplaceable role as a source of information and data necessary in the verification and testing of the proposed model principles and algorithms.

1.3.1 Model Dimensions

Several programs have been developed for the simulation of hydraulic processes using different calculation methods. One of the basic distinction of these programs is their dimensionality.

If the flow is predominantly one-dimensional (1D), this means that one component of the point velocity exceeds the other two components of the point velocity by a significant amount. In this case, the flow is described by 1 equation of motion and 1 continuity equation. An example of 1D flow is flow in straight prismatic channels and pipes.

In a two-dimensional (2D) flow, one component of the point velocity is significantly smaller in magnitude than the other two components of the point velocity. An example of two-dimensional flow is flow in straight non-prismatic channels where the vertical component of velocity is neglected. In this case, the flow is described by 2 equations of motion (in components) and 1 continuity equation.

All 3 components of the point velocity are significant for flow in channels and pipe bends and for flow behind an obstacle. In such a situation, a three-dimensional (3D) description of the flow is applied using 3 equations of motion in the components and 1 continuity equation [8].

Some of the most common software are:

- *1-D*
    - HEC-RAS – hydraulic objects on streams,
    - MIKE 21 - transport model and movement of sediments,
    - HEC-HMS – complete hydrologic processes of the dendritic watershed system.
- *2-D*
    - HEC-RAS 2-D,
    - FESWMS – finite-element surface-water modelling system for two-dimensional flow in the horizontal plane,
    - MIKE 21 C – development in the riverbed and channel planform.
- *3-D*
    - ANSYS Fluent – model of fluid flow, heat and mass transfer and chemical reactions,
    - Flow-3-D – complex hydraulic issues related to planning, design and operation of a hydraulic system,
    - OpenFOAM – complex fluid flows involving chemical reactions, turbulence and heat transfer, as well as acoustics, solid mechanics and electromagnetics

For this thesis, the program HEC-RAS 2D was used.

1.3.2 HEC-RAS 2D Model

HEC-RAS (Hydrologic Engineering Center's River Analysis System) is a software which allows users to perform one-dimensional steady flow, one and two-dimensional unsteady flow calculations, sediment transport/mobile bed computations, and water temperature/water quality modelling [15].

For the calculation of two-dimensional (2D) steady flow, i.e. modelling the free surface flow of a fluid flowing through a riverbed with a variable bed under the influence of gravity acceleration, the Saint-Venant (SV) equations in full dynamic form are used. These equations are derived using the same principles as the more general Navier–Stokes equations, which describe the flow of an incompressible viscous fluid. The program can also solve a simplified version of the Saint-Venant equations, that is the diffusion wave method, which compared to the full SV equations neglects inertial forces. By solving the SV equation in its full form, it is possible to solve more cases, but by using the diffusion wave the program will work faster and can also solve many cases, such as steady flow in prismatic beds. At setting up the calculation, it is easy to choose which variant of the calculation is required. These equations are supplemented by a continuity equation that expresses the law of conservation of mass [8; 6].

Using the Saint-Venant equations, the notation of which can be seen in 1.3.2.1, in other words the shallow water equations, the following assumptions and simplifications are introduced:

- small bottom slope,
- vertically averaged variables,
- flow area perpendicular to the bottom,
- horizontal level at the cross-section point,
- hydrostatic pressure distribution along the vertical,
- small streamlined curvature,
- neglect of acceleration in the vertical direction.

$$\underbrace{\frac{\partial Q}{\partial t}+\frac{\partial}{\partial x}\cdot\left(\beta\cdot\frac{Q^2}{S}\right)}_{\text{Inertial force}}=\underbrace{-g\cdot S\cdot\frac{\partial y}{\partial x}}_{\text{Compressive}}+\underbrace{g\cdot S\cdot i_0}_{\text{Gravitational}}-\underbrace{g\cdot S\cdot i_E}_{\text{Frictional}}$$

Kinematic wave

Diffusion wave

Dynamic wave

1.3.2.1 Saint-Venant's equation [8]

Where:

$Q\ (m^3 \cdot s^{-1})$ - flow rate,
$S\ (m^2)$ - flow area,
$t\ (s)$ – time,
$x\ (m)$ - coordinates in the direction of flow,
$y\ (m)$ - coordinate perpendicular to the flow direction,
$g\ (m \cdot s^{-2})$ - gravitational acceleration,
$\beta\ (-)$ - Boussinesq number,
$i_0\ (-)$ - bottom slope,
$i_E\ (-)$ - slope of the energy line.

Each term in the Saint-Venant equation (1.3.2.1) represents a controlling force of motion. The equation consists of an inertial force component and an external force component, i.e. surface and volume forces. The surface forces are forces compressive from normal stress and frictional from shear stress. The first term expresses the inertial force, which is in the form of local and convective acceleration components. The second term of the equation represents the compressive force, which is in the form of a surface force from the hydrostatic pressure difference. The third term of the equation stands for the gravitational force, which is in the form of volumetric force and is the component of the gravitational acceleration in the direction of flow. The last term in the equation is the frictional force, which is a form of surface force [9].

From the notation of the equation, the simplest kinematic wave solves only the gravitational and frictional components. The more complex diffusion wave also addresses the pressure component. If all components are considered, it is called the dynamic wave [9].

The HEC-RAS program solves the shallow water equations in full dynamic form using the finite volume method. This implicit solution allows for larger computational time steps than explicit methods. It also provides greater computational stability than traditional methods such as finite element method and difference methods. The finite volume method uses the integral form of the equations, which are based on the laws of conservation of mass, momentum, etc. The domain to be solved is divided into a finite number of small control volumes of the mesh. The calculation is performed over the entire volume and its surface [9].

1.4 Hybrid Modelling

By combining numerical and physical modelling, benefits of both approaches are used to investigate hydraulic structures. Such combined modelling is called hybrid modelling. First, the problem is described using a numerical model and variant simulations are used to optimize the hydraulic solution. The resulting solution is then verified on the hydraulic model in the laboratory and refined if necessary. Experience gained in numerous practical applications indicates that the combination of numerical and physical modelling represents a useful approach towards a significant efficiency enhancement of the hydraulic research, which manifests itself particularly in the decrease in number of options that need to be tested on a hydraulic model in the laboratory. The combination of physical and numerical modelling leads to their complementarity. The blending of methods favourably influences the economic and time aspects of research implementation, the quality of results and the complexity of results [4].

Examples of hydraulic research carried out by the Department of Hydraulic Structures of the Czech Technical University in Prague include research on the Přelouč waterworks, research on the Děčín waterworks, research on boulder shoots on the Lower Elbe, research on the lock and navigation stage České Vrbné.

2 NUMERICAL MODELLING OF MAZOUROV WEIR

2.1 Watercourse Characteristics

The area of interest is located on the Sázava River, which rises as the Stružný Brook on the southern slopes of the Žďár Hills. The pond Velké Dářko is built on this stream, from which Sázava flows out of the lake at an altitude of 612 metres above sea level (MASL). The total length of the stream is 224.6 km and the catchment area is 4349 km^2. The Sázava River flows through a richly populated and agriculturally exploited landscape with developed industry and is therefore significantly influenced by human activity along its entire length. The largest towns on the river include Žďár nad Sázavou, Havlíčkův Brod, Světlá nad Sázavou and Ledeč nad Sázavou. The largest tributary of the Sázava River in terms of length of its course, area of the drainage basin and water capacity is the Želivka River. In the upstream section, approximately to the town of Přibyslav, the river flows through a forested valley with a rocky bottom and a relatively high gradient. Further downstream, the Sázava flows through a rather agricultural landscape, with the riverbed in a deep valley, in many places with rocky slopes. In some parts, the longitudinal gradient increases, creating rapids, while in other parts the flow is narrower, deeper and with smaller velocities. In the downstream part of the stream, it is almost a continuous cascade of weirs and surges. The stream channel itself is not significantly morphologically modified, however, there are numerous cross structures. The Sázava River is a right-bank tributary of the Vltava River, which it flows into in the town of Davle [19].

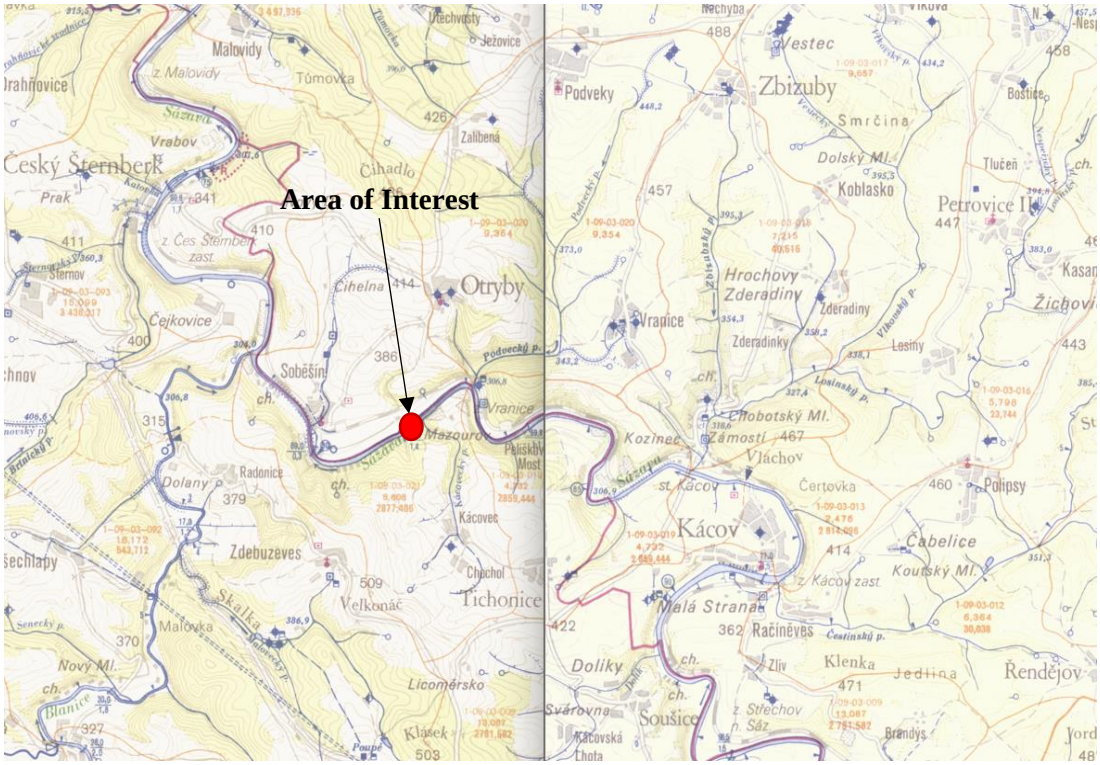

Figure 1 Water-management map showing the area of interest

2.2 Sediment Regime and Morphology

In general, the sediment regime describes sediment production, stability, transport and sedimentation in the channel itself and on adjacent land. The sediment regime also has an important influence on channel formation and stability. Loss of stability, caused by the erosion of the topsoil or subsoil and the movement of material to other locations, occurs due to erosion processes [20].

The site of main interest above the Mazourov weir (river km 81.28) is located in an area of significant erosion and gully erosion. 7.4 kilometres above the Mazourov weir, the Čestínský brook, whose catchment area is classified as an area of up to very strong erosion, flows into the Sázava River in the village of Kácov. In the case of problematic upstream parts of the streams, as in this case, it is assumed that the problems arising in these parts of the catchment area can be easily subsequently propagated to the backbone streams, e.g. by an inappropriate flow regime, siltation of the stream or, on the contrary, increased erosion of the stream.

Anti-erosion measures on watercourses include, for example, linear stabilization of watercourse beds, stabilization of the riverbed using cross structures or damming of rapids and ravines. Localized stabilization of watercourse channel disturbances (e.g. stabilization of bank embankments) can also be considered as anti-erosion measures. Most of the problematic ravines are currently stabilised by riparian treatments, which prevent further erosion.

Monitoring of suspended solids to quantify erosion and sedimentation processes is carried out by the Czech Hydrometeorological Institute (CHMI). Quantitative assessment of suspended solids is based on daily observation of suspended solids at selected water gauging stations. The basic data evaluated is the average daily concentration of suspended solids at the selected gauging stations. Based on these data, further calculations are made. For example, evaluation of sediment flow rate, evaluation of sediment runoff from the catchment and, where appropriate, evaluation of specific sediment runoff. Specifically, on the Sázava River, sediment and suspended solids are monitored in two profiles, Sázava – Nespeky and Sázava - Zruč nad Sázavou.

The morphology of the entire Sázava basin is rugged, sloping northwards. The river basin is made up of several hills concentrated in the south of the basin with the highest point of the basin being the hill Křivý Javor in the Hills of Žďár with an altitude of 824 m. In the northern direction, the river flows mainly through the lowlands. The terrain of the whole area mostly ranges in altitude from 197 MASL to 807 MASL.

2.3 Description of the Current State of Mazourov Weir Structure

The area of interest that is the subject of the present modelling is located between river kilometres 81.28 and 82.00 of the Sázava River.

There is a cross barrier at river kilometre 81.28, which is a privately owned weir. The Mazourov weir is in a damaged state, it does not have a structure allowing fish migration and its sports sluice requires reconstruction. The owner of the Mazourov weir decided to use a gradient of about 1.23 m and build a small hydropower plant on the right bank of the river. The investor decided to reconstruct the weir at the same time as the construction of the small hydroelectric power station. In this particular case, the reconstruction of the weir means an increase of its crest. At present, the crest of the weir is between 307.40 and 307.94 MASL. After the reconstruction, the weir crest will be constant over the entire width of the structure at 307.80 MASL. The single proposals for a small hydropower plant, fish passage and sports sluice are dealt with later in the thesis.

The cross-barrier river structure is a fixed straight weir oriented diagonally to the axis of the channel with a mean length of 104.68 m. At present, there is a 13.22 m long and 6.1 m wide raft sluice in the central part of the weir, which historically used to be used for rafts floating timber from the logging site to the processing site. The current layout of the weir and its surroundings can be found in the image figure 2 [18].

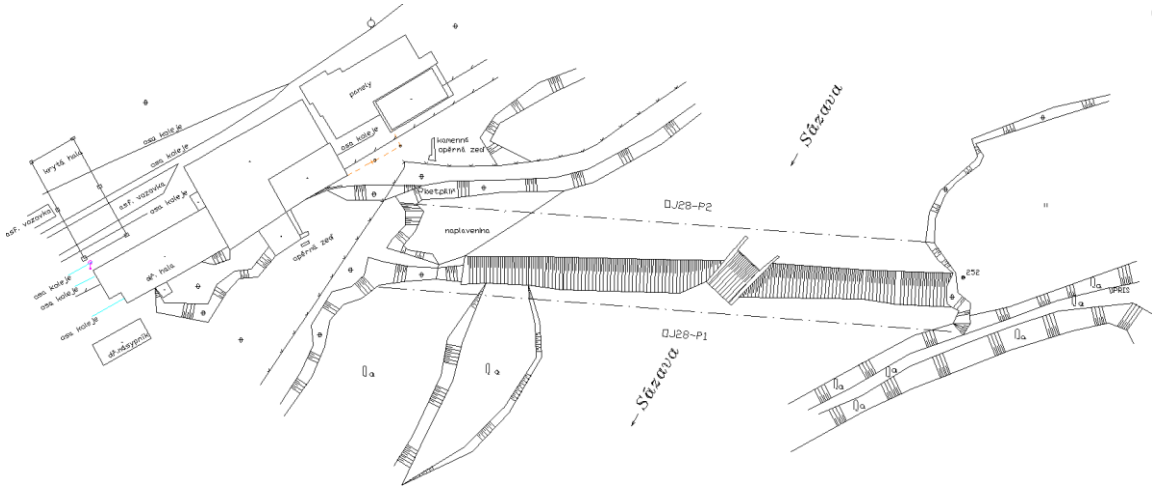

Figure 2 Current layout of the Mazourov weir structure

The main aim of the reconstruction is to ensure the stability of the structure during the period of flood flows through the Sázava River. The reconstructed (raised) Mazourov weir crest will also help the water management and energy purposes. The scope of the proposed reconstruction will also ensure the construction of a fish passage structure to make the weir profile migratory-friendly for fish and other

aquatic animals. The design of the new sports sluice will enable safer crossing of the weir structure in the context of water sports activities that are very widespread on the Sázava River.

For the present thesis, a layout of the weir was created. In the layout proposal, small hydroelectric power plant was placed on the right bank of the river, a slot fish passage was placed right next to the power plant and a sports sluice for tourist navigation was placed at the place of current raft sluice. Using a 2D numerical model of steady flow, the layout will be adjusted to ensure the optimal function of the facilities with maximum probability.

2.4 Model Inputs

2.4.1 Hydrology Data

One of the most important bases of the work is the hydrology data provided by CHMI processed in 2016. These are the m-day flow data and n-year flow data, which are attached in table 1. M-day data refer to the average daily flows that are reached or exceeded in a given river profile for M-days in a normal (average) year. In contrast, n-year data contain information on maximum flows that are reached or exceeded once every N years over the long term.

Table 1 Hydrology data from CHMI

M – day flow data

30	60	90	120	150	180	210	days
34.7	22.9	16.9	12.9	10.2	8.37	7.07	$m^3 \cdot s^{-1}$

240	270	300	330	355	364	days
6.02	5.08	4.32	3.54	2.65	1.95	$m^3 \cdot s^{-1}$

N – year flow data

1	2	5	10	20	50	100	years
121	173	247	311	378	474	553	$m^3 \cdot s^{-1}$

To design a safe sports sluice, a fish passage to allow fish migration, and a reliably functioning small hydroelectric plant, knowing water levels corresponding to each flow was crucial. This data was provided to the author by the Povodí Vltavy, State Enterprise. However, provided materials referred to outdated hydrology data connected to the current lowered crest of the weir (307,40 - 307,94 MASL).

Thus, determining elevation levels for individual flows for the raised crest of the weir was required. To solve this problem, calculation of overtopping over the weir body was performed. By calculation, it was found that at a hundred-year water flow of Q_{100} = 553 $m^3 \cdot s^{-1}$, the level would be at 311.29 MASL. The data from the state enterprise indicated that a hundred-year flow of 559 $m^3 \cdot s^{-1}$ would reach an elevation of 311.24 MASL. Table 2 is attached bellow for a clear summary of flows ($m^3.s^{-1}$) and corresponding elevations (MASL) for both the reconstructed raised weir with a weir crest of 307.8 MASL and the current damaged lower weir.

For future development of the topic of the thesis, 2 variants (processes) are distinguished. Materials referring to outdated hydrology data connected to the current lowered crest of the weir are called Variant A, while data connected to the raised crest of the weir (newly reconstructed) are considered as Variant B.

Table 2 Elevations for current (A) and proposed (B) weir structure

M – day flow data

30	60	90	120	150	180	210	days
34.7	22.9	16.9	12.9	10.2	8.37	7.07	$m^3 \cdot s^{-1}$
307.94	307.81	307.74	307.69	307.66	307.64	307.62	Var. A
308.11	308.03	307.98	307.94	307.92	307.90	307.88	Var. B

240	270	300	330	355	364	days
6.02	5.08	4.32	3.54	2.65	1.95	$m^3 \cdot s^{-1}$
307.60	307.59	307.58	307.58	307.57	307.55	Var. A
307.87	307.85	307.84	307.83	307.81	307.75	Var. B

N – year flow data

1	2	5	10	20	50	100	years
121	173	247	311	378	474	553	$m^3 \cdot s^{-1}$
308.40	308.89	309.50	309.92	310.30	310.81	311.22	Var. A
308.58	308.95	309.56	310.04	310.41	310.89	311.29	Var. B

For a visual comparison of the flood flow regime before and after the reconstruction of the weir, which will increase the overflow edge of the weir crest across the entire width of the weir to 307.80 MASL, a graph of the capacity curves is attached as figure 3. Calculations of the proposed renovation are seen below in table 3.

Table 3 Calculations of total weir overflow

Level (MASL)	h_0 (m)	m	σ	$\sqrt{2g}$	$h_0^{3/2}$	b_0	Q ($m^3.s^{-1}$)
307.80	0.000	0.00	1.00	4.429	0.000	91.00	0.00
308.00	0.200	0.38	1.00	4.429	0.090	90.99	14.47
308.20	0.403	0.40	1.00	4.429	0.256	90.98	41.24
308.40	0.609	0.42	1.00	4.429	0.476	90.98	80.48
308.60	0.818	0.43	0.98	4.429	0.740	90.97	125.07
308.80	1.024	0.43	0.87	4.429	1.036	90.96	155.25
309.00	1.228	0.43	0.77	4.429	1.360	90.95	180.22
309.20	1.431	0.43	0.69	4.429	1.711	90.94	204.51
309.40	1.633	0.43	0.63	4.429	2.087	90.94	227.74
309.60	1.836	0.43	0.59	4.429	2.489	90.93	254.29
309.80	2.040	0.43	0.56	4.429	2.914	90.92	282.54
310.00	2.244	0.43	0.54	4.429	3.362	90.91	314.34
310.20	2.448	0.43	0.52	4.429	3.830	90.90	344.78
310.40	2.652	0.43	0.51	4.429	4.318	90.89	377.51
310.60	2.856	0.43	0.50	4.429	4.827	90.89	413.65
310.80	3.063	0.43	0.50	4.429	5.362	90.88	459.37
311.00	3.268	0.43	0.49	4.429	5.907	90.87	495.80
311.20	3.473	0.43	0.48	4.429	6.472	90.86	537.63
311.29	3.565	0.43	0.48	4.429	6.730	90.86	553.18

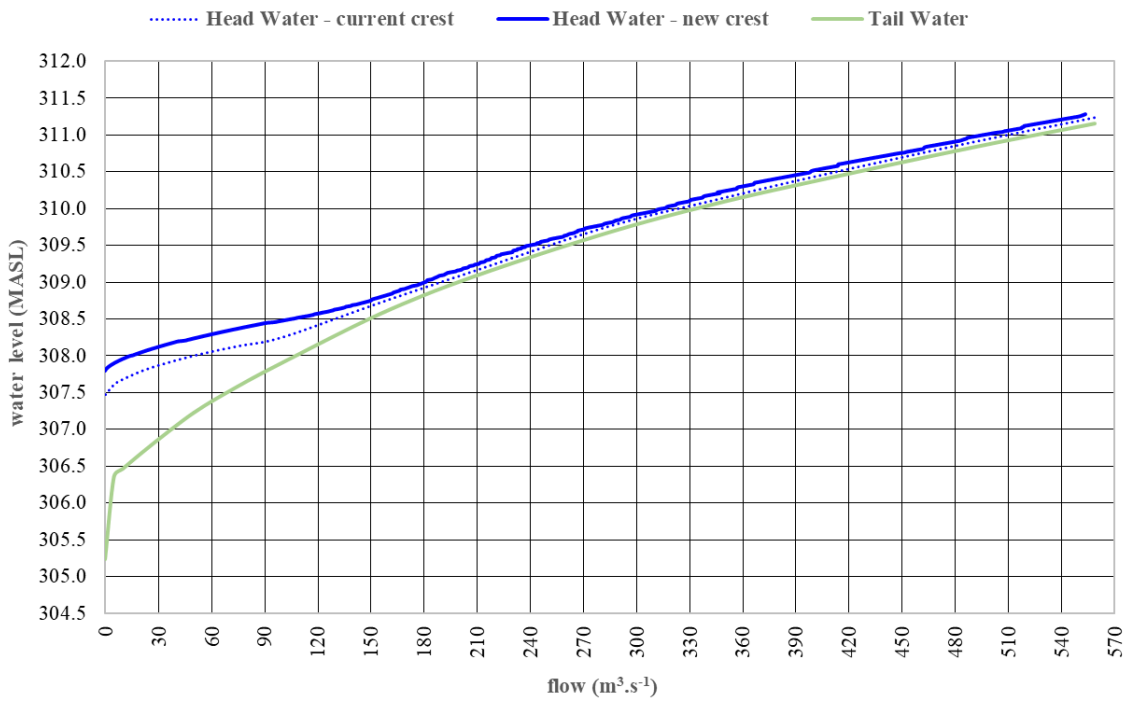

Figure 3 Graph of capacity curves

The light green capacity curve plots the tailwater levels, the dotted blue curve shows the current state of measured flows with corresponding water levels, and the bold blue depicts the capacity curve of calculated proposed state. These calculations were made disregarding the operation of the small hydropower plant and are seen in table 3. The hydropower plant will only affect the water levels during the period when the plant is operating. In the chapter 2.4.5, the calculation of levels during operation of the HPP is described in detail. In addition, the effect of the operation of the power plant will only occur between the m-day flows of approximately Q_{240d} and Q_{20d}.

From the plotted capacity curves, the tailwater curve and the headwater curve converge towards each other with increasing flow. For a 100-year Q_{100} flow of 553 $m^3.s^{-1}$, the difference between the headwater and tailwater levels is 7 cm. In reality, the difference in levels is almost imperceptible to humans. As the flow rate increases, the influence of the weir on the upstream area decreases. This fact has been confirmed by aerial photographs in figure 4 taken during floods in 2006.

The current Act No. 254/2001 Coll. The water act, issued in the Czech Republic, defines three possible levels of flood activity: first level - state of alertness, second level - state of emergency, third level - state of threat. The flood activity level is a simple numerical indication of the situation in terms of the extent to which the population and its property are at risk from a possible or ongoing flood. At the end of March and at the beginning of April in 2006, flood activity stage 3 was exceeded with a maximum flow of Q_{max} 396 $m^3.s^{-1}$, which is higher than Q_{20}. The attached photograph shows the flooded Mazourov weir with minimal backwater flooding. The photograph was taken during

the monitoring of the flood situation and provided by the Povodí Vltavy, State Enterprise. The photograph shows the entire project area of interest, which is the (flooded) weir and neighbouring land, as well as the land of the Sawmill and part of the paved access road to the area.

Figure 4 Aerial photograph of floods in 2006

For further designs of the objects and their calculations it was necessary to determine the minimum residual flow in the river. Minimum Residual Flow (MRF) is the minimum flow that must be maintained in a watercourse in a given profile or reach to maintain its basic water management and ecological functions. The values of the minimum residual flow were determined according to the Methodological Guideline of the Department of Water Protection of the Ministry of the Environment of the Czech Republic, seen as table 4 [13].

Table 4 Minimal residual flow

Flow Q_{355d}	Minimal residual flow
< 0.05 $m^3 . s^{-1}$	Q_{330d}
0.05 – 0.5 $m^3 . s^{-1}$	$(Q_{330d} + Q_{355d}) . 0.5$
0.01 – 5.0 $m^3 . s^{-1}$	Q_{355d}
> 5.0 $m^3 . s^{-1}$	$(Q_{355d} + Q_{364d}) . 0.5$

Thus, a flow of Q_{355d} of 2.65 $m^3.s^{-1}$ must be maintained in the river to ensure sufficient oxygenation of the tailwater area. It was determined that due to the gradual filling of individual sluices, the minimum residual flow rate will be achieved at the headwater level of 307.81, i.e. at a flow rate of MRF, 1 cm of water will overflow the weir crest. The MRF will be secured in the riverbed at all times when operating the small hydropower plant.

2.4.2 Solid Weir

As part of the reconstruction of the body of the fixed weir itself, it will be raised to a constant height of the crest at 307.80 MASL. In cross-section, the weir will have the shape of trapezoidal spillway, with a steeper rising face at a slope of 1 : 3 and a gradual spillway designed at a slope of 1 : 5. The crest thickness will be 20 cm and the sloping weir spillway will end at a height of 0.80 m above the level of the modified bed in the tailwater area. In the downstream area, the overflow surface will be finished with a vertical face at the level 305.24 MASL. Basic data on the dimensions and elevations of the proposed weir can be found in the figure 5 below and in the corresponding attached drawing.

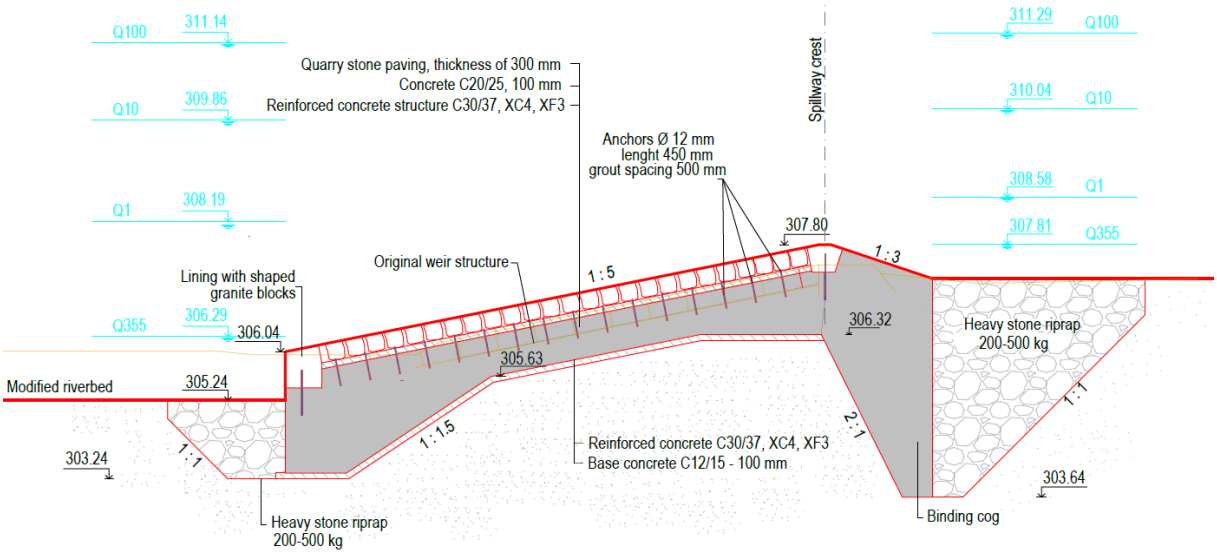

Figure 5 General cross section of the reconstructed weir

The capacity of the fixed weir was determined by calculating the overflow over the fixed edge according to the mathematical equation for an imperfect flooded overflow:

$$Q = \frac{2}{3} \times \mu \times \sigma \times b_0 \times \sqrt{2g} \times h_0^{3/2}$$

2.4.2.1 Weir overflow equation [6]

Where:

m (-) - overflow coefficient, *m= (2/3).μ,*

σ (-) -flooding coefficient,

b_0 *(m)* - length of the overflow edge,

g $(m.s^{-2})$ - acceleration of gravity,

h_0 *(m)* - overflow height.

Table 5 Calculations of weir overflow

Level (MASL)	h_0 (m)	m	$\sqrt{2g}$	$h_0^{3/2}$	b_0	Q ($m^3.s^{-1}$)
307.80	0.000	0.00	4.429	0.000	91.00	0.00
307.82	0.020	0.38	4.429	0.003	91.00	0.43
307.84	0.040	0.38	4.429	0.008	91.00	1.23
307.86	0.060	0.38	4.429	0.015	91.00	2.25
307.88	0.080	0.38	4.429	0.023	91.00	3.47
307.90	0.100	0.38	4.429	0.032	91.00	4.85
307.92	0.120	0.38	4.429	0.042	91.00	6.37
307.94	0.140	0.38	4.429	0.052	90.99	8.04
307.96	0.160	0.38	4.429	0.064	90.99	9.82
307.98	0.180	0.38	4.429	0.077	90.99	11.73
308.00	0.200	0.38	4.429	0.090	90.99	14.47
308.02	0.221	0.40	4.429	0.104	90.99	16.70
308.04	0.241	0.40	4.429	0.118	90.99	19.05
308.06	0.261	0.40	4.429	0.133	90.99	21.49
308.08	0.281	0.40	4.429	0.149	90.99	24.03
308.10	0.301	0.40	4.429	0.165	90.99	26.67
308.11	0.312	0.40	4.429	0.174	90.99	28.03

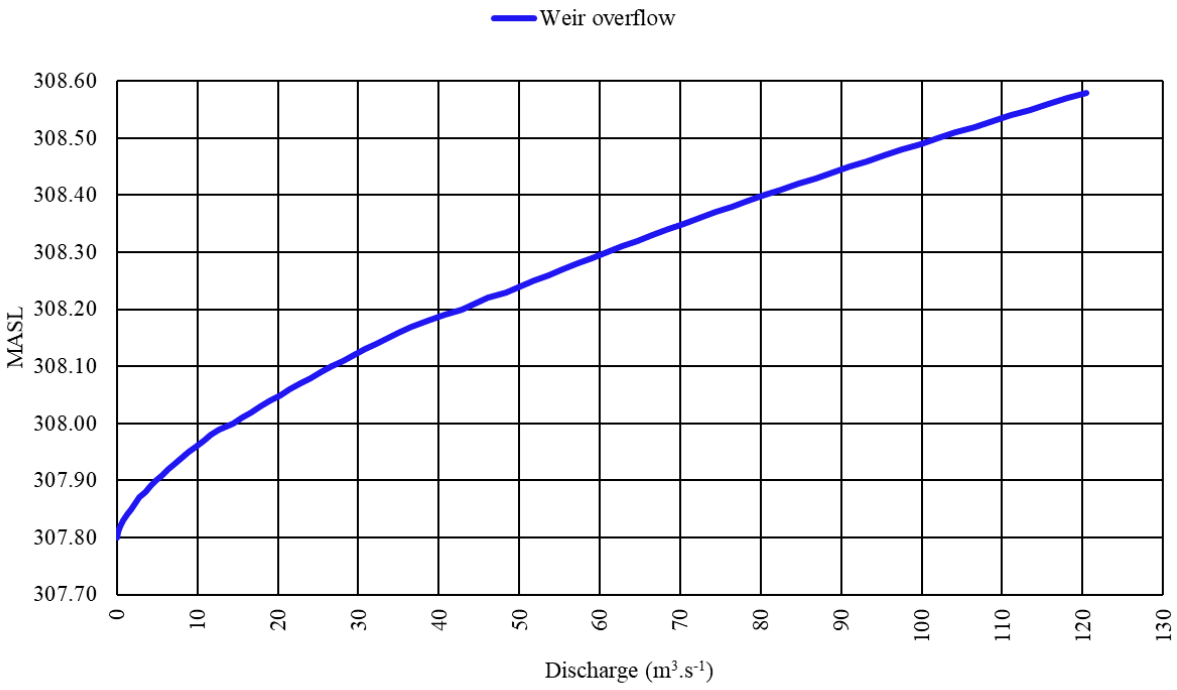

Figure 6 Graph of capacity curve of the weir

The attached calculation table above contains only a range of m-day flow rates. These flows are not influenced by tailwater; therefore, the flooding coefficient is equal to 1. These calculations were very crucial for the design of the elevations of the overflow edges of the fish passage and the sports sluice. At the same time, these calculations were important for the subsequent determination of the average annual production of the small hydropower plant. When the power station is not in operation, the overflow beam reaches a height of 31 cm at a flow of Q_{30d} through the entire riverbed. At this moment 28.03 $m^3.s^{-1}$ overflows the spillway edge of the weir alone (excluding the fish passage and the sport sluice). A weir capacity curve, figure 6, is included for visual clarity as well.

As part of the reconstruction of the weir, during which the weir crest will be raised, modifying the riverbed in the downstream area was considered. Such a modified prismatic channel was used to calculate the hydraulic jump. The calculation of the hydraulic jump was made to ensure maximum safety during sports rafting. The calculation indicated that the second reciprocal depth of the hydraulic jump is below the depth of the tailwater, which means that a neared hydraulic jump is formed. Its length is 8.85 metres. In such scenario, there is no need to construct a stilling basin. Knowing the length of the hydraulic jump is essential for designing the length of the sports sluice's piers.

The hydraulic jump was calculated using the following formulas:

$$y_k = \sqrt[3]{\frac{q^2}{g}}$$

2.4.2.2 Hydraulic jump - Critical depth equation [7]

$$y_2 = \frac{y_1}{2} \times \left(\sqrt{1 + 8 \left(\frac{y_k}{y_1} \right)^3} - 1 \right)$$

2.4.2.3 Hydraulic jump – 2nd reciprocal depth equation [7]

$$L_s = 3 * y_d$$

2.4.2.4 Hydraulic jump - lenght of the hydraulic jump [7]

Where:

y_k *(m)* – critical depth,
q *($m^3.s^{-1}.m^{-1}$)* -flow rate,
$y_{1,2}$ *(m)* – reciprocal depths,
y_d *(m)* – tail water depth,
L_s *(m)* – hydraulic jump length.

2.4.3 Sports Sluice

In the Czech Republic, there is currently no valid standard or methodology that serves as a basis for the design of sports sluices. A document recommending a design procedure, defining terms, summarising the necessary hydraulic calculations, or establishing criteria for safe sports sluices has not yet been published. For this thesis, the unofficial requirements of the Water Tourism and Sports Association (AVTS) were adopted.

The sports sluice is tied into the structure of the fixed weir in place of the existing raft sluice. In the longitudinal direction, the sports sluice is a sloping ramp with a slope of 8.0% over a length of 18.24 m. The crest of the inflow sill of the sports sluice reaches the level of 307.52 MASL. The entrance part of the sports spillway is situated 2.2 m in front of the overflow edge of the weir in the direction of the upstream area. In the direction of the headwater, the forward entrance section will slightly decrease to the bottom elevation of 306.56, which corresponds to the existing condition. The width of the sluice is 2.5 m, which is the minimum width specified by the AVTS. The pillars of the sluice consist of reinforced concrete walls with a thickness of 90 cm, which reach a flow height

of Q_1, i.e. 308.58 MASL in the upstream area and 308.19 MASL in the downstream area. By calculations, it was determined that for 355 days a year there is a water depth of 29 cm in the sports spillway itself, which ensures that the weir will be passable almost all year round. The sloping sliding part of the sports sluice will be terminated at 305.84 MASL.

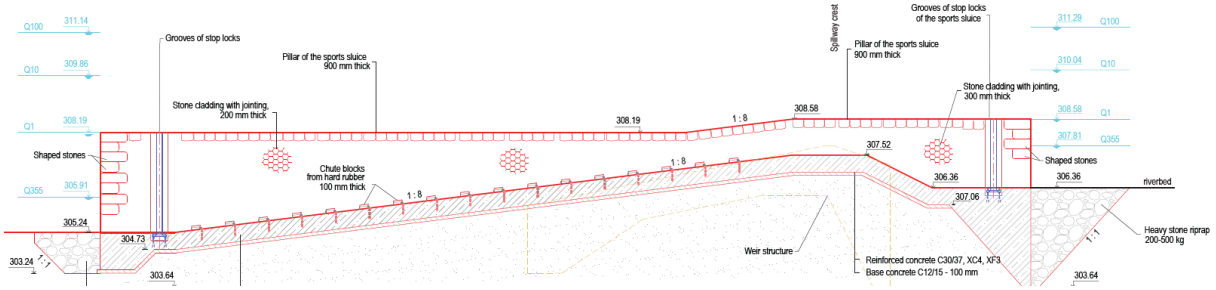

Figure 7 General cross section of sports sluice

The capacity of the sports sluice is solved as a perfect overflow over a wide crest according to mathematical formulas:

$$h_K = \sqrt[3]{\frac{Q^2}{g \times b^2}}$$

2.4.3.1 Equation of the critical height of the sluice [6]

$$h_c = h_K \times \chi$$

2.4.3.2 Decreased height of the overflow capacity of sluice

$$H = \frac{Q^2}{\varphi^2 \times b^2 \times h_c^2 \times 2g}$$

2.4.3.3 Equation of the overflow height of sports sluice

Where:

h_k *(m)* – critical depth of the sluice,
b (m) – sluice width
H (m) – overflow height,
χ *(-)* - overflow coefficient (0,833),
φ *(-)* -overflow shape coefficient (0,91).

Table 6 Capacity of sports sluice

Q ($m^3.s^{-1}$)	b (m)	$\frac{Q^2}{g.b^2}$	h_k (m)	χ	h_c (m)	σ	2g	E	Level (MASL)
0.00	2.5	0.000	0.00	0.833	0.000	0.91	19.62	0.000	307.52
0.20	2.5	0.001	0.09	0.833	0.072	0.91	19.62	0.075	307.60
0.40	2.5	0.003	0.14	0.833	0.115	0.91	19.62	0.120	307.64
0.60	2.5	0.006	0.18	0.833	0.150	0.91	19.62	0.157	307.68
0.80	2.5	0.010	0.22	0.833	0.182	0.91	19.62	0.190	307.71
1.00	2.5	0.016	0.25	0.833	0.211	0.91	19.62	0.221	307.74
1.20	2.5	0.023	0.29	0.833	0.239	0.91	19.62	0.249	307.77
1.40	2.5	0.032	0.32	0.833	0.264	0.91	19.62	0.276	307.80
1.60	2.5	0.042	0.35	0.833	0.289	0.91	19.62	0.302	307.82
1.80	2.5	0.053	0.38	0.833	0.313	0.91	19.62	0.327	307.85
2.00	2.5	0.065	0.40	0.833	0.335	0.91	19.62	0.350	307.87
2.20	2.5	0.079	0.43	0.833	0.357	0.91	19.62	0.373	307.89
2.40	2.5	0.094	0.45	0.833	0.379	0.91	19.62	0.396	307.92
2.60	2.5	0.110	0.48	0.833	0.399	0.91	19.62	0.417	307.94
2.80	2.5	0.128	0.50	0.833	0.420	0.91	19.62	0.438	307.96
3.00	2.5	0.147	0.53	0.833	0.439	0.91	19.62	0.459	307.98
3.20	2.5	0.167	0.55	0.833	0.459	0.91	19.62	0.479	308.00
3.40	2.5	0.189	0.57	0.833	0.478	0.91	19.62	0.499	308.02
3.60	2.5	0.211	0.60	0.833	0.496	0.91	19.62	0.518	308.04
3.80	2.5	0.236	0.62	0.833	0.514	0.91	19.62	0.537	308.06
4.00	2.5	0.261	0.64	0.833	0.532	0.91	19.62	0.556	308.08
4.20	2.5	0.288	0.66	0.833	0.550	0.91	19.62	0.574	308.09
4.40	2.5	0.316	0.68	0.833	0.567	0.91	19.62	0.593	308.11

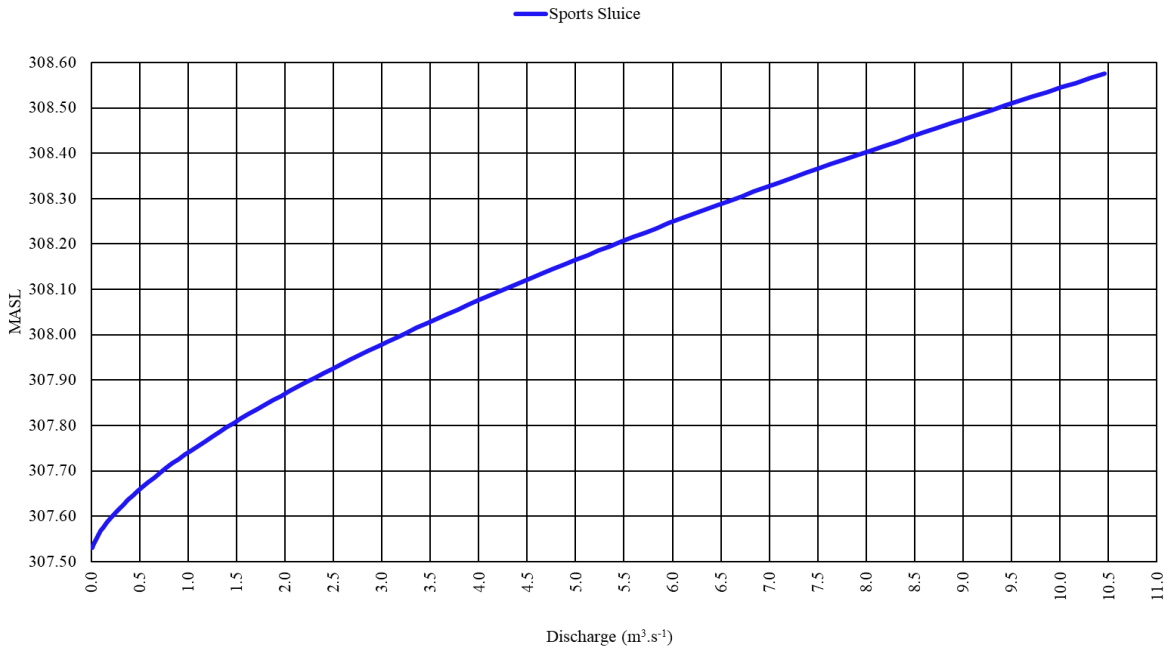

Figure 8 Graph of capacity curve of sports sluice

The attached calculation table above (Table 6) contains only a range of m-day flow rates. Based on the calculations, it was decided that the elevation of the overflow edge of the sports spillway would be 307.52 MASL, which is 28 cm lower than the overflow edge of the weir. With a 30-day water flow (34.7 $m^3.s^{-1}$) through the entire river profile, 4.40 $m^3.s^{-1}$ will pass through the sports spillway alone and the water depth in the spillway will be 59 cm. A sports sluice capacity curve is included for visual clarity as well, see figure 8.

Although the sport sluice is designed so that the height of the piers is capable of safely carrying the Q_1 flow without exceeding the height of the piers by overtopping, crossing the river at such high flows is strongly discouraged. Navigation bans on rivers occur when the water level is such that the safety of navigation is compromised on the relevant section of the watercourse and also when flood activity stages (hereinafter referred to as FS) 2 and 3 are declared. From the Reporting Profile Registration Sheet No. 152 - Kácov, it was found that the 1st stage of flood activity, alertness, of the Sázava River location of interest occurs when the flow exceeds 67.1 $m^3.s^{-1}$. The second FS - emergency - occurs at a flow of 97 $m^3.s^{-1}$ and the third level of flood activity - threat - at a flow of 189 $m^3.s^{-1}$ [17].

2.4.4 Fish Passage

In designing the fish passage, the Fish Passage Standard was followed. The Standard gives an overview of the individual steps and procedures for restoring the permeability of migration barriers on watercourses. The standard is based on TNV 75 2321 - Clearance of river barriers for fish migration and P ČSN 75 2323 - Ensuring downstream migration of fish in watercourses [21].

To ensure the migratory accessibility of the Mazourov weir for fish and other aquatic animals, a fish passage was designed, located at the left wall of the small hydropower plant on the right bank of the Sázava River. In the longitudinal direction, the fish passage is a rectangular bypass channel in the zigzag shape with a slope of 1 : 39.0. The flow profile is divided in the longitudinal direction by regular barriers made of precast concrete or boulders with intermediate openings for lagoons/pools. The difference in level between the two adjacent pools is 100 mm. A total of 15 slots forms 14 pools, overcoming a gradient of 1.53 m. Regularly alternating openings with widths of 650 and 350 mm are created between the individual prefabricated barrier blocks (slots) to allow the passage of aquatic animals. The clear length of the individual pools is designed to be 4.01 m, with an axial distance of 4.17 m between adjacent pools. The minimum depth at the exit of the fish ladder is designed to allow for carp migration of 0.6 m.

The basic dimensions of the partition can be seen in the general cross-section in the figure 9 below. Gaps between individual dividers, in our case boulders, are alternately spaced, the average gap size being 450 mm. Total width of 1350 mm must be maintained. Irregular placement of boulders is advised for its nature-like appearance and for formation of better natural conditions which makes

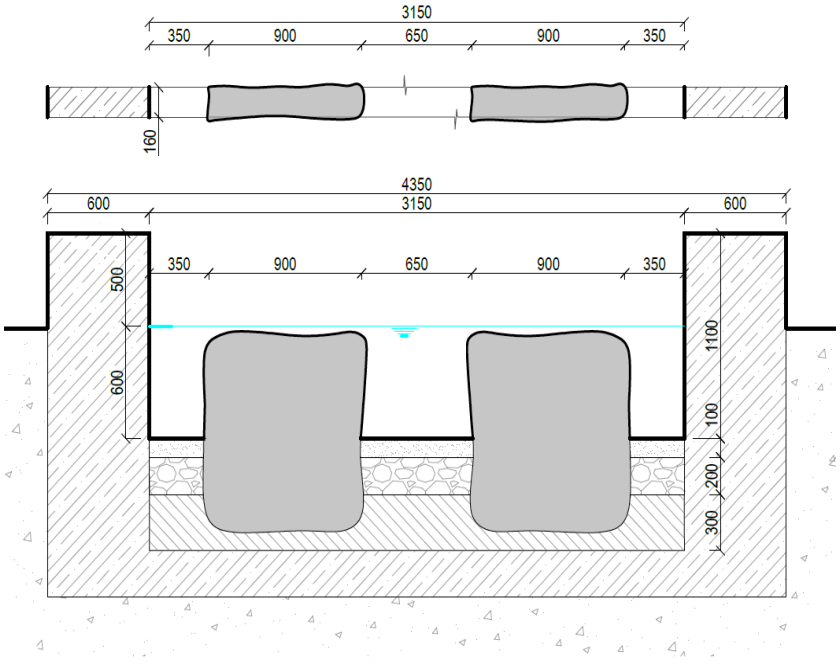

Figure 9 General cross section of the fish passage

the fish passage more attractive for animals. The entrance to the fish passage in the tailwater area is designed at the level of 305.75 MASL with the minimum water level in the downstream at 306.28 MASL. On the exit side of the fish passage, its foundation joint will extend to the level of 306.40 MASL.

The capacity of the fish passage was determined by calculating the flooded spillway over the fixed edge according to a mathematical formula:

$$Q = \frac{2}{3} * \mu * \sigma * \sum b_0 * \sqrt{2g} * h^{3/2}$$

2.4.4.1 Fish passage capacity [6]

where:

μ (-) - overflow coefficient for boulders (0,65),
σ (-) - flooding coeffverageicient (0,96),
b_0 *(m)* - length of the overflow edge, total width of openings,
g ($m.s^{-2}$) - acceleration of gravity,
h (m) - overflow height.

Table 7 Capacity of fish passage

Level [(MASL)]	μ	σ	$\sum b$	$\sqrt{2g}$	h [m]	$h^{3/2}$	Q ($m^3.s^{-1}$)
307.25	0.70	0.96	1.35	4.43	0.00	0.000	0.00
307.30	0.70	0.96	1.35	4.43	0.03	0.005	0.01
307.35	0.70	0.96	1.35	4.43	0.08	0.023	0.06
307.40	0.70	0.96	1.35	4.43	0.13	0.047	0.13
307.45	0.70	0.96	1.35	4.43	0.18	0.076	0.21
307.50	0.70	0.96	1.35	4.43	0.23	0.110	0.30
307.55	0.70	0.96	1.35	4.43	0.28	0.148	0.40
307.60	0.70	0.96	1.35	4.43	0.33	0.190	0.51
307.65	0.70	0.96	1.35	4.43	0.38	0.234	0.63
307.70	0.70	0.96	1.35	4.43	0.43	0.282	0.755
307.75	0.70	0.96	1.35	4.43	0.48	0.333	0.89

Level (MASL)	m	s	$\sum b$	$\sqrt{2g}$	h [m]	$h^{3/2}$	Q ($m^3.s^{-1}$)
307.80	0.70	0.96	1.35	4.43	0.53	0.386	1.03
307.85	0.70	0.96	1.35	4.43	0.58	0.442	1.18
307.90	0.70	0.96	1.35	4.43	0.63	0.500	1.34
307.95	0.70	0.96	1.35	4.43	0.68	0.561	1.50
308.00	0.70	0.96	1.35	4.43	0.73	0.624	1.67
308.05	0.70	0.96	1.35	4.43	0.78	0.689	1.85
308.10	0.70	0.96	1.35	4.43	0.83	0.756	2.03
308.11	0.70	0.96	1.35	4.43	0.84	0.770	2.06

The attached calculation table (Table 7) above contains only a range of m-day flow rates. Based on the calculations, it was decided that the elevation of the overflow edge of the fish passage would be 307.27 MASL, which is 53 cm lower than the overflow edge of the weir and 25 cm lower than the overflow edge of the sports sluice. The different height elevations of the spillway edges of the individual objects are important in optimising the efficiency of a small hydropower plant.

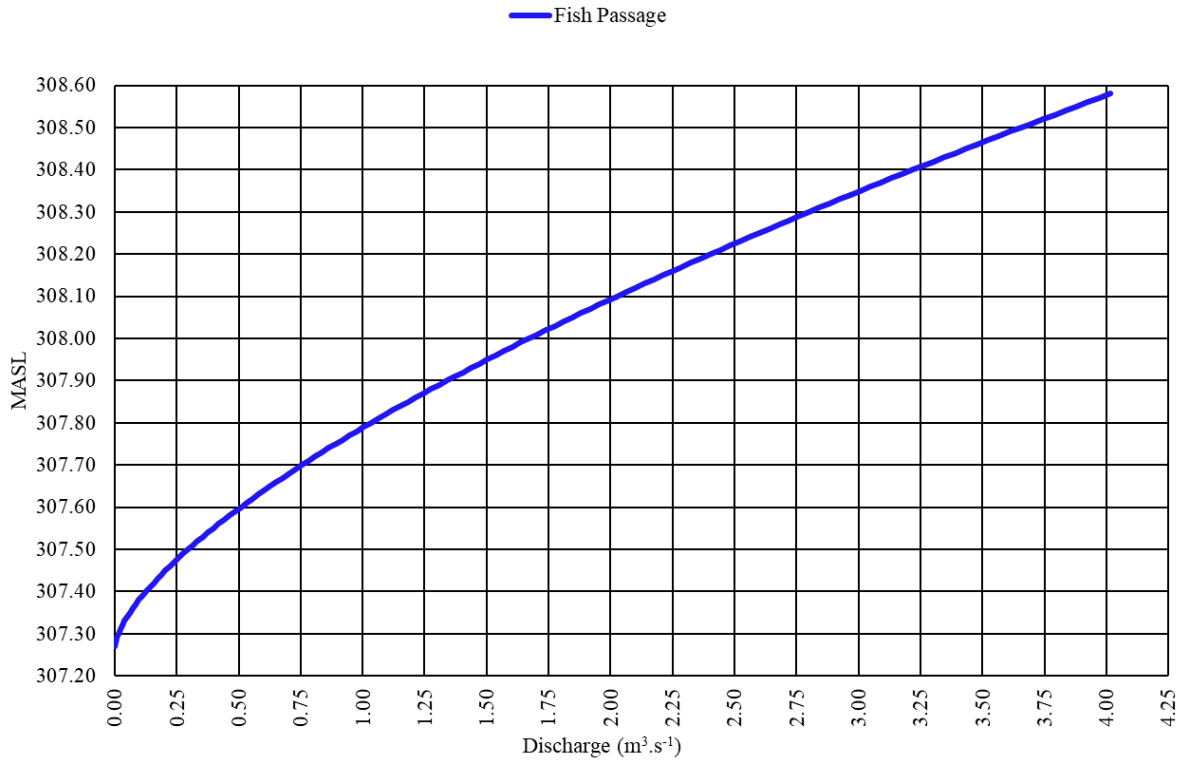

Figure 10 Graph of capacity curve of the fish passage

With a 30-day water flow (34.7 $m^3.s^{-1}$) through the entire river profile, 2,06 $m^3.s^{-1}$ will pass through the fish passage alone and the water depth in the spillway will be 84 cm. A sports sluice capacity curve (figure 10) is included for visual clarity as well. The theoretical flow through the fish passage corresponds to the value prescribed in TNV 75 2321 - Passage of migration barriers through fish passages. The technical standard stipulates that for a Q_{355day} flow of 1.0 to 5.0 $m^3.s^{-1}$, the minimum percentage for the fish passage must be 40%, which in our case is 1.06 $m^3.s^{-1}$. At the MRF flow rate, 1.06 $m^3.s^{-1}$ will flow through the fish passage.

A detailed overview of the proposed slot-type fish passage parameters for carp waters is found in the table 8

Table 8 Main parameters of the Fish Passage

Head water (Q_{355d})		307.81	MASL
Tail water (Q_{355d})		306.28	MASL
Head	dH	1.53	m
Total constructional fish pass length	L	60.00	m
Total fish pass slope	i	0.03	1:39
Rated pool water levels difference	dh	0.10	m
Pools width	b_t	3.15	m
Pool net length	dt	4.01	m
Min. number of pools	n_{min}	14.00	pcs
Pool average depth	h	0.70	m
Mean pool velocity	v	0.48	$m.s^{-1}$
Disipation energy in pool	P_t	118	$W.m^{-3}$
Slots amount in partition	n	3	pcs
Slot length (fish pass axial direction)	dp	0.16	m
Distance from entrance to 1st slot	d_1	0.80	m
Distance from exit to last slot	d_2	0.80	m
Net head between pools	dh	0.10	m

Discharge	Q	1.06	$m^3.s^{-1}$
Min. number of slots	n	15.00	pcs
Distance between slots (axial)	d_0	4.17	m
Velocity in slot	v	0.99	$m.s^{-1}$
Section area	S	0.81	m^2
Opening width	b_o	0.45	m
Opening height	h_o	0.60	m
Coefficient	C_s	0.70	-
Flow characteristics	Fr	0.41	-
Dissipation energy in pool	Ps	1042	W

To finally summarize the calculations, the following reminders are important: the weir crest is located at 307.80 MASL, the bottom of the inlet of the sports spillway is located at 307.52 MASL and the bottom of the fish passage outlet is located at 307.27 MASL. From the calculated m-day flows through the sports spillway, the fish passage and the spillway over the weir body, the total capacity of the weir profile is determined for different water levels in the weir and can be seen below in table 9.

Table 9 Total capacity of weir profile without HPP

Level (MASL)	Fish Passage ($m^3.s^{-1}$)	Sports Sluice ($m^3.s^{-1}$)	Weir Structure ($m^3.s^{-1}$)	Total Discharge ($m^3.s^{-1}$)
307.25	0.000	0.000	0.00	0.00
307.30	0.01	0.000	0.00	0.01
307.35	0.06	0.000	0.00	0.06
307.40	0.13	0.000	0.00	0.13
307.45	0.21	0.000	0.00	0.21
307.50	0.30	0.000	0.00	0.30
307.55	0.40	0.040	0.00	0.44
307.60	0.51	0.20	0.00	0.71
307.65	0.63	0.43	0.00	1.06
307.70	0.76	0.71	0.00	1.47
307.75	0.89	1.03	0.00	1.92
307.80	1.03	1.40	0.00	2.43
307.81	1.06	1.47	0.15	2.69
307.85	1.18	1.79	1.71	4.69
307.90	1.34	2.22	4.85	8.41
307.95	1.50	2.68	8.91	13.10
308.00	1.67	3.16	14.47	19.30
308.05	1.85	3.67	20.26	25.77
308.10	2.03	4.21	26.68	32.91
308.11	2.06	4.32	28.03	34.41

The hydraulic calculations of the weir, the fish passage and the sports sluice show that at the residual flow rate Q_{355d} = 2.65 $m^3.s^{-1}$ the level in the spillway will rise to the level of 307.81 MASL, while the sports sluice will carry the flow rate Q_S = 1.47 $m^3.s^{-1}$, the fish passage Q_R = 1.09 $m^3.s^{-1}$ and weir overflow will be Q_J = 0.15 $m^3.s^{-1}$.

A graph of the capacity curves is attached below to clearly illustrate the gradual increase in flow as a function of water level. The graph as figure 11 corresponds to the state in which the power plant is not operating. The yellow curve corresponds to the dependence of the flow rate on the water level in the fish passage, the red curve shows the Q-H dependence of sports sluice, the green curve represents the size of the overflow beam over the weir crest. The thick blue curve is the sum of the flow rate through the individual sluices and the overflow across the weir.

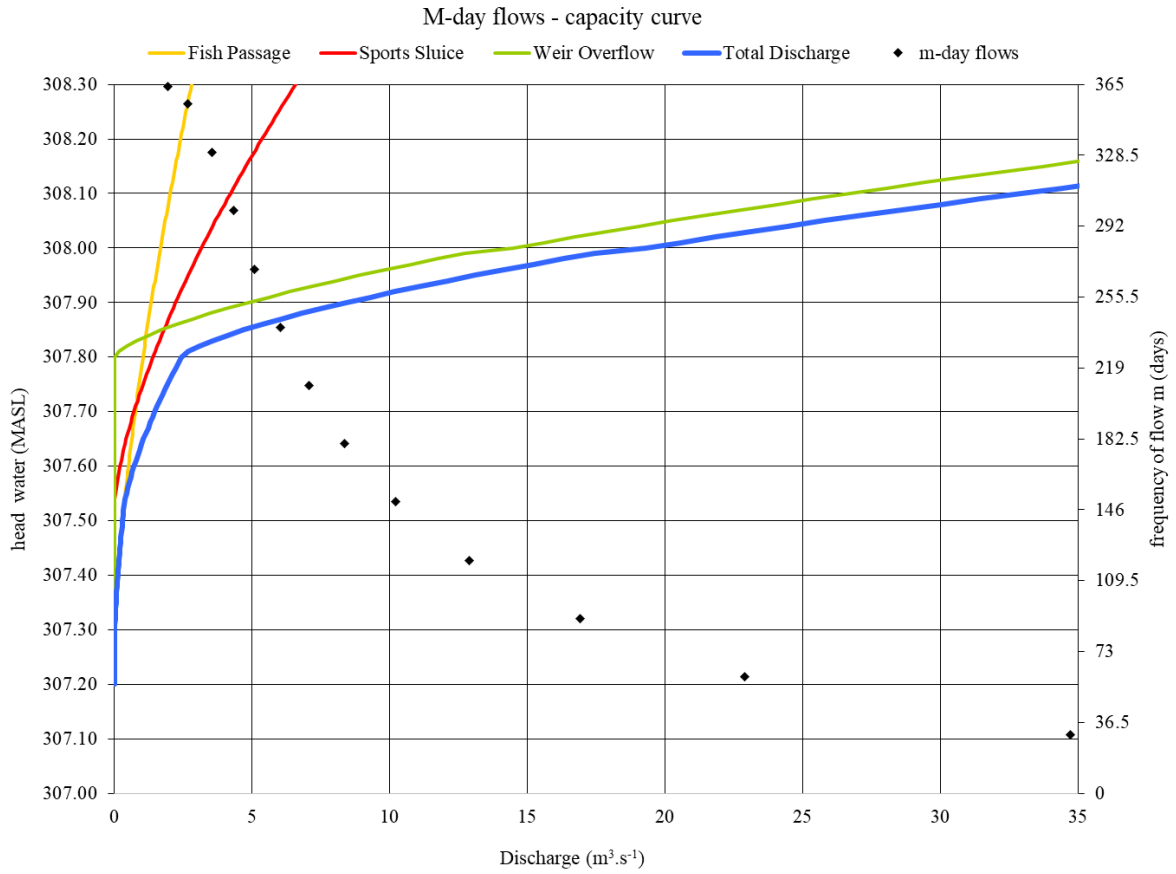

Figure 11 Combined graph of individual capacity curves

The curve chart attached and described above is valid only when the power plant is not operating. In that case, the fish passage is filled first, then a flow through the sport sluice is added, and the level in the pool area rises to 307.81. At this point, a 355-day flow is flowing through the river and 1 cm of water is overflowing the crest of the weir. Minimal residual flow in Sázava river is secured.

The state of the levels that occur during the operation of the power plant is dealt with in the next chapter 2.4.5.

2.4.5 Water Management Design Proposal of Small Hydropower Plant

This chapter focuses mainly on the hydraulic design of a small hydropower plant. The hydraulic design includes the number and the type of turbine units, positions of water levels, minimum and maximum turbine head, expected turbine power and considered losses. The construction part of the design of small hydropower plant in Mazourov is described in chapter 4.

The hydrology data provided by CHMI in 2016, seen at table 1, was the basis for the design of the small hydropower plant. The elevation of the repaired and reinforced crest of the weir at river kilometre 81.28 corresponds to 307.80 MASL.

2.4.5.1 Turbine Type

One of the first tasks was to decide which type of turbine is the most suitable for the given location and hydrological conditions. Considering the usable gradient and average flows of the Sázava River, the Kaplan turbine was chosen. Kaplan turbines automatically adjust its runner blades and wicket gates to suit changing water conditions. This unique adaptability enables consistently high efficiency over a range of flow and head conditions. The high variability of flows in the Sázava River was one of the factors why Kaplan turbine type was chosen [1].

In general, Kaplan turbine models include PIT, vertical, bulb, Z, and S. Individual turbines vary in their applicability to gradients and their power output. Kaplan PIT and S-turbine units are generally favoured for economic solutions in small hydro applications with outputs up to about 10 MW. Their design provides good accessibility of various components and assures reliability and long service life. Meanwhile, the bulb turbine is a very common solution for high outputs at low headsites. Both bulb and PIT turbines feature higher full-load efficiency and higher flow capacities than vertical Kaplan turbines [1]. For the design of small hydropower plant in Mazourov, the PIT model of Kaplan turbine was chosen. General drawing of a Kaplan PIT turbine is seen on figure 12.

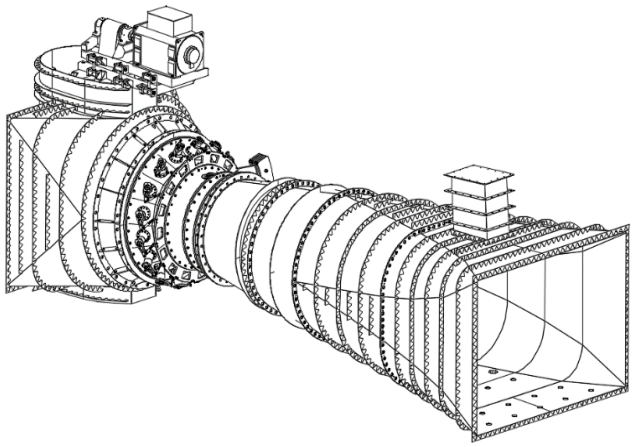

Figure 12 Trigonometry drawing of Kaplan turbine used for the design of HPP in Mazourov

Parameters of the main technology are:

- turbine type: Kaplan PIT
- number of turbines: 2
- impeller diameter: 1300 mm
- speed: 170 rpm
- 1 turbine power: 95 kW
- Gradient: 0,8 – 1,5 m
- transmission: belt drive, 170/660 rpm
- generator: horizontal, asynchronous
- generator speed: 600 rpm
- generator output: 90 kW

2.4.5.2 Turbine Capacity, Losses, Energy Production

The maximum usable flow of the turbines (turbine capacity) was set at 12 $m^3.s^{-1}$. For the respective turbine type used, efficiencies were determined as a function of flow and gradient. The minimum turbine efficiency is 69.3% at a flow rate of 2.28 $m^3.s^{-1}$. Therefore, the minimum usable flow is estimated to be about 2.28 $m^3.s^{-1}$. As the flow rate increases, the efficiency increases to a maximum value of 90.5% at a maximum usable flow of 12 $m^3.s^{-1}$.

The following losses were considered for calculations of the expected annual production of the turbine:

- turbine efficiency $0,776 < \mu_T (-) < 0,905$,
- the efficiency of the electrical generator $\mu_G (-) = 0,94$,
- losses on the coarse and fine screens $y (m) = 0,05$.

The following hypothesis was used in the calculation of the power plant output and the subsequent determination of the annual energy production:
If the flow rate in the upstream area (pool area) is smaller than Q_{355d} – the power plant is not in operation. As soon as the flow becomes greater than Q_{355d} and as soon as the minimum usable flow of the turbine is reached, the power plant switches on. The considered gradient equals the difference between the upstream and downstream water levels minus the losses on the screens. The losses on the screens were considered to be constant.

In our particular case, to optimize the function of HPP, the plant switches on at the upstream water level of 307.86, when the minimum turbine capacity is exceeded while ensuring a minimum residual flow in the remaining river profile. At this water level, the turbine starts operating, taking flow from the rest of the riverbed. At this moment, while the turbine is running, the level in the pool area

does not rise with increasing flow. On the contrary, when the minimum turbine head requirement is met, the water level drops to 307.81 with the MRF being secured. Any excess flow above the MRF is used only by the HPP. The flow through the plant gradually increases without any increase in the upstream area. The discharge increase situation with constant water level is visible in the graph bellow between the flow rates of 5.35 $m^3.s^{-1}$ and 14.69 $m^3.s^{-1}$. Once the maximum flow rate of 12 $m^3.s^{-1}$ is reached, the level in the pool area starts to rise, which increases the overflow beam of the weir. In our case, the maximum head is reached at the upstream water level of 307.81 with the flow through the entire river profile of 14.69 $m^3.s^{-1}$. The flow rate of 14.69 $m^3.s^{-1}$ includes both the minimum residual flow through the riverbed by individual sluices and the maximum turbine capacity of the plant. The efficiency of the power plant is at its maximum. This status lasts until the gradient of the power plant drops below 80 cm. The decrease in the gradient is due to the increase of tailwater level. The minimum gradient of 80 cm between the headwater and tailwater level occurs at a flow rate of 55.93 $m^3.s^{-1}$. At this flow rate, the water level in the pool area is 308.17 MASL and the tailwater level is at 307.32 MASL The power plant is, at this moment, disconnected. Once the power plant is disconnected, all flow through the profile passes through the fish ladder, sports sluice and overflows the crest of the weir.

Table 10 Capacity and elevations of the weir structure with HPP in operation

Level [(MASL)]	Fish Passage ($m^3.s^{-1}$)	Sports Sluice ($m^3.s^{-1}$)	Weir ($m^3.s^{-1}$)	HPP ($m^3.s^{-1}$)	Total Discharge ($m^3.s^{-1}$)
307.80	1.03	1.40	0.00	0.00	2.43
307.81	1.06	1.47	0.15	0.00	2.69
307.82	1.09	1.55	0.43	0.00	3.08
307.83	1.12	1.63	0.80	0.00	3.55
307.84	1.15	1.71	1.23	0.00	4.09
307.85	1.18	1.79	1.71	0.00	4.69
307.86	1.21	1.88	2.25	0.00	5.35
307.81	1.06	1.47	0.15	3.36	6.04
307.81	1.06	1.47	0.15	3.99	6.67
307.81	1.06	1.47	0.15	4.66	7.34
307.81	1.06	1.47	0.15	5.37	8.05
307.81	1.06	1.47	0.15	6.11	8.80

Level (MASL)	Fish Passage ($m^3.s^{-1}$)	Sports Sluice ($m^3.s^{-1}$)	Weir ($m^3.s^{-1}$)	HPP ($m^3.s^{-1}$)	Total Discharge ($m^3.s^{-1}$)
307.81	1.06	1.47	0.15	6.89	9.58
307.81	1.06	1.47	0.15	7.71	10.39
307.81	1.06	1.47	0.15	8.56	11.24
307.81	1.06	1.47	0.15	9.43	12.12
307.81	1.06	1.47	0.15	10.34	13.03
307.81	1.06	1.47	0.15	11.28	13.97
307.81	1.06	1.47	0.15	12.00	14.69
307.82	1.09	1.55	0.43	12.00	15.08
307.83	1.12	1.63	0.80	12.00	15.55
307.84	1.15	1.71	1.23	12.00	16.09
307.85	1.18	1.79	1.71	12.00	16.69
307.90	1.34	2.22	4.85	12.00	20.41
307.95	1.50	2.68	8.91	12.00	25.10
308.00	1.67	3.16	13.74	12.00	30.57
308.05	1.85	3.67	20.25	12.00	37.77
308.10	2.03	4.21	26.67	12.00	44.91
308.15	2.21	4.77	33.68	12.00	52.66
308.17	2.29	5.00	36.64	12.00	55.93

For visual representation of this table, a capacity curve is attached, see figure 13.

The gross annual production was calculated to be approximately 466 MWh. The net annual production after the deduction of 1.25% of the gross annual production is therefore 461 MWh. The economic evaluation of the power plant construction is not the subject of the thesis. However, it has been found that since 2012 the purchase price of electricity for small hydropower plants in new locations has been on a downward trend. For 2021, the price was set at 2.85 CZK/MWh. Therefore, the annual revenue from the sale of electricity generated by the small hydroelectric power plant at the Mazourov weir is estimated to amount to CZK 1,300,000.

Table 11 Turbines output

	Q_m ($m^3.s^{-1}$)	Q_{HPP} ($m^3.s^{-1}$)	H_1 (MASL)	H_2 (MASL)	H (m)	P (kW)	G (kWh)
Q364	1.95	0.00	307.76	306.24	1.470	0.0	0.00
Q355	2.65	0.00	307.81	306.29	1.470	0.0	0.00
Q330	3.54	0.00	307.83	306.31	1.470	0.0	0.00
Q300	4.32	0.00	307.85	306.33	1.470	0.0	0.00
Q270	5.08	0.00	307.86	306.36	1.450	0.0	0.00
Q240	6.02	3.33	307.81	306.44	1.320	36.7	13 205.84
Q210	7.07	4.38	307.81	306.46	1.300	47.5	30 312.51
Q180	8.37	5.68	307.81	306.47	1.290	61.1	39 120.01
Q150	10.20	7.51	307.81	306.49	1.270	79.6	50 667.76
Q120	12.90	10.21	307.81	306.52	1.240	105.7	66 690.46
Q90	16.90	12.00	307.91	306.605	1.255	125.7	83 281.29
Q60	22.90	12.00	308.09	306.72	1.320	132.2	92 833.86
Q30	34.70	12.00	308.19	306.95	1.190	119.2	90 490.48
	55.93	12.00	308.17	307.32	0.8	80.1	23 914.48
Q1	121.00	0.00	308.58	308.19	0.340	HPP disconnected	

The estimate of average annual production was calculated as the cumulative sum of kWh for individual m-day flows from Q_{364d} to Q_{30d}. The last two rows of the Table 11 are included only to give an idea of the further development with increasing flow but are not included in the annual production.

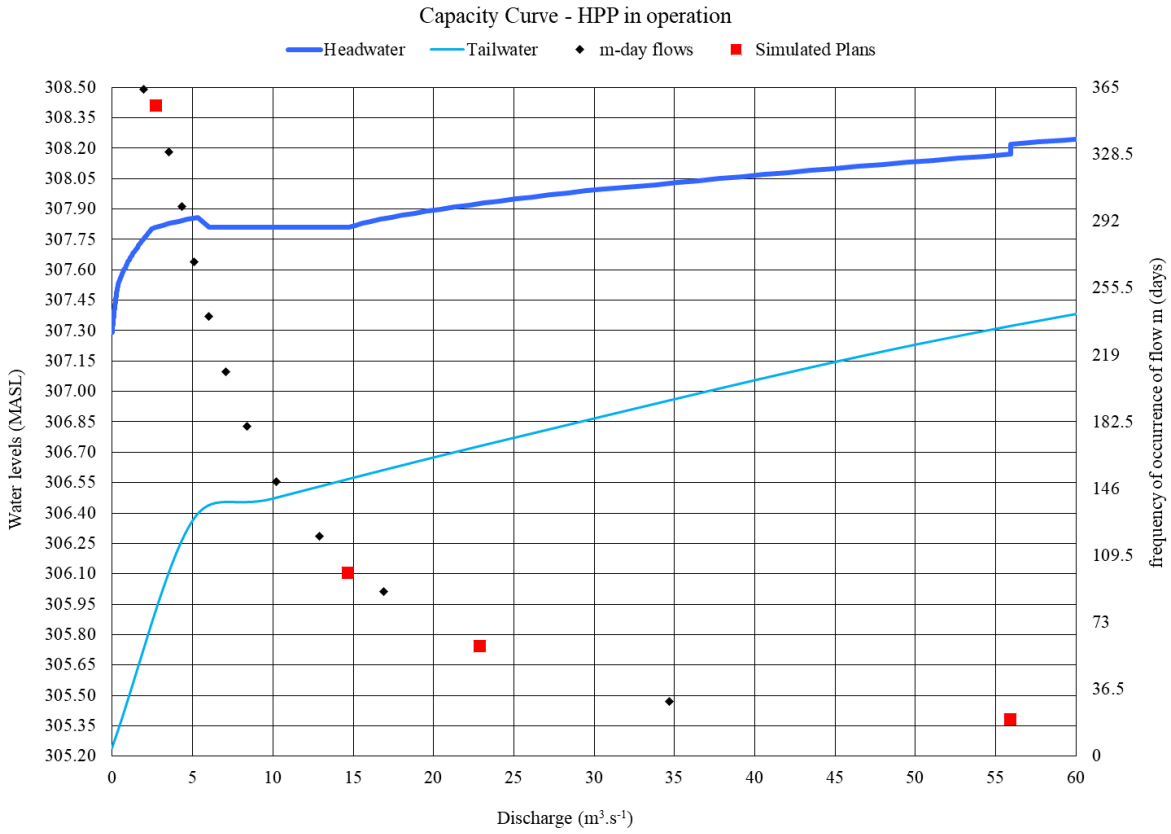

Figure 13 Graph of capacity curve of the weir with HPP in operation

2.5 Creating the Model

2.5.1 Developing a Terrain Model

When creating a terrain model, it is essential to have representative data in the main channel and the overbank areas as well. The data must stand for the ground surface well in locations affected by the water movement. The software HEC-RAS uses DTM data for bare earth ground surface. It is essential to have an adequate number of cross sections that accurately depict the channel and overbank geometry. Another important part of developing a representative model is choosing the right grid-cell size. For overbank areas, it is possible to choose a larger cell size, however, for the main channel, the grid-cell size needs to be small enough to capture more abrupt changes [2].

The digital terrain model from figure 14 was compiled based on 2-point surveys carried out as part of the processing of the technical-operational records from 2000 and the flood risk map from 2013. The points contained 3D information, which enabled the creation of a terrain model in Autocad Civil software, which was subsequently exported to geotif format. Digital Terrain Model of the Czech Republic of the 5th generation (DMR 5G) in S-JTSK, Bpv was used to create a detailed elevation model outside the Sázava River channel. Its accuracy may be limited, especially in the overgrown area, and it cannot be used for the riverbed itself. The channel gauging was carried out in the whole section of station 68.9 - 106.00 km of the Sázava River by tachymetry. The survey outputs include bank lines, bed lines and the connected river axis. The alignment captures all significant changes in channel course. In addition, all significant elevation edges in the channel vicinity that are important from a hydrodynamic perspective were measured.

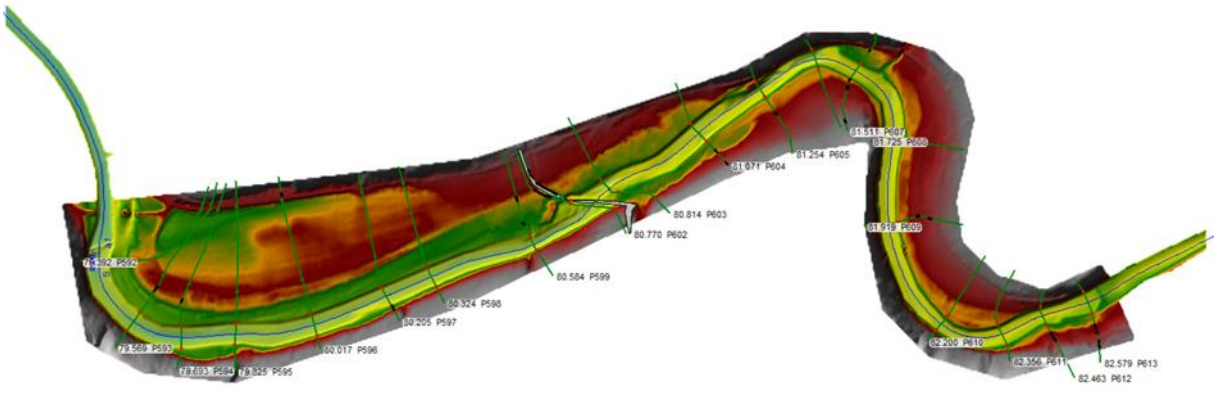

Figure 14 Remote view of the digital terrain model of Sázava river

In the 2D modelling area of interest around the Mazourov weir, which is the subject of the thesis, there are exactly 4 surveyed transverse profiles/sections: P600, P602, P603, P604. All of them are visible in the figure below. In this figure 15, the inline structure P601 of the current Mazourov weir structure is seen between the sections P600 and P602. Individual transversal terrain sections are also shown in the figures below.

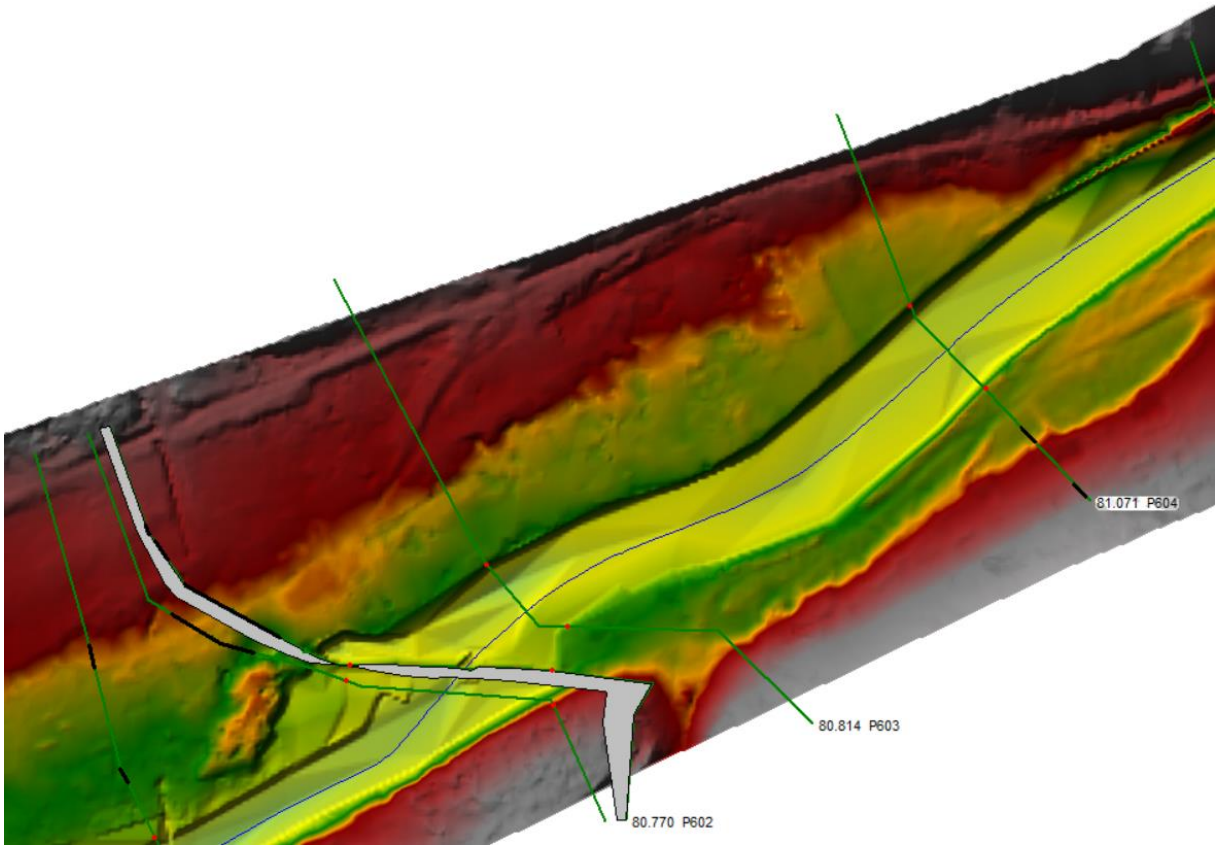

Figure 15 Close up of the modelled area with sections P600, P602, P603 and P604

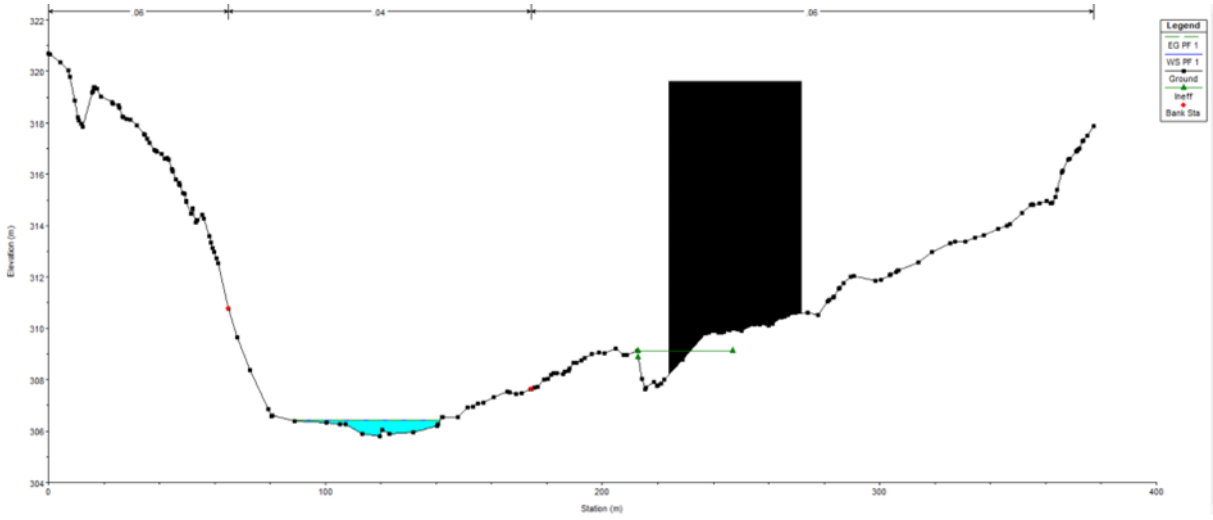

Figure 16 Cross section P600 at river kilometer 80.754

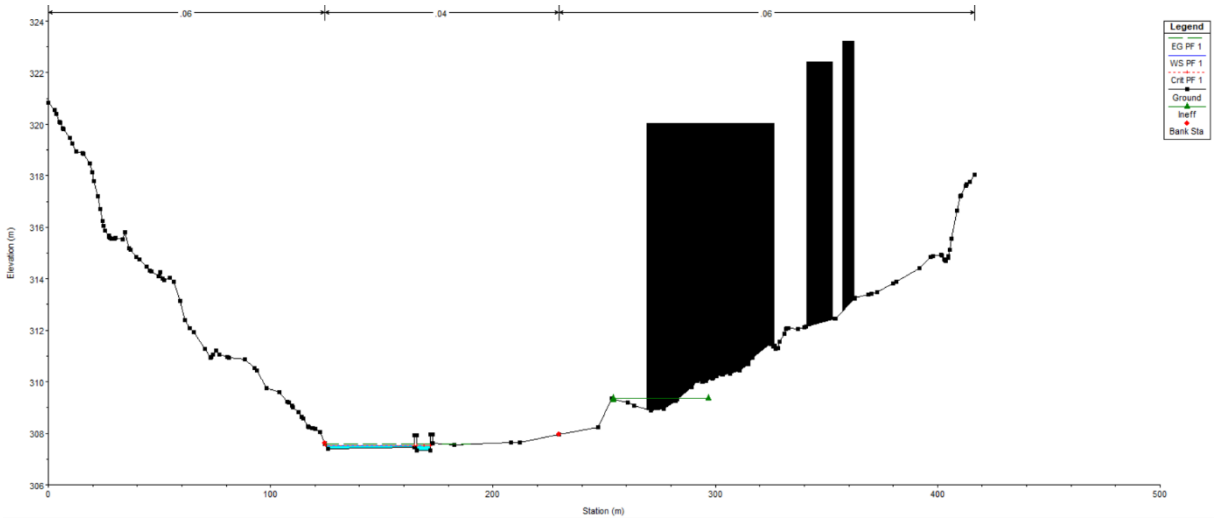

Figure 18 Cross section P602 at river kilometer 80.770

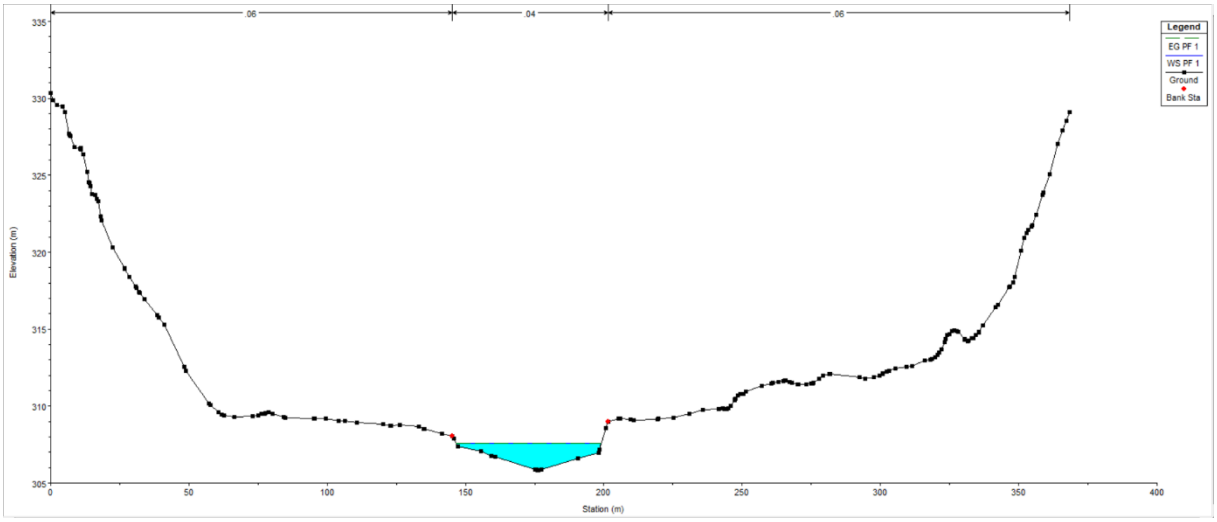

Figure 17 Cross section P603 at river kilometer 80.814

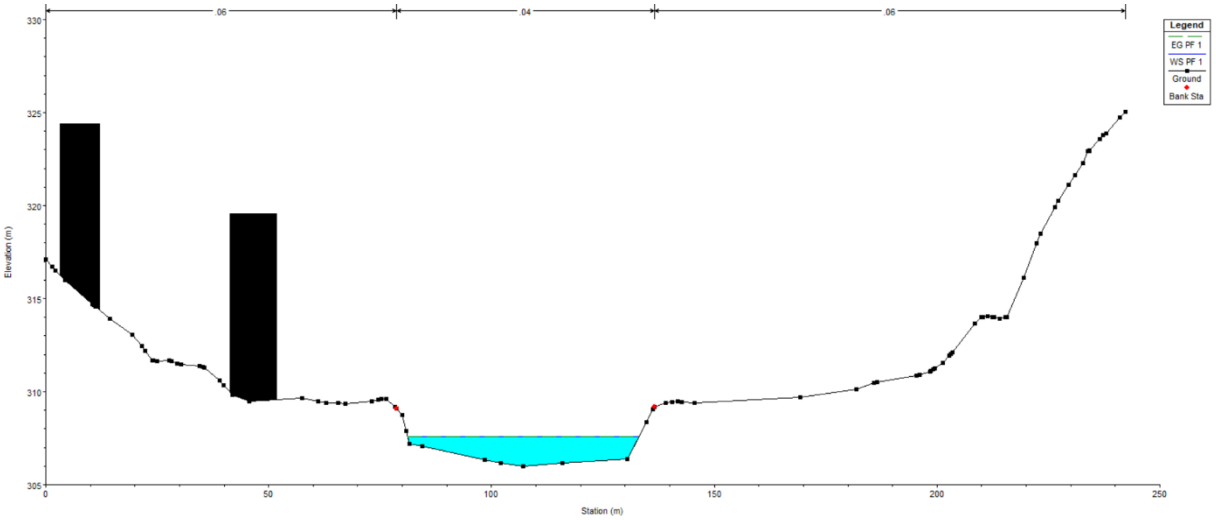

Figure 19 Cross section P604 at river kilometer 81.071

2.5.2 Geometries of the Model

To perform 2D modelling in HEC-RAS, 2D Flow Area must be created. For more accurate results alongside of structures of shorelines, breaklines can be added as well. Before computations, boundary conditions must be assigned to both the upstream and downstream area. The computational area named 2D Flow Area is generally created using a CxD m polygon grid. The size of polygons is chosen according to the required accuracy of the results and to the extent of modelled area. In general, as the size of the computational cell decreases, the result becomes more accurate. At the same time, the computation time increases considerably. Each of the cells has a defined centre at which the flowing water level at a given time is calculated.

For our modelling, four different geometries were created. The geometries differ in size of modelled area, in cell size of the generated mesh and the use of breaklines and their cell spacing. The individual geometries were then used for computational simulations - Plans, which are explained in more detail in chapter 2.6 and table 13.

2.5.2.1 Geometry A

For modelling Plan 1, Plan 2, Plan 3 and Plan 4 of the current state of the weir (Variant A), a considerably detailed 2D Flow Area was created. The geometry is depicted on figure 20. Geometry A was created using a 1x1 m polygon grid. Since the modelled area is not very large, it was possible to create a relatively detailed mesh.

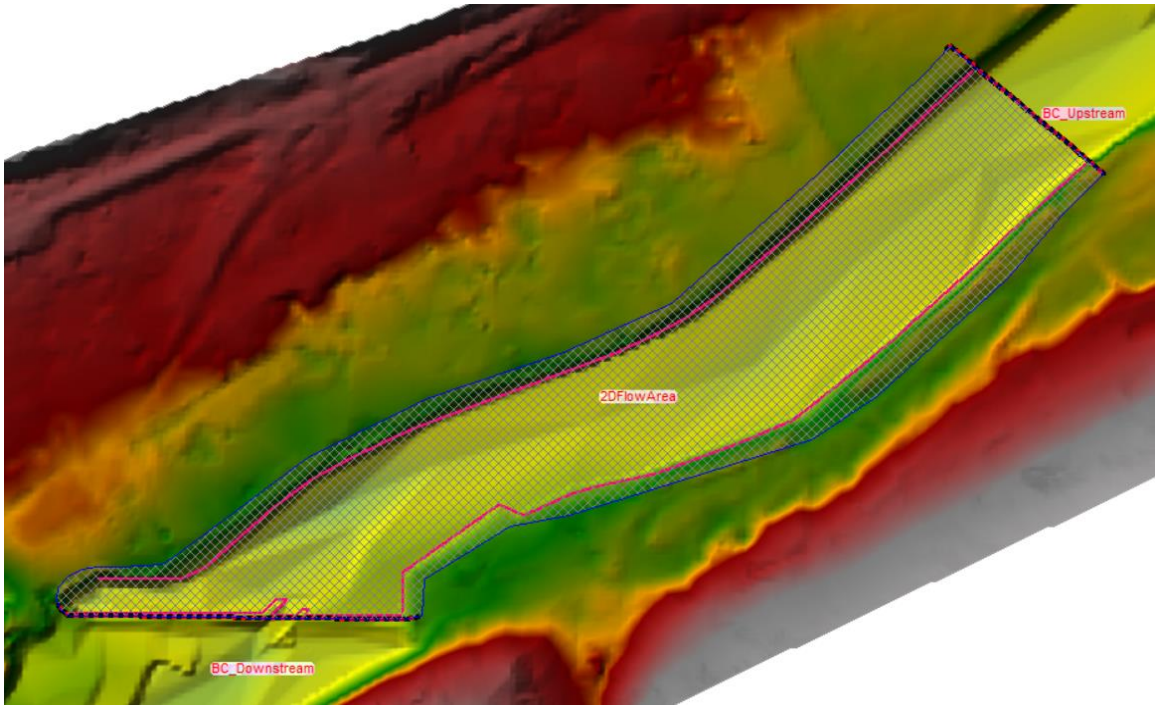

Figure 20 Geometry A: 2D flow area with mesh, breaklines and boundary conditions

To ensure accurate results in the weir area, exactly three separate breaklines were inserted into the 2D Flow Area. First breakline is situated near the weir structure, making the results at the end of the flow area more detailed with spacing ranging from 0.1 m to 0.5 m. The second and the third breaklines were both put close to the riverbanks with spacing of the cells from 0.3 m to 1.0 m. For further calculations and simulations, a mesh was created inside the 2D Flow Area using 32 523 cells from computation points and enforced breaklines with average cell size being 0.70 m^2. The maximum cell size was computed to be 2.20 m^2 and the minimum cell size estimated to be 0.01 m^2. The created 2D flow area with generated mesh, breaklines and boundary conditions can be seen for clear visual representation in figure 20, while in figure 21, the enforced cell spacing of breaklines is depicted.

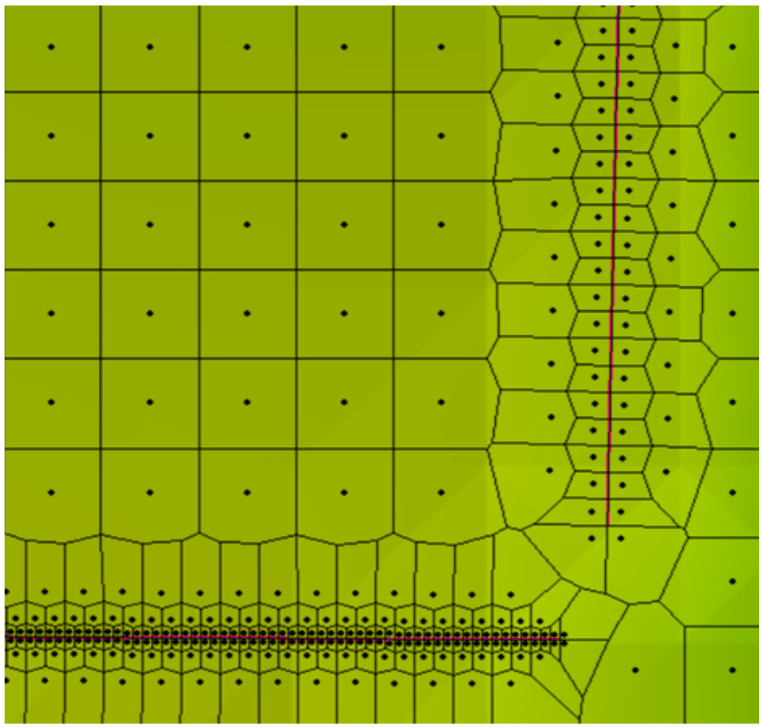

Figure 21 Geometry A: cell spacing of breaklines

2.5.2.2 Geometry B

A new geometry B was created to model the control one-year flow Q_1, which includes a larger 2D flow area. This geometry was created to monitor how far the water would spill at such a large flow rate. Since the flow area is large, the polygons of the computational grid were increased to 4x4 m. Increasing the cell size of the computational grid results in a decrease in computational accuracy. However, since this is a high flow rate, which neglects the power plant function, it is possible to do it. At the same time, by increasing the size of the polygons, a reduction in computation time is achieved. The mesh contains 4 916 cells from computation points and enforced breaklines with average cell size

being 9.70 m^2. The maximum cell size was computed to be 29.72 m^2 and the minimum cell size estimated to be 0.19 m^2.

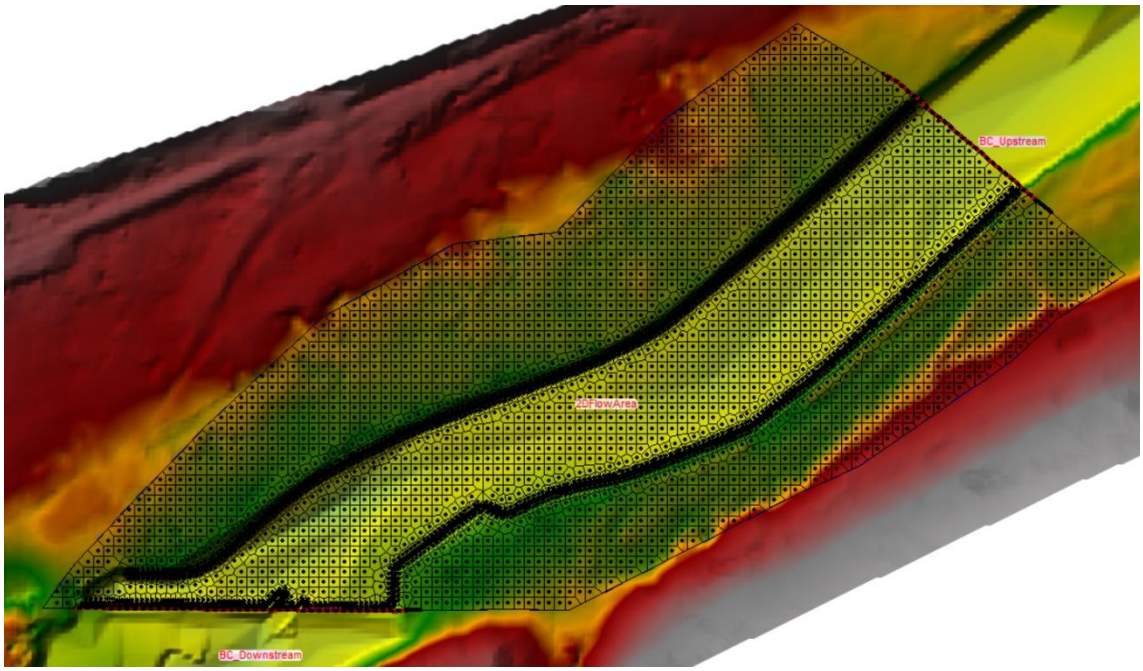

Figure 22 Geometry B: 2D flow area, mesh, breaklines and boundary conditions

Geometry B in figure 22 contains breaklines as well as geometry A alongside of both riverbanks and the weir structure. In the case of geometry B, the spacing of breakline cells ranges from 1 to 2 m for weir breakline and 1 to 4 m for both riverbanks.

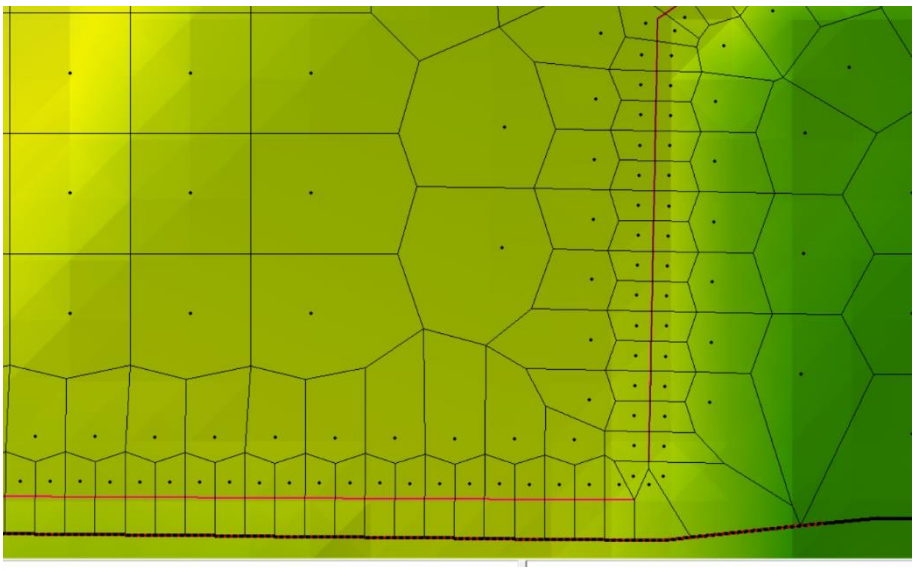

Figure 23 Geometry B: enforced breaklines with spacing

2.5.2.3 Geometry C

Geometry C, seen in figure 24, was created for the new design that consists of fish passage, sports sluice, and small hydropower plant (Variant B). The geometry C was used for simulating river flow for Plan 1, Plan 2, Plan 3 and Plan 4. A detailed flow area was created using a mesh with grid cell size spacing 1x1m. Mesh of the 2D flow area contains 30 566 cells as computation points. The maximum cell size is 2.22 m^2, minimum cell size 0.01 m^2 and the average cell size 0.72 m^2. To ensure accurate results in the weir area, four separate breaklines were inserted: close to weir structure, right and left riverbank and entrance to the inlet channel of the small HPP. Minimum breakline spacing for the weir structure is 0.2 m, while the maximum spacing is 1 m. For both riverbanks, minimum breakline spacing is 0.25 m, maximum spacing 0.75 m and lastly, minimum breakline spacing for the inlet channel is 0.2 m, while the maximum spacing is 1 m.

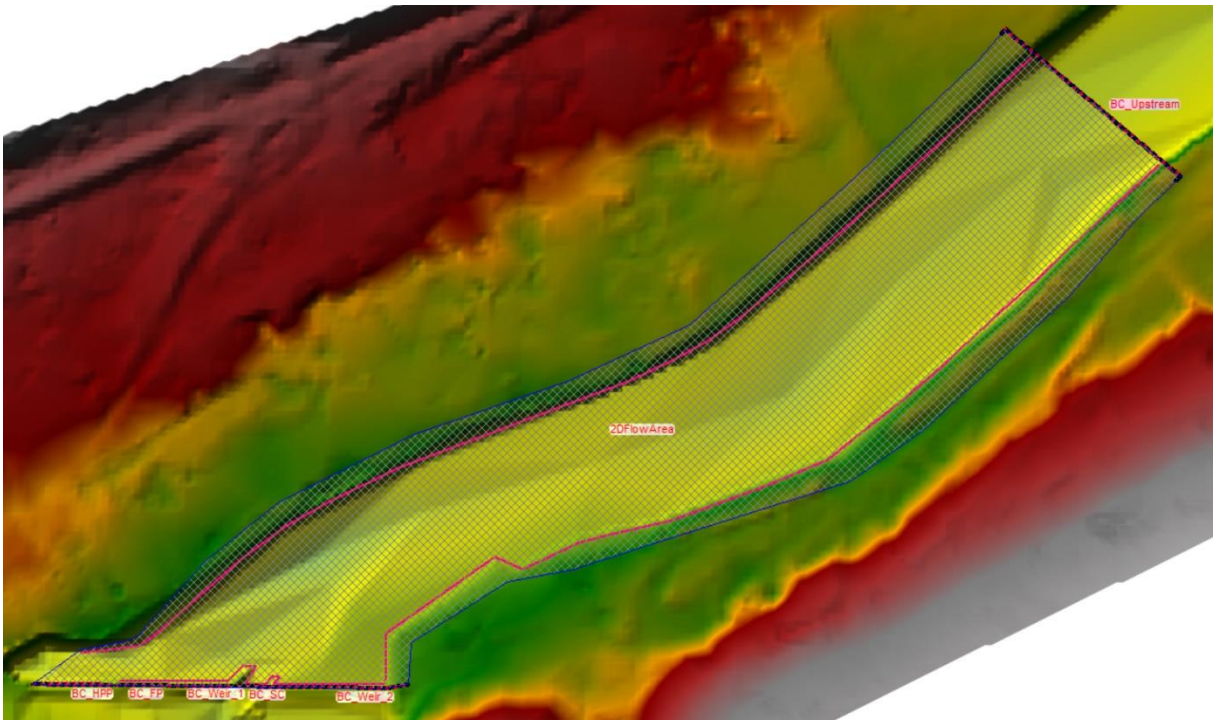

Figure 24 Geometry C: 2D flow area, mesh, breaklines and boundary condition lines

2.5.2.4 Geometry D

Geometry D was created solely for Variant B (weir crest at 307.80 MASL) and Plan 5 (Q_1). Created 2D flow area consists of 5 062 computation points creating mesh of grid cell size spacing 4x4m. The maximum cell size is 31.16 m^2, minimum cell size 0.09 m^2 and the average cell size 9.54 m^2. Geometry C contains breaklines as well as the rest of geometries used. There are breaklines alongside of both riverbanks, the weir structure and at the inlet channel of HPP. In the case of geometry C seen in figure 25, the spacing of breakline cells ranges from 0.5 to 3 m for weir and HPP breakline and from 1 to 4 m for both riverbanks.

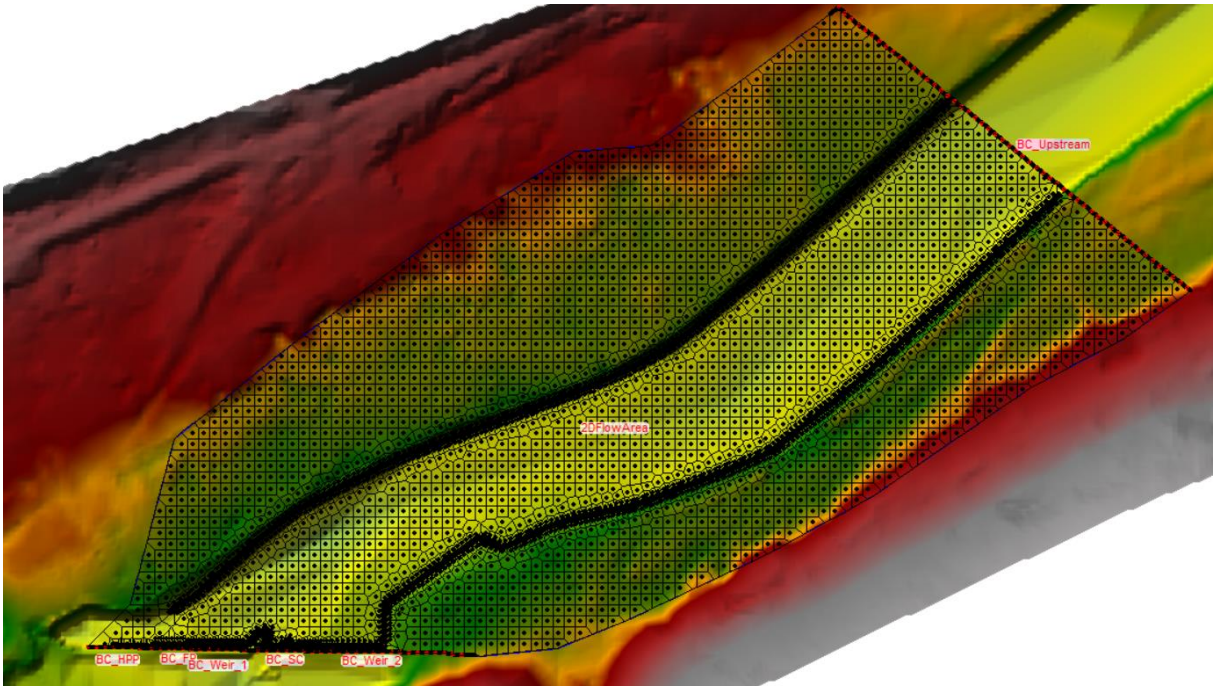

Figure 25 Geometry D

2.5.3 Surface Characterisation

The surface in a hydraulic model is typically described by its roughness. Thus, roughness coefficients are one of the main variables used in calibrating a hydraulic model. Generally, for a free flowing river, roughness decreases with increased stage and flow. However, if the banks of a river are rougher than the channel bottom (due to trees and brush), then the composite n value will increase with increased stage. Specifically, in 2D modelling, Manning's n values are spatially varying within 2D Flow Areas, which produces more accurate results of river flows.

The influence of diverse types of terrain surfaces on the flowing water was expressed by the roughness coefficient value given in the table:

Table 12 Manning's n values of Terrain

Left Overbank (LOB)	Channel	Right Overbank (ROB)
0.06	0.04	0.06

2.6 Boundary Conditions

HEC-RAS has a wide range of boundary and initial conditions that can be applied to a model. Boundary conditions consist of external boundary conditions along the perimeter of the 2D area, internal boundary conditions, and global boundary conditions (Meteorological Data) that are applied to the entire model (i.e., precipitation, wind, etc.). By defining the boundary conditions, it is determined where water flows into the model and out again. In the case of the upstream boundary condition, the magnitude of the modelled flow is defined. In the case of the downstream boundary condition, the water level that the flow reaches is defined for the area where the water flows out of the model [2].

The following boundary conditions were used in the model:

- flow hydrograph,
- rating (capacity) curve.

The rating curve was only used for areas where the flow leaves the 2D region, whereas the flow and level conditions were applied to both entering and leaving the area. The flow condition was positive for flow entering the area and on contrary negative for leaving the area.

The upstream boundary condition for all simulations was a constant flow hydrograph, but the value of flow varied in each plan. The first modelling variant was devoted to the minimum residual flow (2.65 $m^3.s^{-1}$). The second variant simulated a flow of approximately Q_{100d} (14.69 $m^3.s^{-1}$), which corresponds to a maximum powerplant intake flow (12 $m^3.s^{-1}$) and MRF in the rest of the river profile (2.65 $m^3.s^{-1}$). The third plan simulated a flow of Q_{60d} (22.90 $m^3.s^{-1}$), the fourth plan modelled the maximum flow at which the plant is still operating (55.93 $m^3.s^{-1}$) and the last modelling variant was the control flow Q_1 (121 $m^3.s^{-1}$). The plans and their assigned flow rates are clearly stated in table 13.

Table 13 Modelled plans with their simulated flow rates

Plan number	Simulated flow	Flow rate ($m^3.s^{-1}$)
Plan 1	Q_{355d} (MRF)	2.65
Plan 2	Q_{100d}	14.69
Plan 3	Q_{60d}	22.90
Plan 4	Q_{20d}	55.93
Plan 5	Q_1	121.00

Plans 2, 3 and 4 study the river flow with the small HPP in operation, while Plans 1 and 5 do not consider the small HPP working.

The downstream boundary conditions were defined by capacity curves and flow hydrographs. For Variant A, only one downstream boundary was used. For variant B, there were 3 different capacity curves and one flow hydrograph applied.

For Variant A, the downstream boundary condition applied was the capacity curve of Mazourov weir. The data used for this curve was provided by Povodí Vltavy, State Enterprise. The Q-H curve corresponds to current state of the weir. The level of current weir crest can be found between 307.40 and 307.94 MASL.

For Variant B, four individual capacity curves were applied as a downstream boundary condition. Therefore, the downstream boundary condition consists of four sub-conditions. The boundary condition of the weir itself is formed by the capacity curve of the reconstructed weir with crest level at 307.80 MASL. The downstream boundary condition of the fish passage is formed by the capacity curve of the same body and the downstream boundary condition of the sports spillway is the capacity curve of the spillway. Lastly, the boundary condition of the powerhouse intake channel is formed by the constant flow hydrograph. Since the flow is leaving the 2D Flow Area at the boundary, the flow condition was negative.

3 RESULTS

To get an accurate understanding of how the proposed reconstruction of the weir structure and the construction of a small hydroelectric power plant, a fish passage and a sports sluice will affect the river flow, hydraulic models in the software HEC-RAS were created. Firstly, a model for the current situation was created. Subsequently, a model for the updated weir condition was created and the river flow for this case was simulated.

3.1 Variant A

The chapter deals with 2D modelling of the current situation, i.e. with the current unrepaired weir and with hydrology data provided by Povodí Vltavy, State Enterprise. The current unrepaired weir crest is between 307.40 and 307.94 MASL.

Five calculation plans were created in HEC-RAS. The plans differ by boundary conditions. The downstream boundary condition is the same for all four plans and it consists of the capacity curve of the Mazourov weir. Upstream boundary conditions is a constant flow hydrograph. The discharge applied as the upstream boundary condition determines the river flow.

3.1.1 Plan 1

Plan 1 responds to a minimum residual flow (Q_{355d}) of 2.56 $m^3.s^{-1}$. At the minimum residual flow in the river, the small hydropower plant is out of operation, 1.06 $m^3.s^{-1}$ flows through the fish passage, 1.47 $m^3.s^{-1}$ flows through the sports sluice and 1 cm of water corresponding to 0.15 $m^3.s^{-1}$ flows over the weir edge.

The results of the depth, streamlines and velocity field in 2D flow area can be seen below. From HEC-RAS simulations for this Plan 1, it was calculated that the model's maximum depth is 2.56 m and the velocity reaches maximum of 0.23 $m.s^{-1}$.

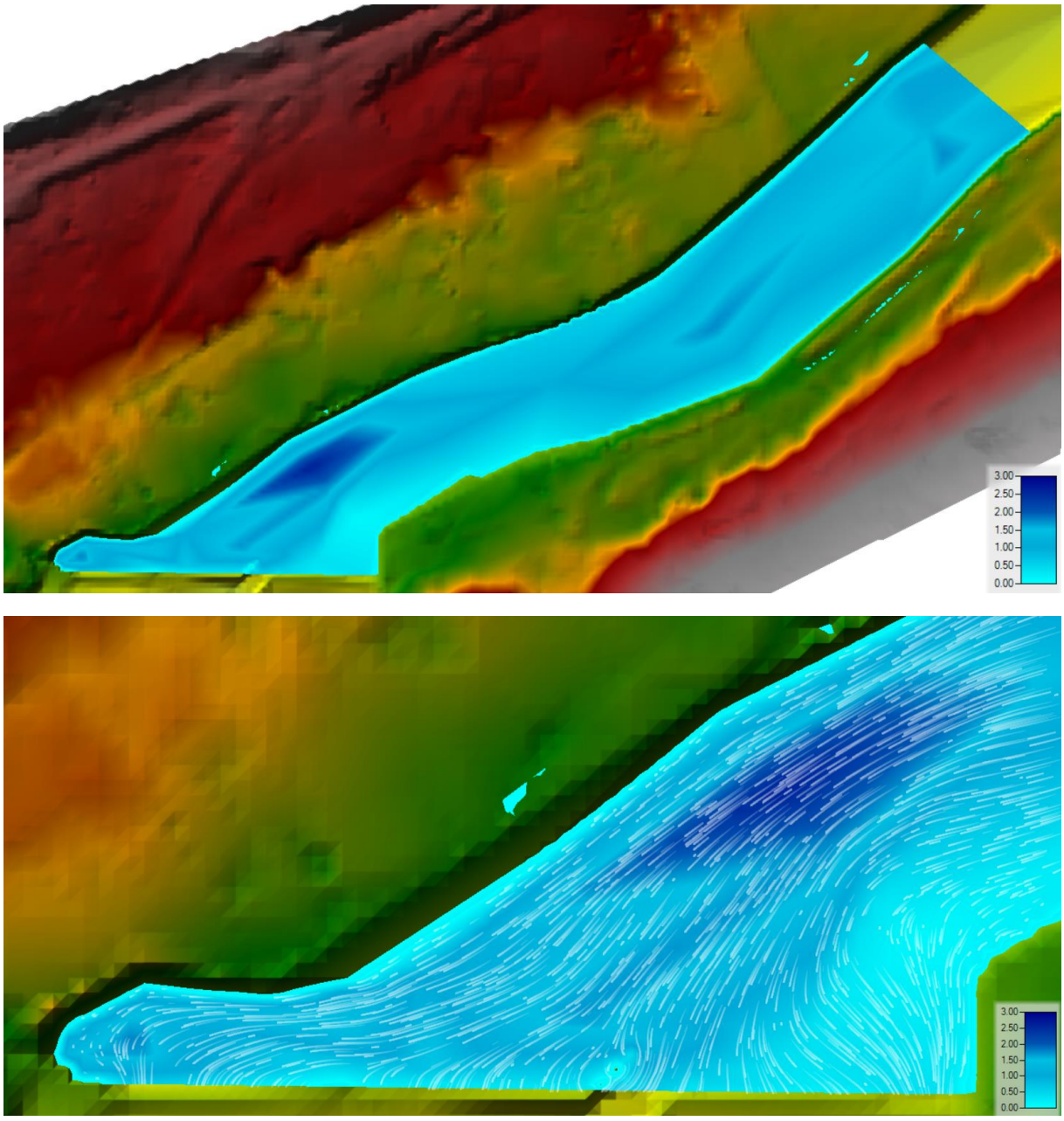

Figure 26 Variant A - Plan 1 – depth and streamlines

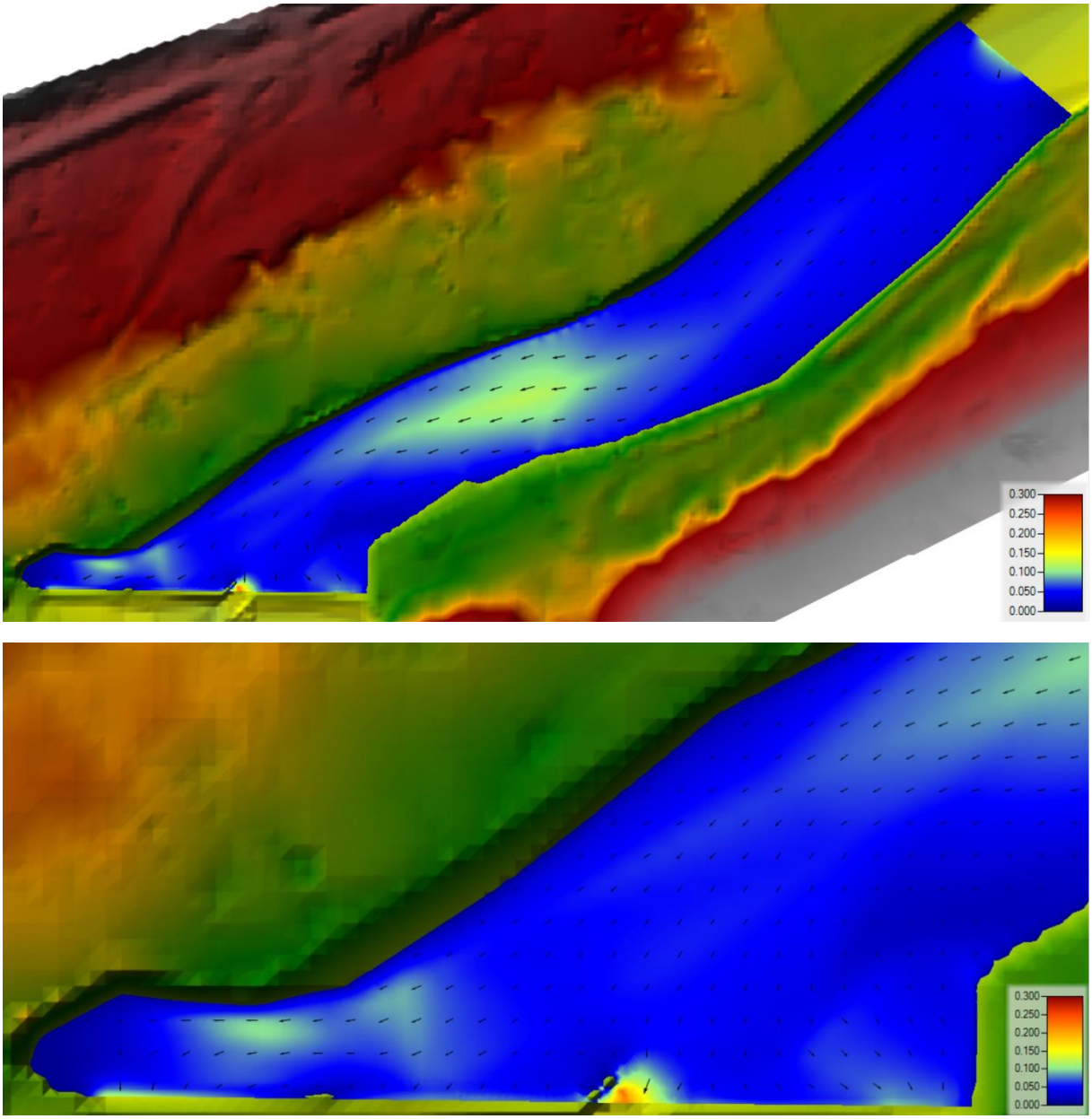

Figure 27 Variant A - Plan 1 - velocity field

3.1.2 Plan 2

The second calculation plan represents the condition at which the flow is exactly 14.69 $m^3.s^{-1}$. This means that a constant flow hydrograph of value 14.69 was used as the upstream boundary condition. Simulated flow of 14.69 $m^3.s^{-1}$ corresponds to approximately Q_{105d}. To simulate this flow is very useful especially for Variant B.

Within the 2D flow area, the maximum depth in the pool area was found to be 2.77 metres. The maximum velocity was determined to be 0.58 $m.s^{-1}$.

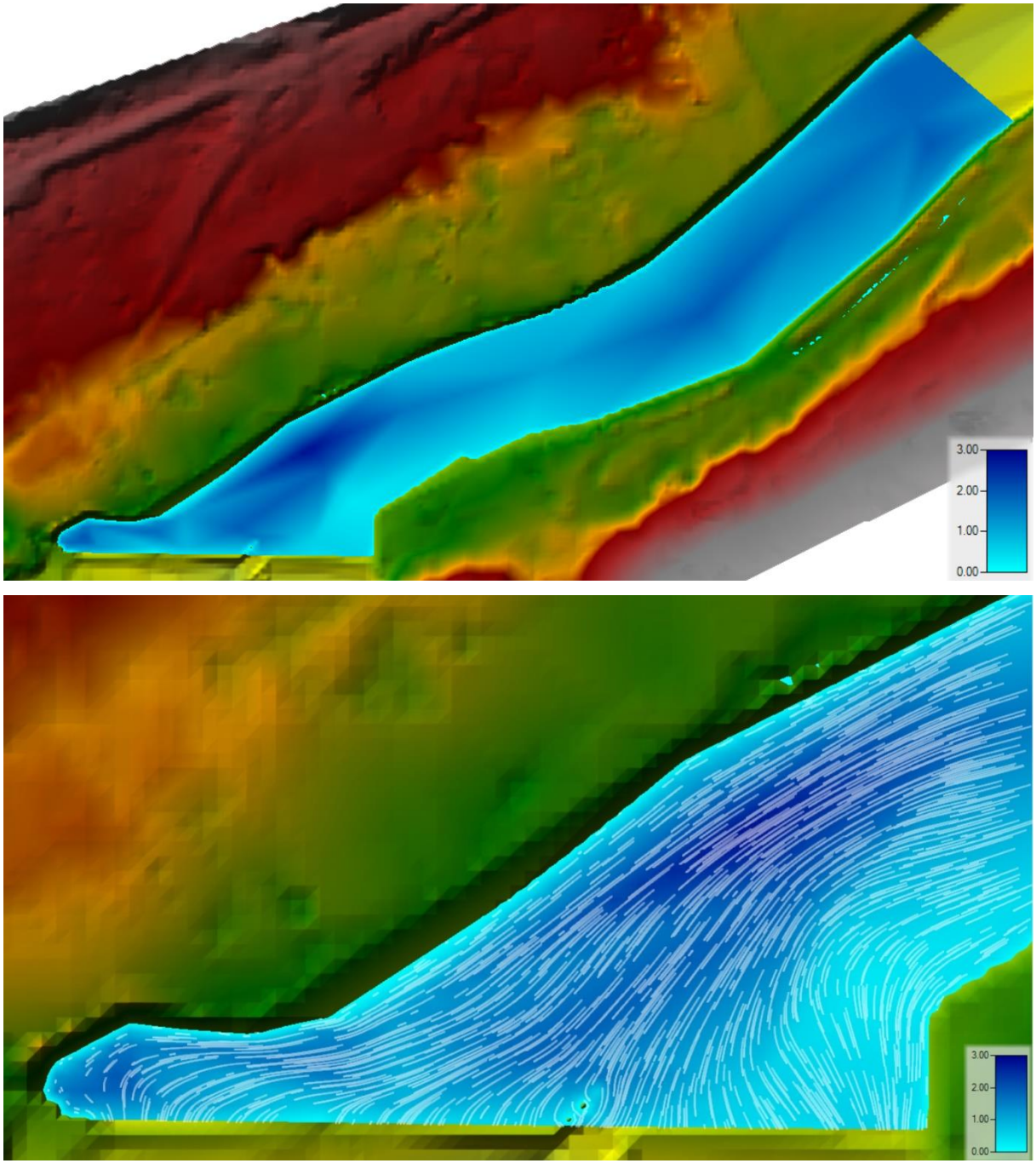

Figure 28 Variant A - Plan 2 - depth and streamlines

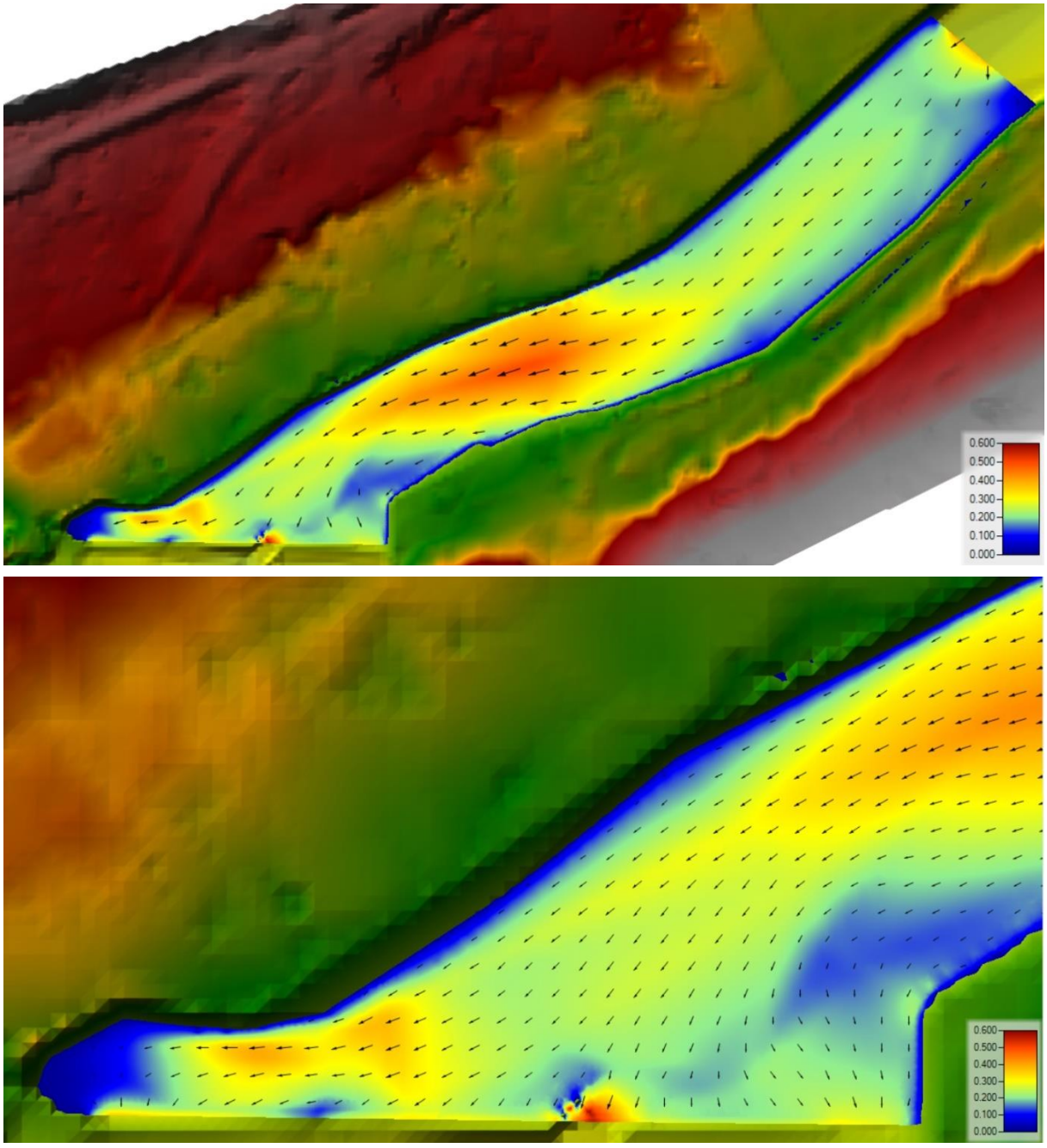

Figure 29 Variant A - Plan 2 - velocity field

3.1.3 Plan 3

Plan 3 depicts a case of 22.90 $m^3.s^{-1}$ corresponding to Q_{60}. The reasoning behind this specific river flow is the fact that for this flow, the hydropower plant is the most efficient. While Q_{60} flows in the riverbed, the HPP's turbines work with the highest gradient of 1.32 m and also use their maximum capacity. Maximum capacity of the turbines is set to be 12 $m^3.s^{-1}$. Excess flow above the maximum capacity of the turbines flows to the remaining weir structures (fish passage, sports sluice and as a weir overflow).

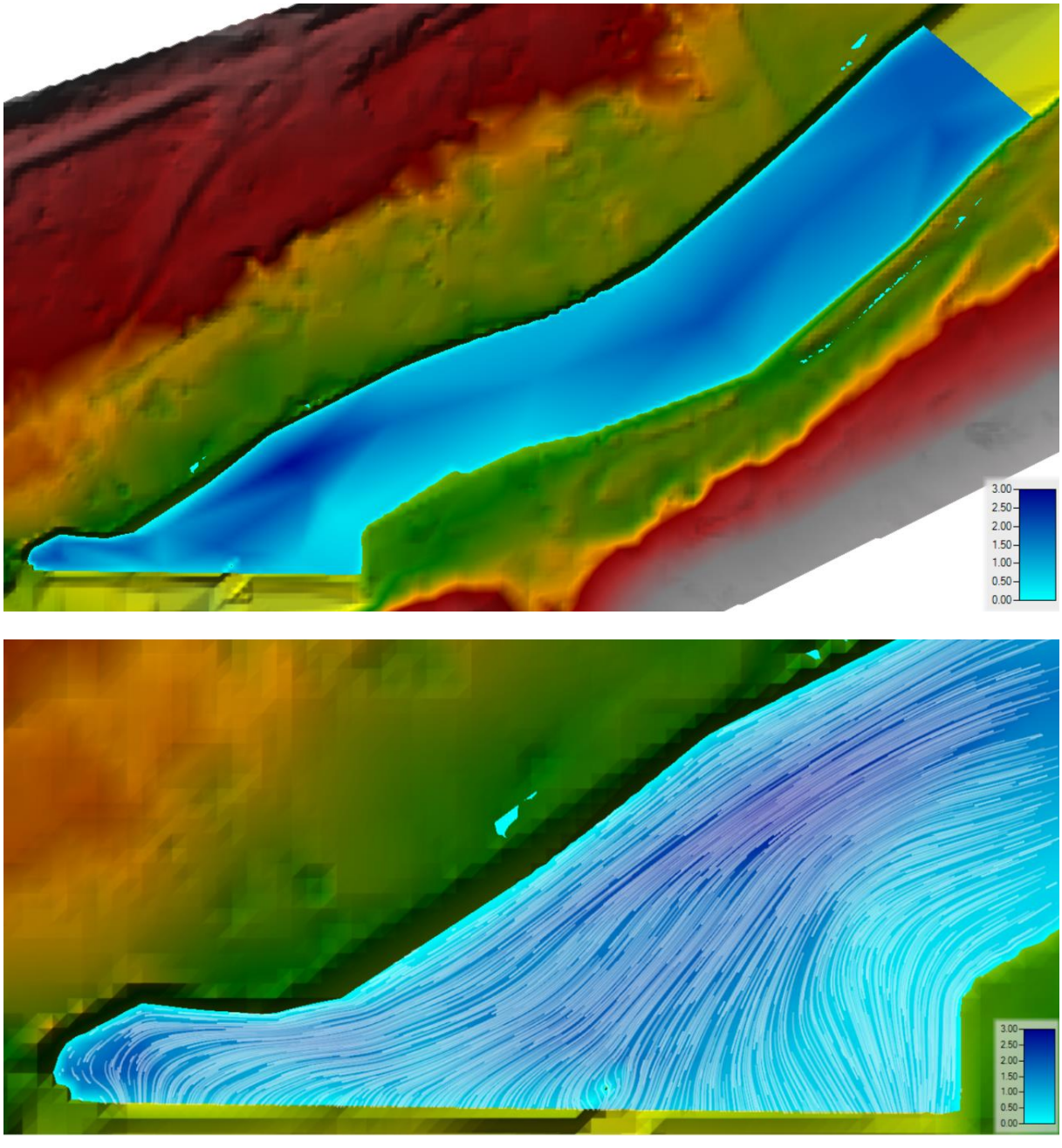

Figure 30 Variant A - Plan 3 – depth and streamlines

The results of depth, streamlines and velocity field can be seen at figure 30 above and figure 31 below. In this case, the maximum depth is 2.86 m while the maximum velocity is 0,68 $m.s^{-1}$.

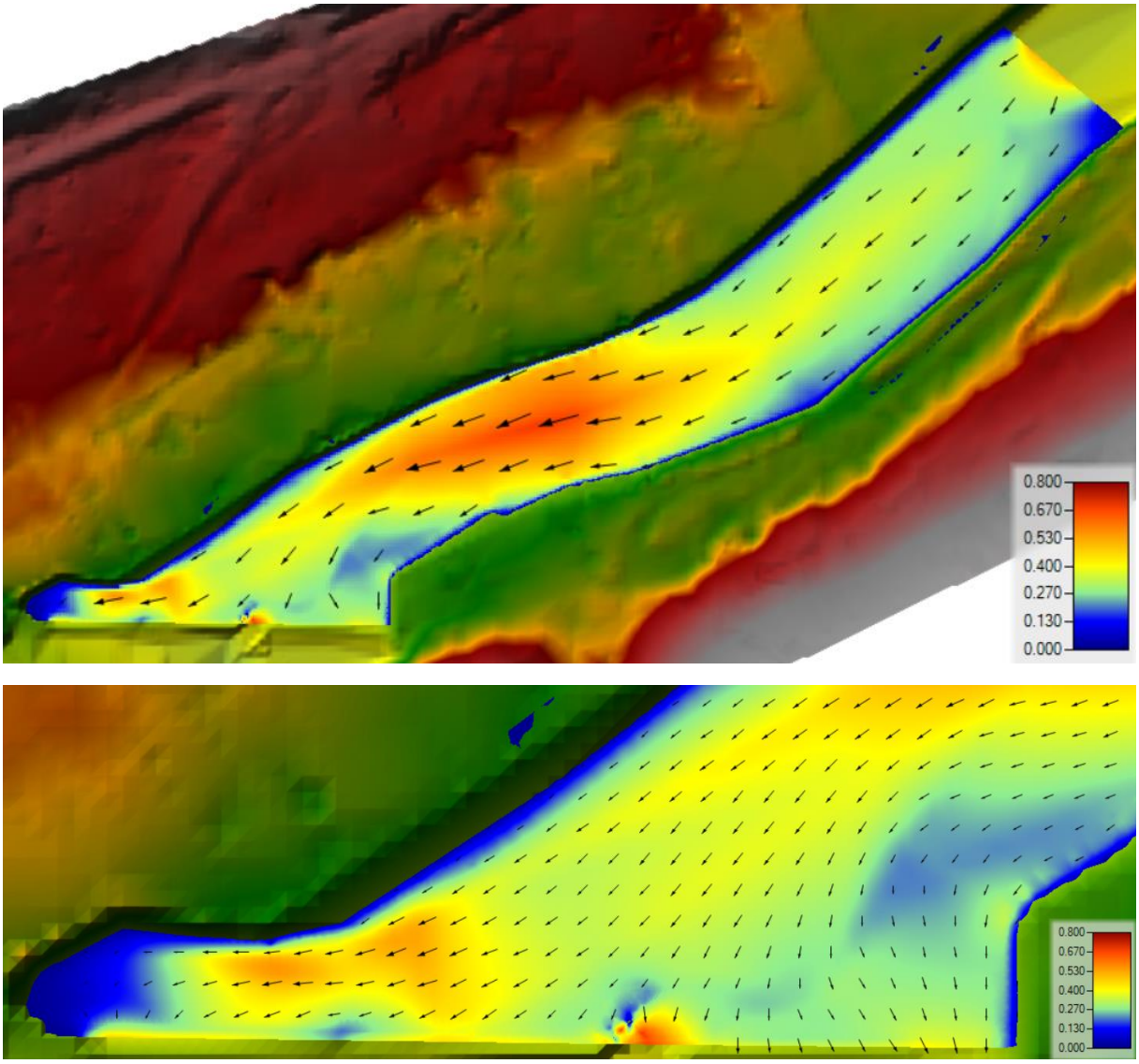

Figure 31 Variant A – Plan 3 - velocity field

3.1.4 Plan 4

The fourth calculated plan depicts a case of 55.93 $m^3.s^{-1}$. It's the maximum flow when the HPP is still in operating mode. Any bigger flow than 55.93 $m^3.s^{-1}$ creates a smaller gradient than 80 cm. If the gradient is lower than 80 cm, the turbines stop working.

Maximum depth for this plan reaches up to 3.10 m while the maximum velocity is 1.25 $m.s^{-1}$.

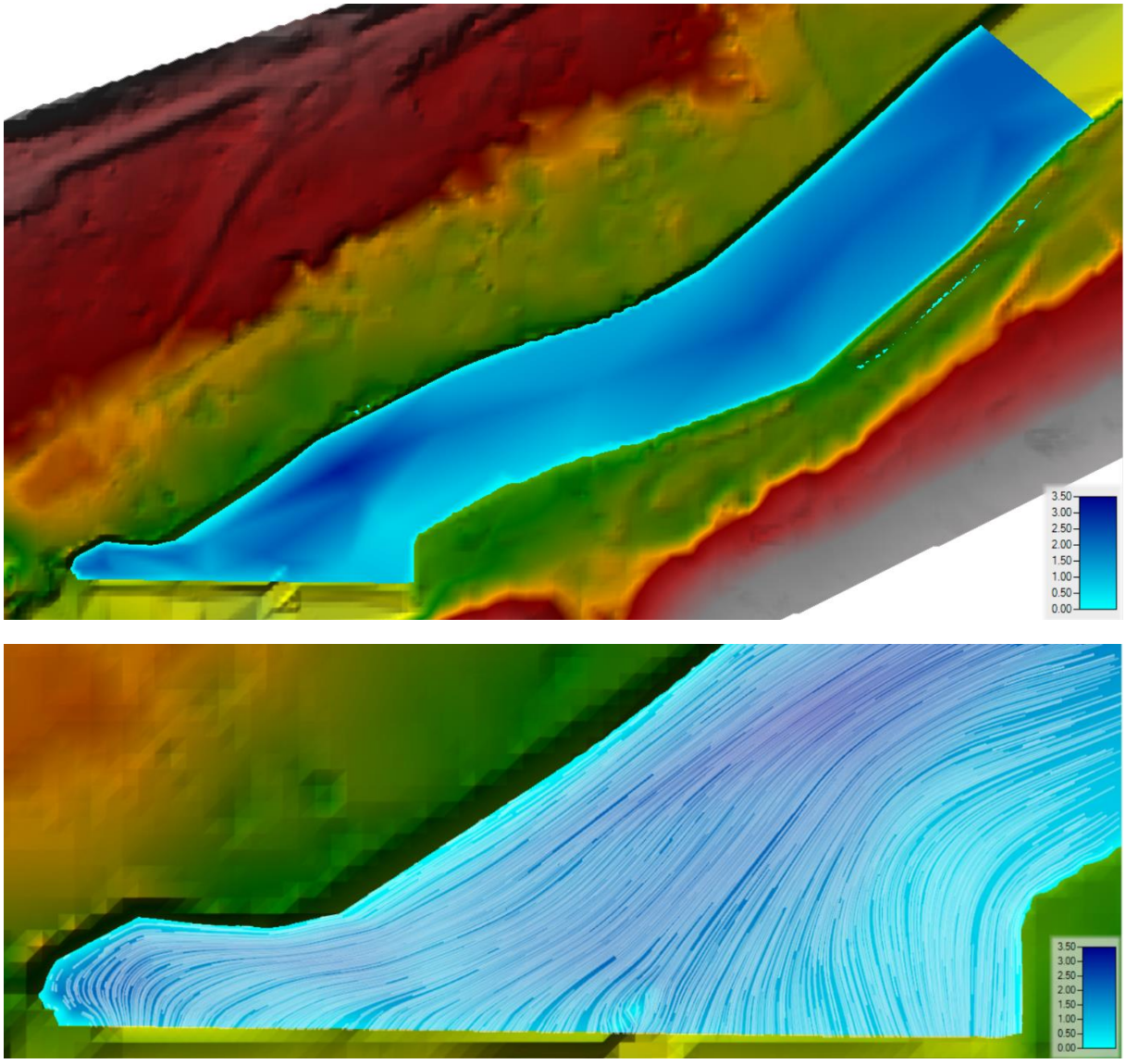

Figure 32 Variant A - Plan 4 – depth and streamlines

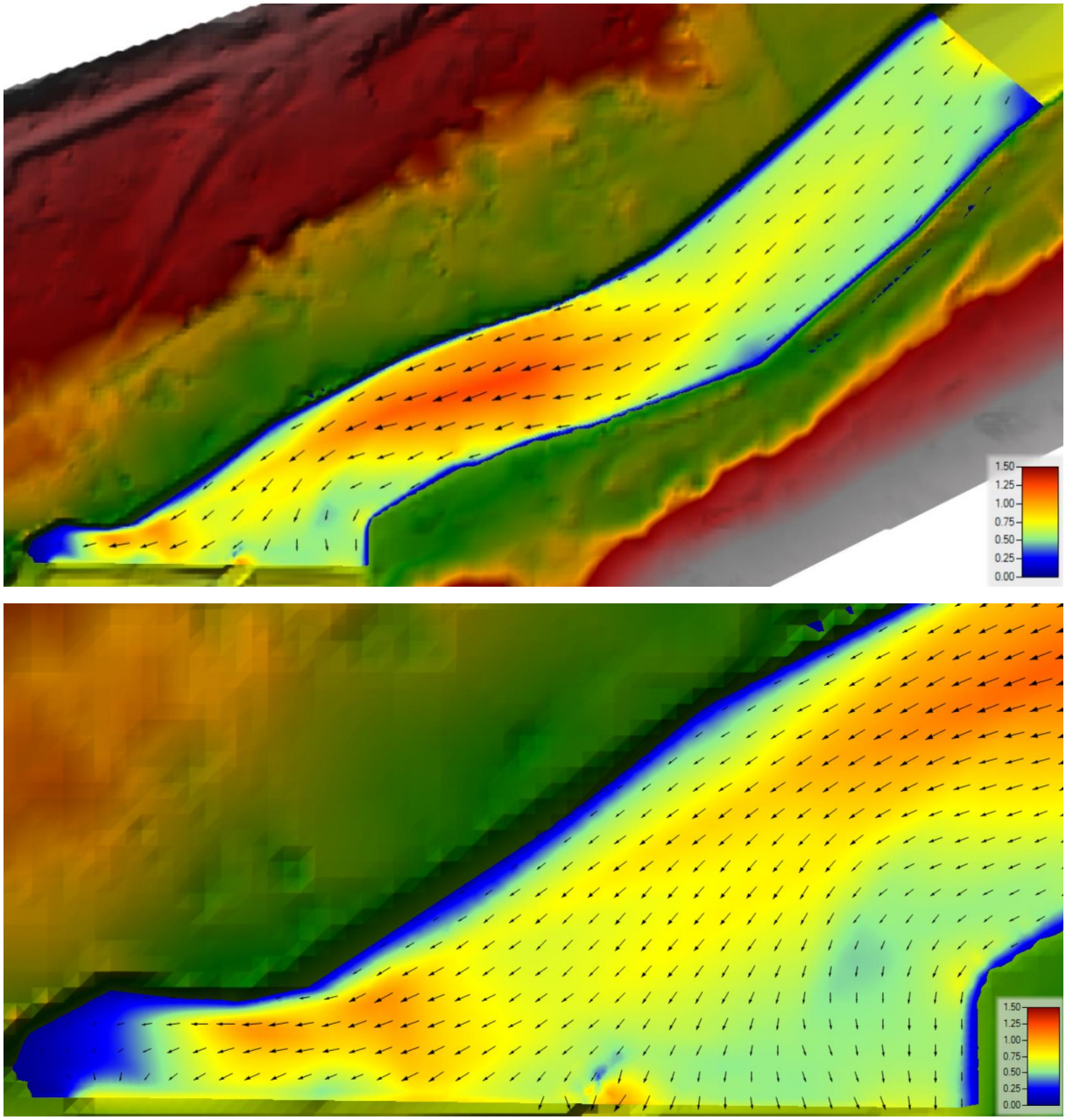

Figure 33 Variant A - Plan 4 - velocity field

3.1.5 Plan 5

Plan 5 was created purely to give an idea of where the water would spill during the control one year flow. At this flow rate, tailwater influence is included in the overflow calculation. The difference between the outputs modelled by the current condition and the new condition is not expected to be very significant.

For this plan, a new larger geometry (2D flow area) was created that was able to accommodate and visually display the spill of the simulated flow. For calculation purposes, the mesh was modified, and its grid cell size was enlarged. The cell size for Plans 1, 2 and 3 and 4 was 1x1m, the geometry

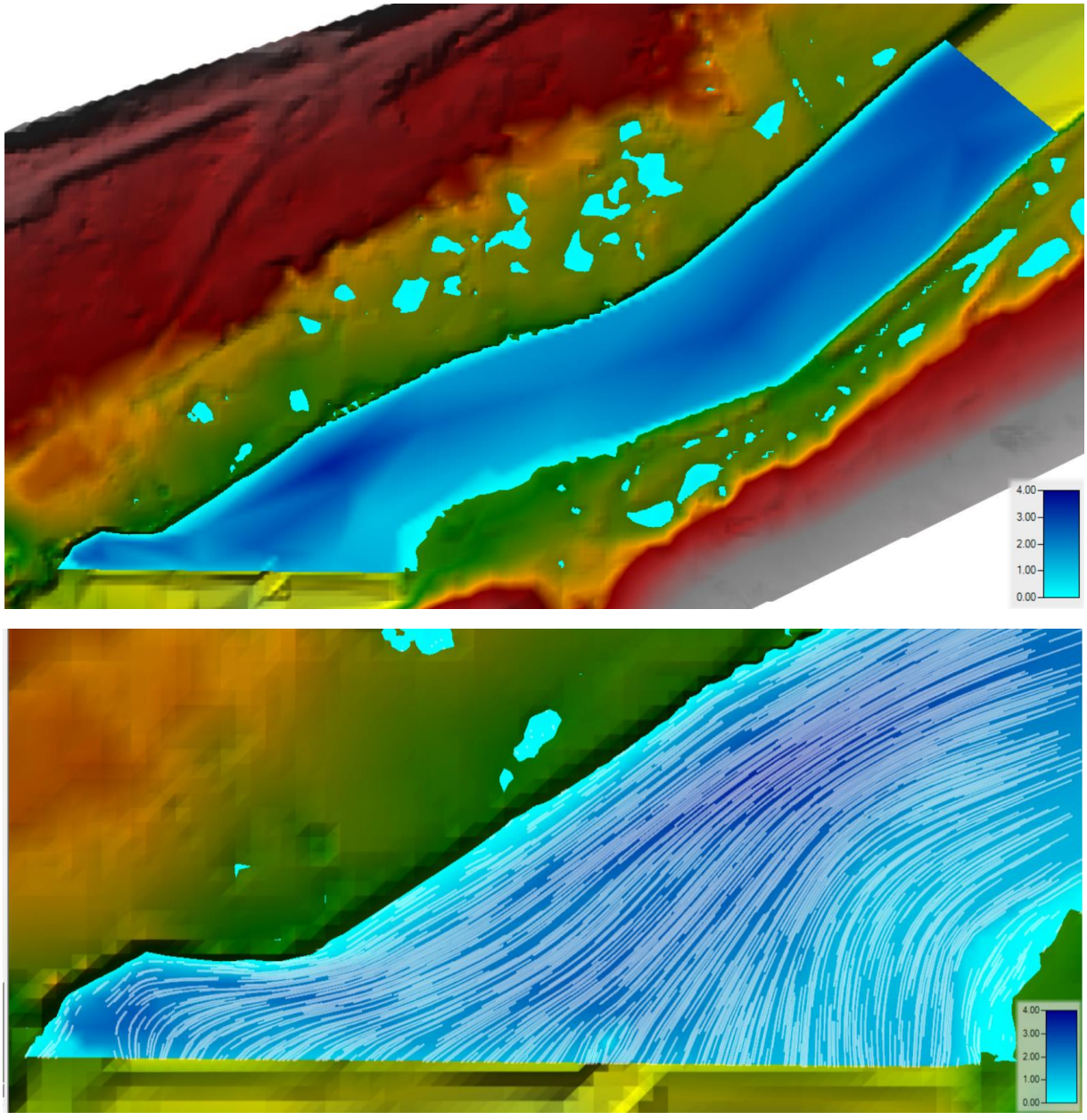

Figure 34 Variant A - Plan 5 – depth and streamlines

of this plan contains a 4x4m cell grid. Since the generated mesh is not very detailed, this calculation plan may contain minor flaws.

Maximum depth reaches up to 3.48 m while the maximum velocity is 1.85 $m.s^{-1}$. HEC-RAS imagery in figure 34 shows off-channel spill on both banks. In reality, these flooded areas are terrain depressions. Flooding will only occur if surface water enters them. As there is no spillage from the Sázava River channel at Q_1 flow, no flooding of these depressions will occur.

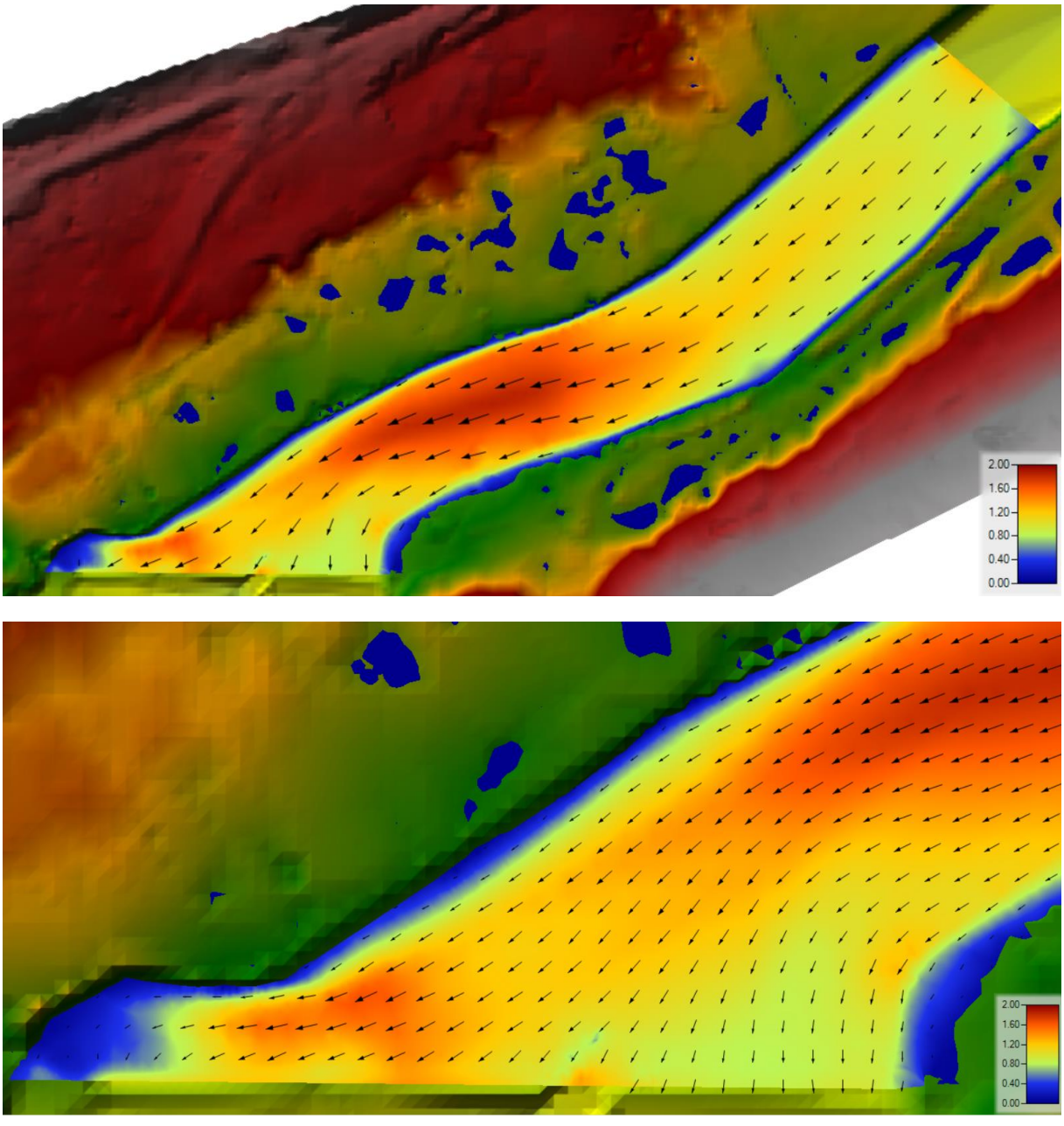

Figure 35 Variant A - Plan 5 - velocity field

3.2 Variant B

Variant B includes the proposed reconstruction of the weir. In this case, reconstruction of the weir means increasing the weir crest to 307.80 MASL, building a small hydropower plant with adjacent fish passage, and building new and safe sports sluice.

To model the new situation, a more detailed 2D flow areas was created – Geometry C and D. Both 2D flow areas contains a total of 4 breaklines that refine the computational mesh created in the area of the right and left banks of the river, near the crest of the weir and at the entrance to the inflow channel of the small hydropower plant.

All plans use a simulation window of 24 hours and computation interval 5 minutes. Mapping output interval as well as hydrograph output interval and detailed output interval is exactly 1 hour. The time step is controlled by courant conditions. Courant conditions are generally concerned with model stability. To have stable outputs, the maximum courant is chosen to be 1, the minimum courant 0.4 and the rest of the parameters connected to advanced time step control and the adjustment of time step based on courant specifically equals 4.

General information about boundary conditions is described in the chapter 2.6. Upstream boundary condition used in all plans (1-5) was constant flow hydrograph, specific performed flows are clearly stated in table 13.

3.2.1 Plan 1

Plan 1 operates with a minimum residual flow (Q_{355d}). The flow rate of 2.65 $m^3.s^{-1}$ is so small that it is used entirely only by the fish passage, the sports sluice and for the weir overflow. Hence, the small hydropower function is not included in Plan 1. The specified constant value in the flow hydrograph which forms downstream boundary condition is thus equal to 0 $m^3.s^{-1}$.

Maximum depth reaches up to 2.74 m while the maximum velocity is 0.5 $m.s^{-1}$.

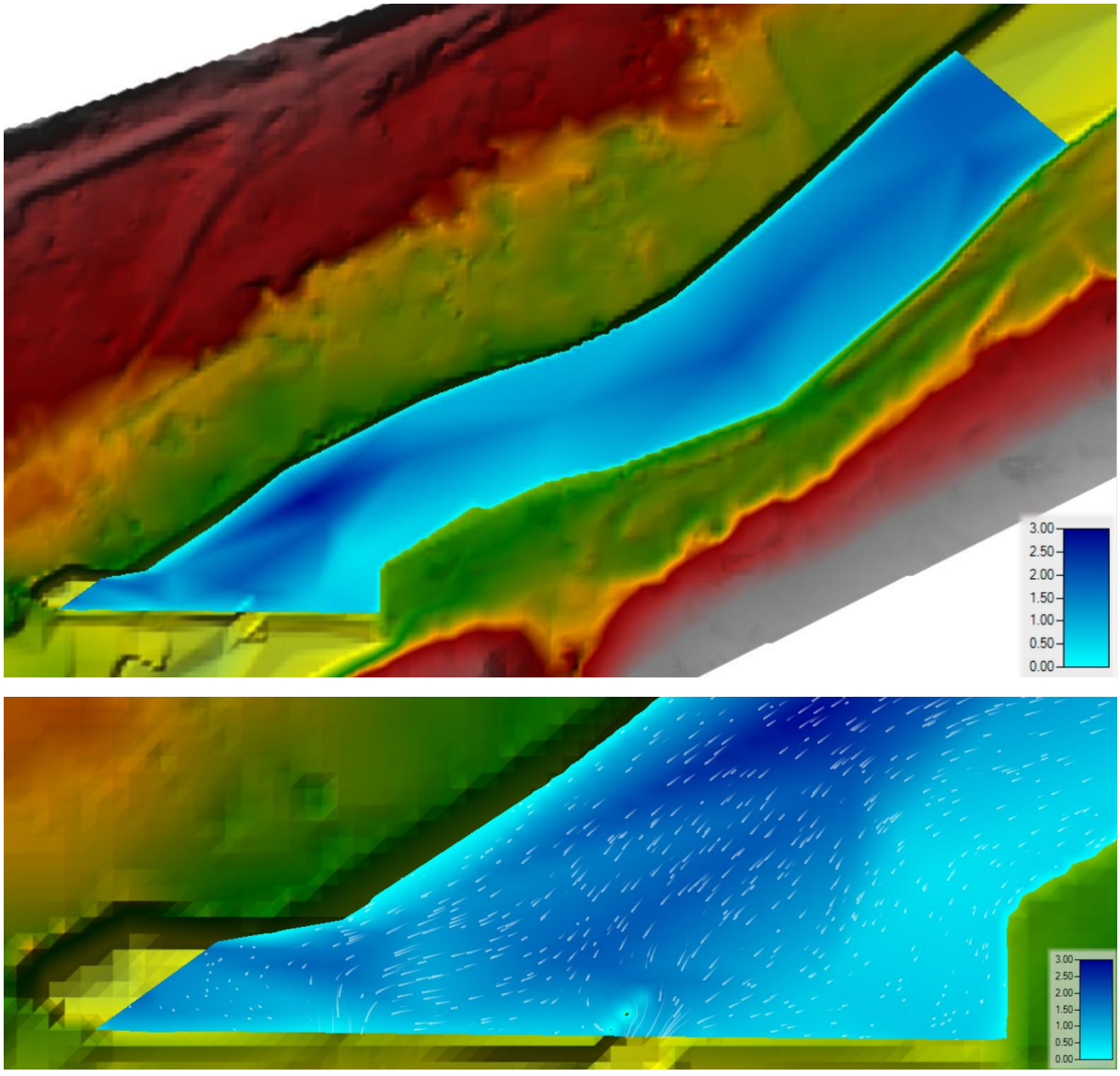

Figure 36 Variant B - Plan 1- depth and streamlines

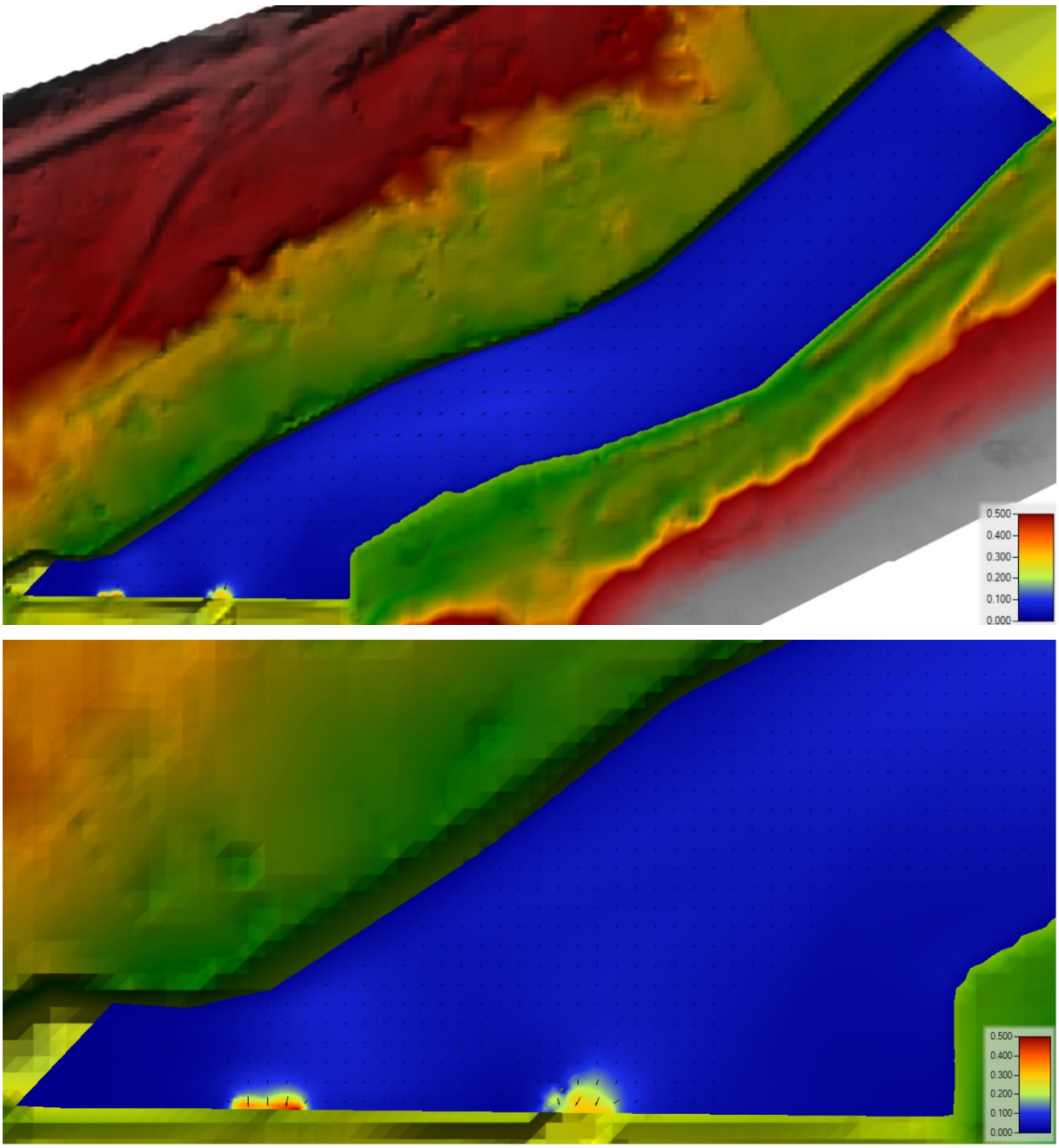

Figure 37 Variant B - Plan 1 - velocity field

3.2.2 Plan 2

Plan 2 represents the condition at which the flow is exactly 14.69 $m^3.s^{-1}$. This means that a constant flow hydrograph of value 14.69 was used as the upstream boundary condition. Under such flow conditions, the capacity of the power plant is fully reached, the power plant is running at its maximum, while only the minimum residual flow is still flowing over the weir, the fish passage, and the sports sluice. Thus, at this time, the head water level is at 307.81 MASL. As the flow rate increases, the level in the overflow rises.

The maximum depth was determined to be 2.85 m and the maximum speed 1.08 $m.s^{-1}$.

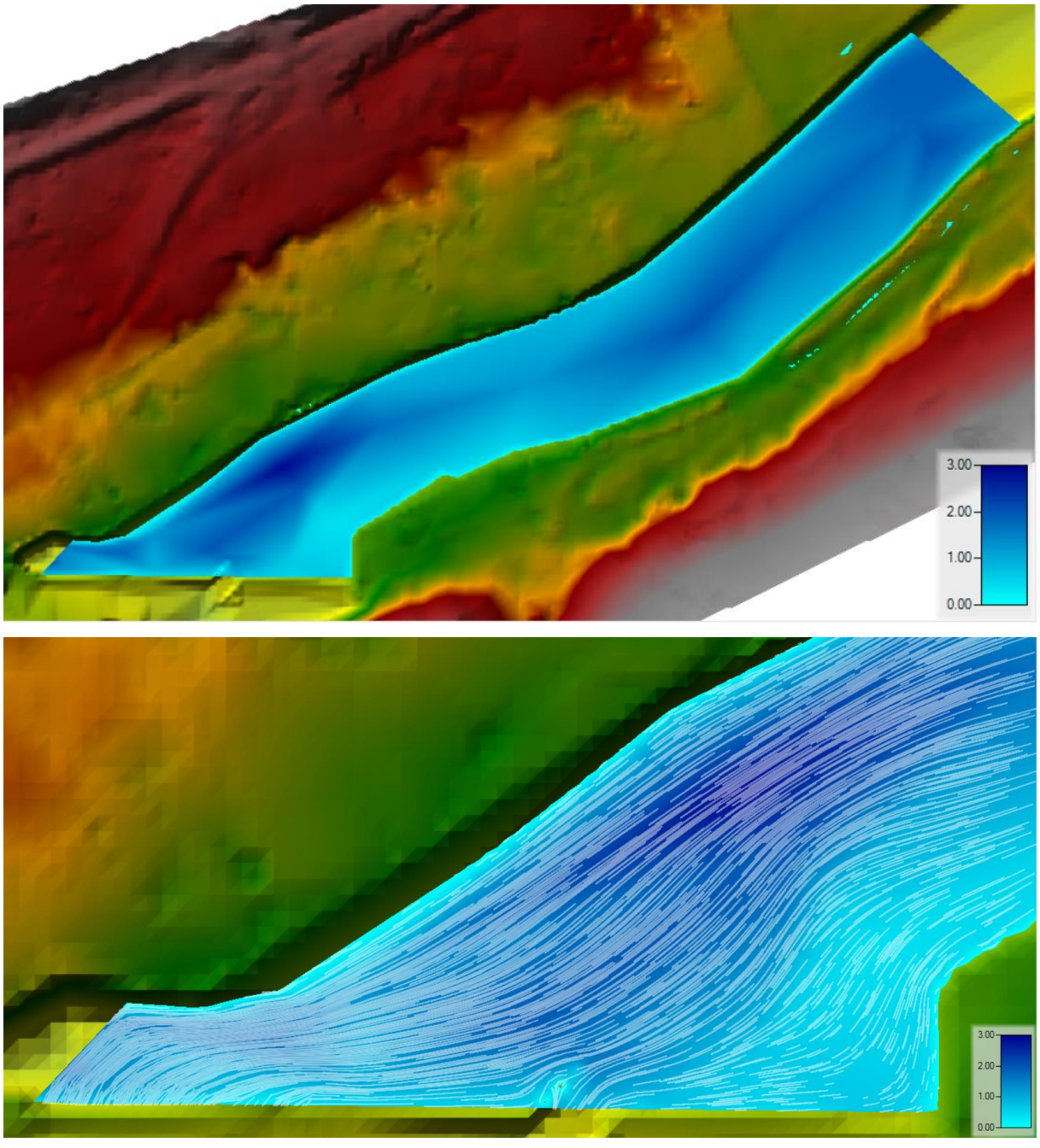

Figure 38 Variant B - Plan 2 - depth and streamlines

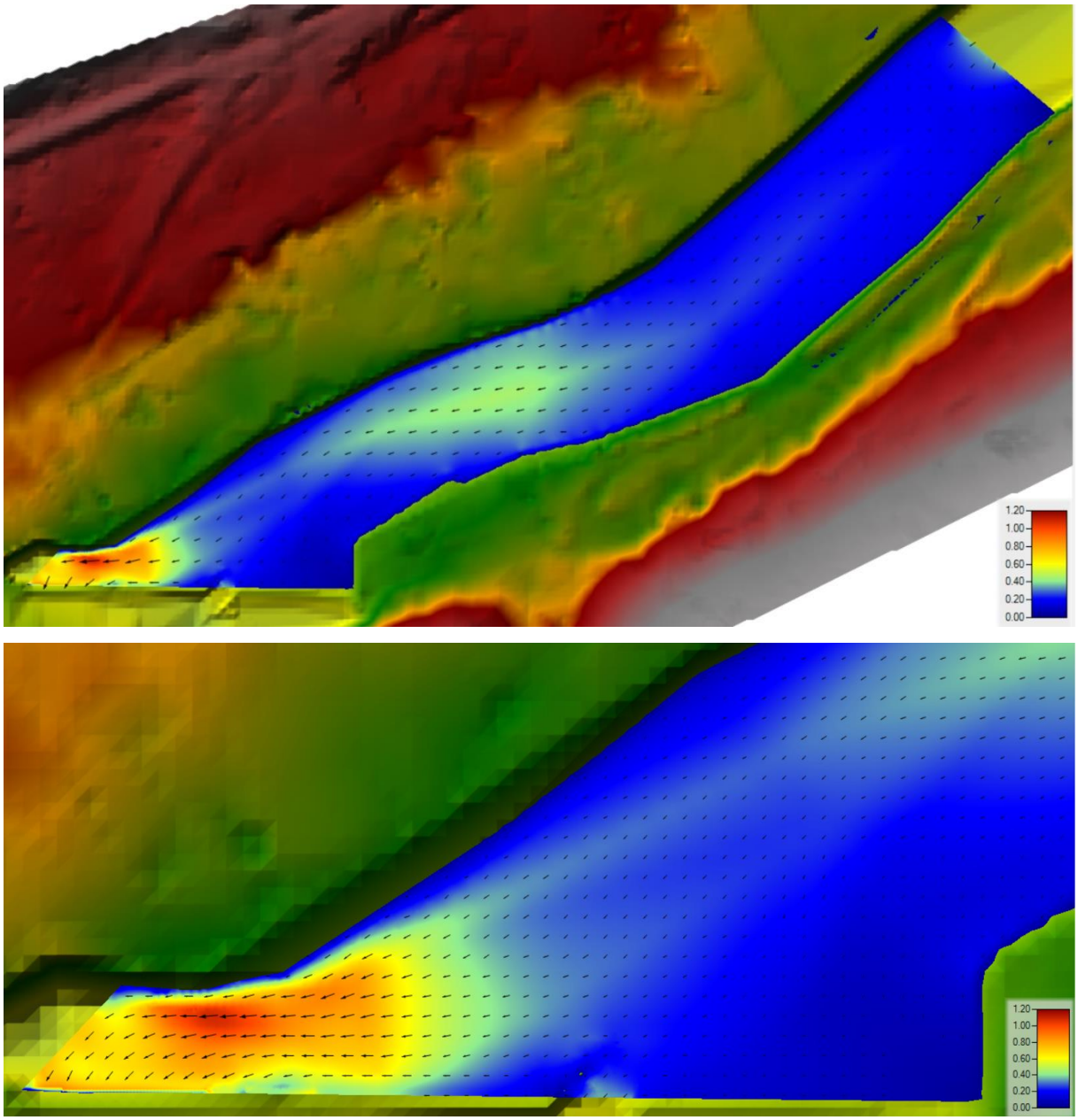

Figure 39 Variant B - Plan 2 - velocity field

3.2.3 Plan 3

Plan 3 depicts a case of 22.90 $m^3.s^{-1}$ corresponding to Q_{60}. The reasoning behind this specific river flow is the fact that for this flow, the hydropower plant is the most efficient. While Q_{60} flows in the riverbed, the HPP's turbines work with the highest gradient of 1.32 m and also use their maximum capacity.

Maximum depth reaches up to 3.24 m while the maximum velocity is 1.13 $m.s^{-1}$ around the area of inlet to the small HPP.

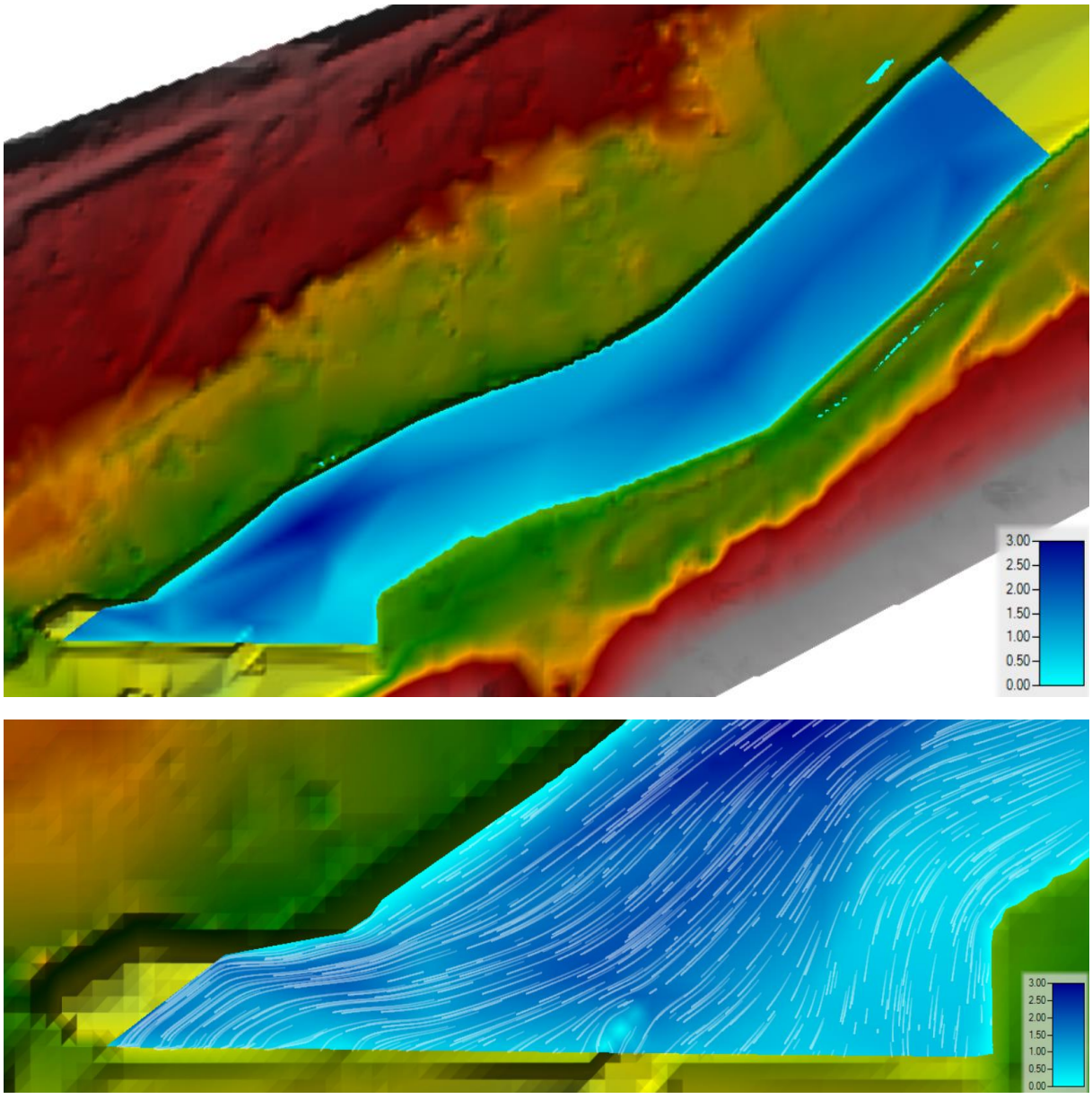

Figure 40 Variant B - Plan 3 – depth and streamlines

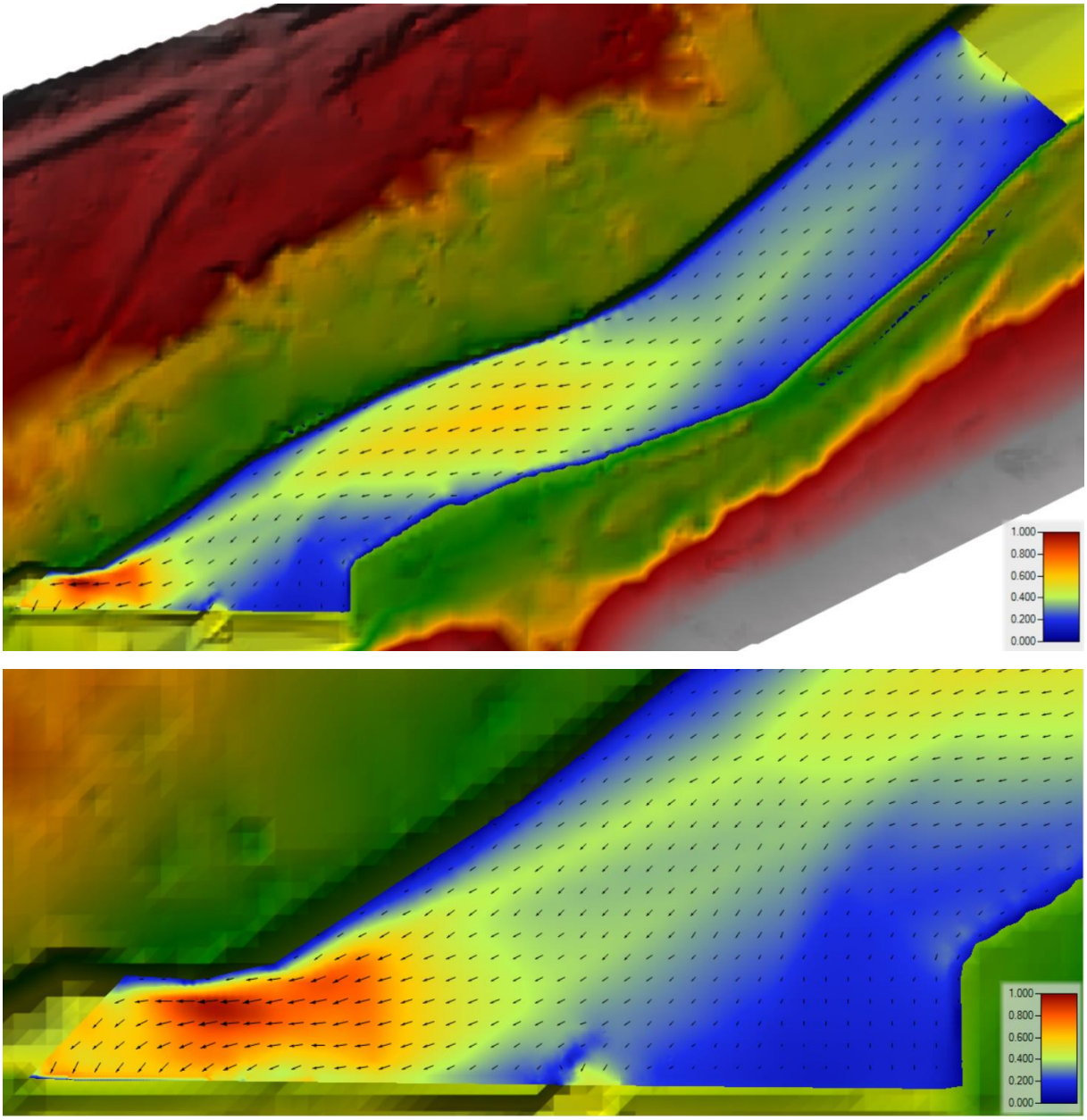

Figure 41 Variant B - Plan 3 - velocity field

3.2.4 Plan 4

The fourth calculated plan depicts a case of 55.93 $m^3.s^{-1}$.

Maximum depth reaches up to 3.24 m while the maximum overall velocity of the 2D flow area is 1.13 $m.s^{-1}$. The maximum velocity closer to the weir structure equals 0.88 $m.s^{-1}$ and is reached by the inlet to the small HPP.

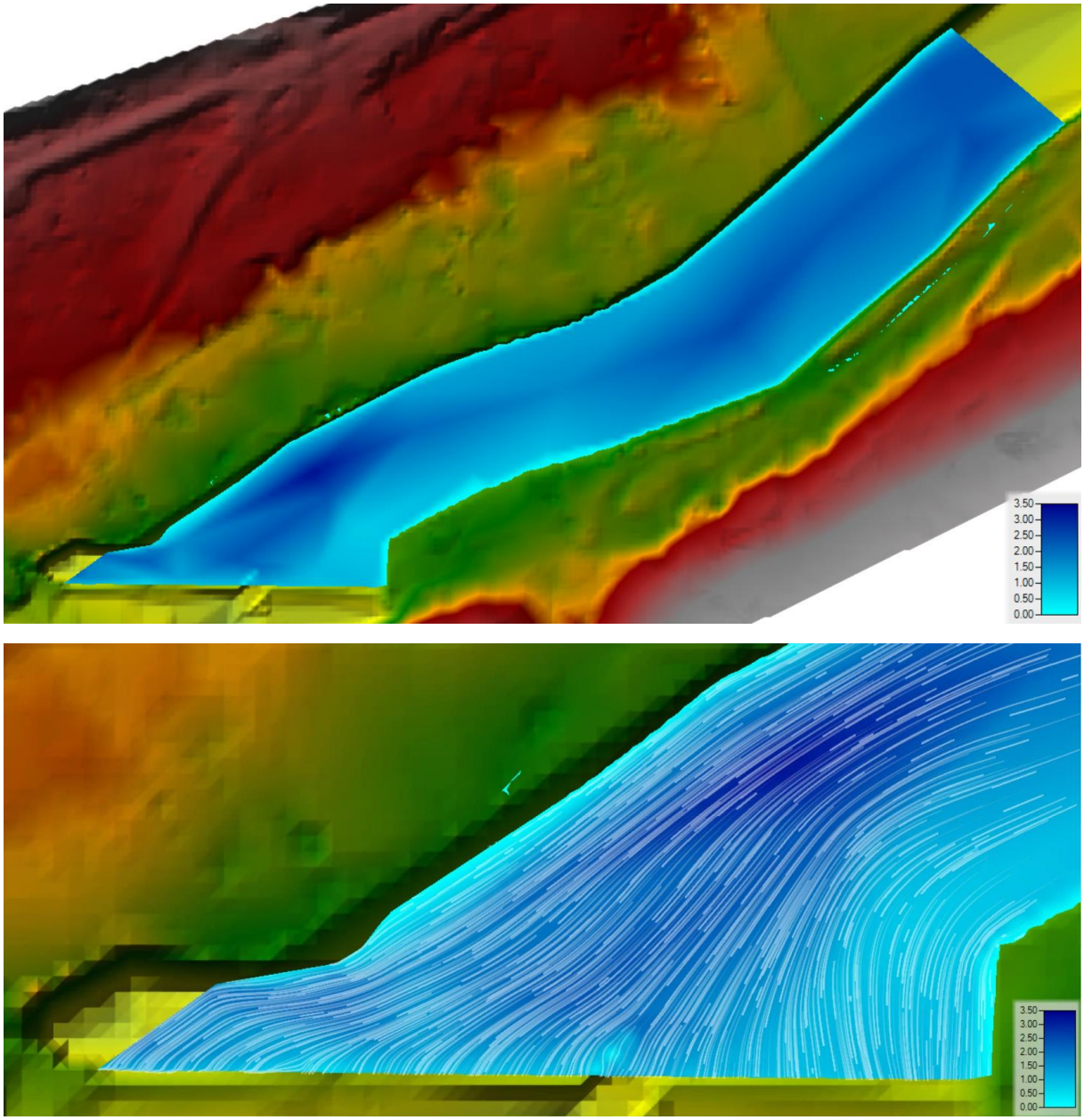

Figure 42 Variant B - Plan 4 –depth and streamlines

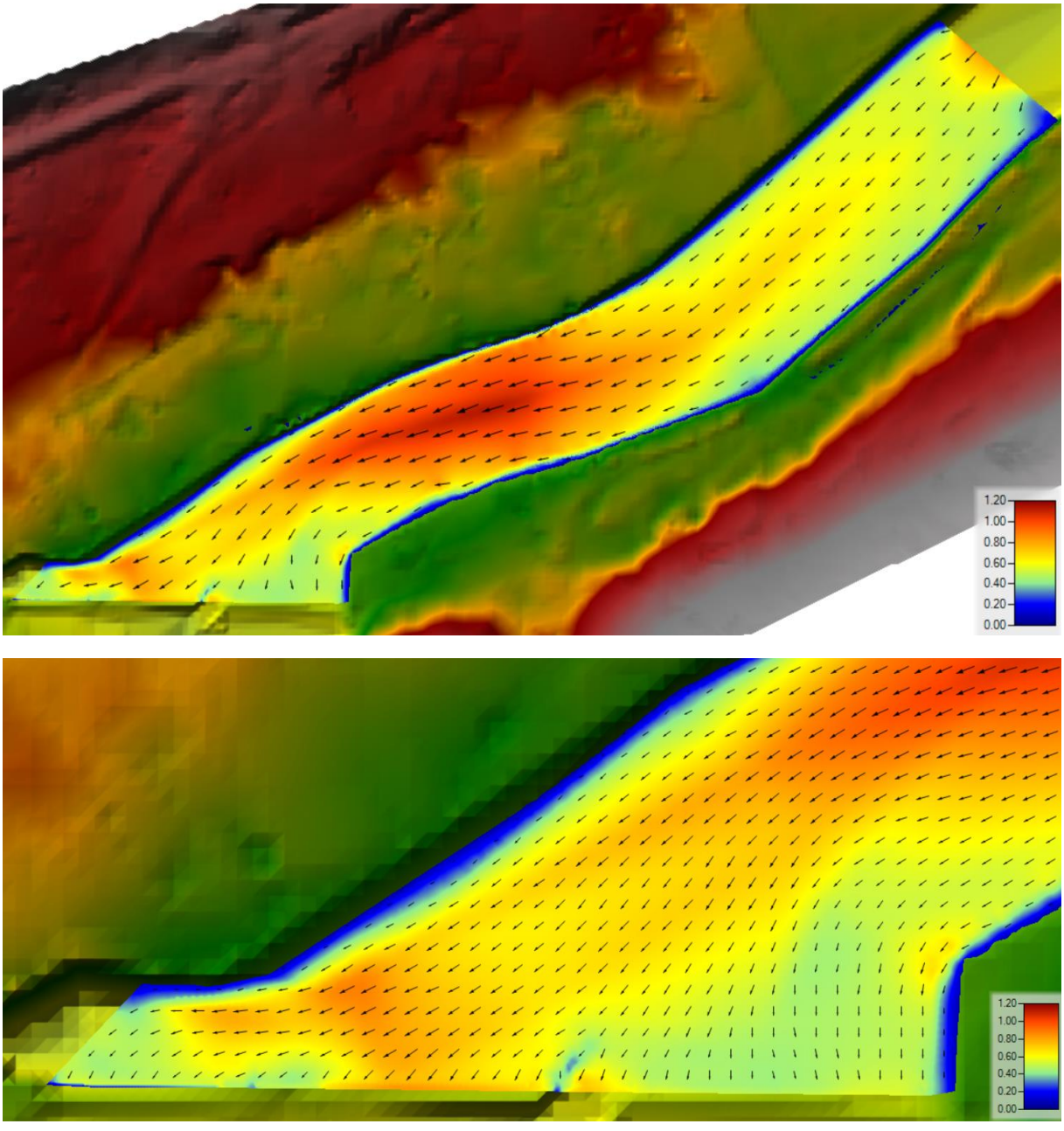

Figure 43 Variant B - Plan 4 - velocity field

3.2.5 Plan 5

The control one-year flow Q_1 is the subject of modelling Plan 5. For this plan, the value of constant flow hydrograph used as the upstream boundary conditions is 121 $m^3.s^{-1}$.

Maximum depth reaches up to 3.71 m while the maximum velocity is 1.65 $m.s^{-1}$.

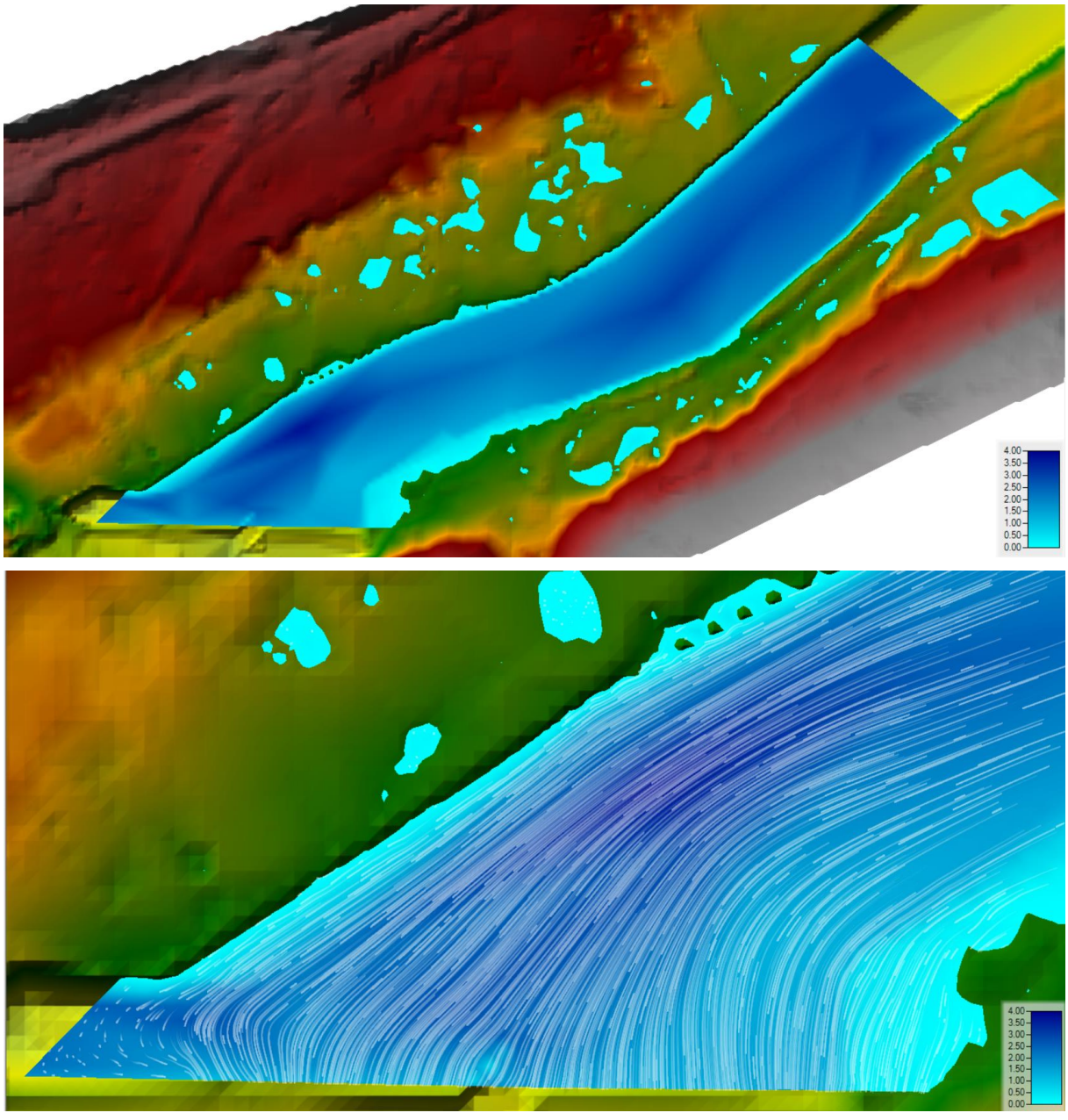

Figure 44 Variant B - Plan 5 – depth and streamlines

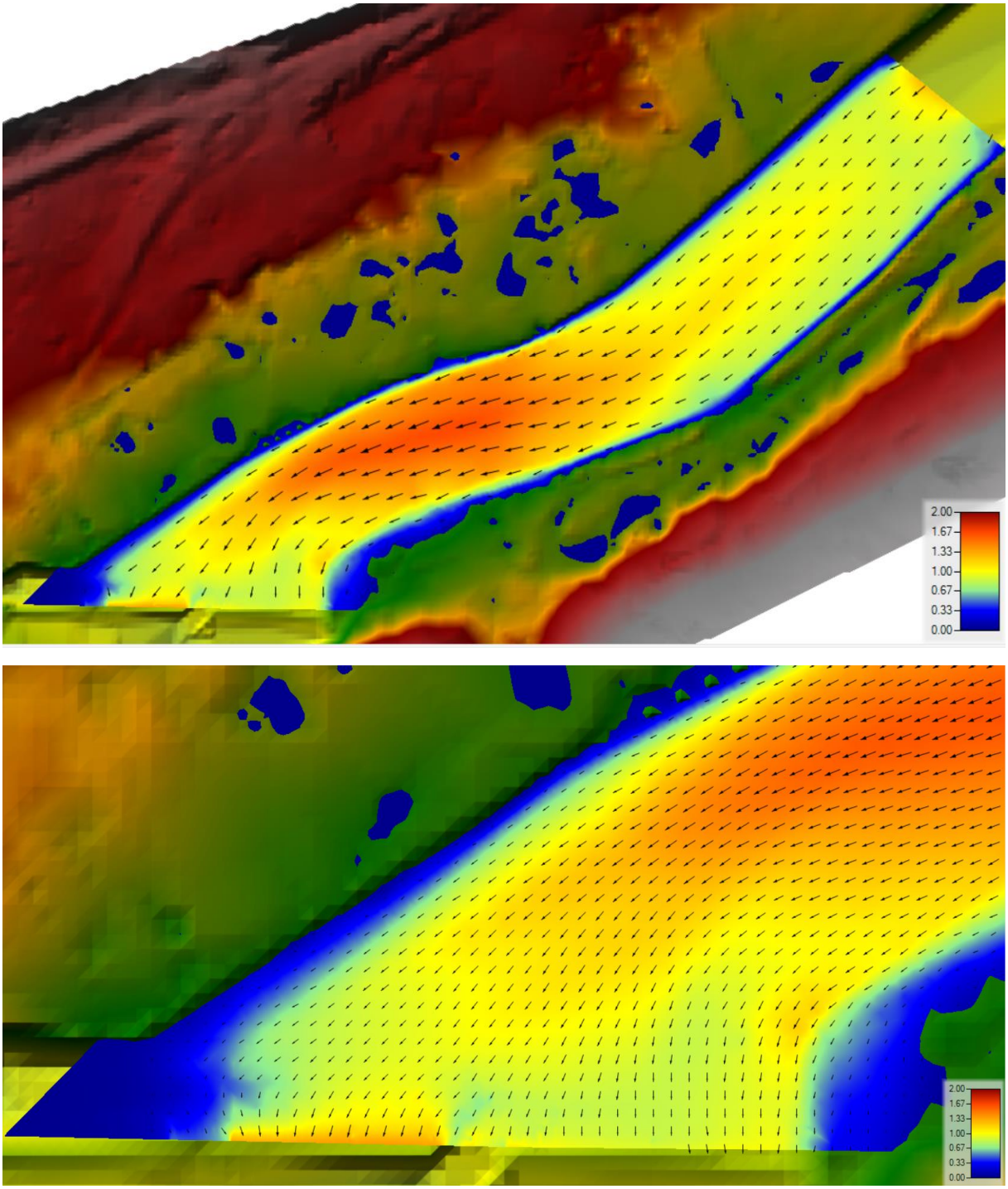

Figure 45 Variant B - Plan 5 - velocity field

3.3 Interpretation of the Results

Using the 2D model in HEC-RAS software, 2 variants A and B were created. For each variant, 5 calculation plans were established. Thus, a total of 10 computational processes were performed. Selected results showing velocity distribution and depth changes with streamlines for each of the ten plans can be found in the previous chapters 3.1 for Variant A as well as Variant B in the chapter 3.2. The interpretation of the results is the focus of this chapter.

3.3.1 Interpretation of Layout of Hydraulic Structures

From the orthophotography images, it was already preliminarily established that a natural inflow channel is being formed in a concave bend of the right bank. This finding was subsequently confirmed during the field survey of the site. This finding has significantly contributed to the possibility of a small hydroelectric power plant being built on the right bank. This claim was finally verified by modelling variant A in HEC-RAS. The situation in the upstream during Q_{355d} is observed from figure 26. It is possible to see that even at minimal residual flow, a significant part of the flow is directed in a concave bend. The location of the small hydropower plant is thus considered suitable.

When proposing the location of a fish passage, the optimal function of the fish passage, the layout of the existing migration barrier, the characteristics of the river channel, the use of the water channel, the morphology of the surrounding terrain, and the possibility of locating the structure on the land are crucial. If a small hydropower plant is part of the migration barrier, the most suitable route for the fish passage is behind the HPP in the offshore part, as a so-called bypass fish channel [17; 13]. In the case of Mazourov weir, this placement was not appliable due to insufficient size of building plots. For this reason, it was decided to place it on the left side of the HPP, in the body of the weir itself.

The sports sluice was placed in place of the current raft sluice. The axis of the riverbed passes through the current sluice's placement. At the same time, it can be observed from the simulations for variant A that the flow direction is the most suitable for passing boaters at this position. There are no significant changes in the x-direction of flow in the area of the channel axis which will make the sluice as safe as possible. After passing over the sport sluice, boaters will not be swept away by the current overflowing the weir and will have sufficient manoeuvring space on both sides.

3.3.2 Interpretation of Selected Variables

To further understand the results from the simulations in HEC-RAS and the affect the proposed reconstruction has, it is necessary to look at the differences of results of selected variables between Variants A and B. Variables selected for interpretation were water depth, velocity distribution, and streamlines. For clarity, 2 tables with the results were created: table 14 containing information on maximum depths in the whole modelled part of the river channel and table 15 with maximum velocity values found in the whole modelled river area.

The maximum reported values of the selected variables were taken from the same place for both variants of the specific calculation plan. Therefore, the values in the tables below correspond to the maximum values that were obtained for each plan throughout the whole modelled area.

Table 14 Maximum depth of the modelled area

	Variant A	**Variant B**
	(m)	
PLAN 1	2.56	2.74
PLAN 2	2.77	2.85
PLAN 3	2.86	2.97
PLAN 4	3.10	3.24
PLAN 5	3.48	3.71

Table 15 Maximum velocity in the modelled area

	Variant A	**Variant B**
	($m.s^{-1}$)	
PLAN 1	0.23	0.50
PLAN 2	0.58	1.08
PLAN 3	0.68	0.95
PLAN 4	1.25	1.13
PLAN 5	1.85	1.65

Here are the basic findings from the tables:

- The maximum depth of the modelled area is greater for the current weir condition - Variant A – in all simulated plans.
- The smallest depth difference between Variants A and B occurs at a flow rate of 14.69 $m^3. s^{-1}$ (Plan 2). At this point, the maximum capacity of the turbine is reached and only the MRF is maintained in the riverbed without any backwater flooding in the overbank.
- The most significant difference in depths between the alternatives occurs when the power plant is not operating – Plans 1 and 5.
- The values of maximum velocities are higher after raising the weir edge and building individual structures - variant B - only at smaller flows. For neither Plan 4 nor 5, the velocities are higher for Variant A.
- The smallest velocity difference occurs at Plan 4, while the HPP is in operation.

– The greatest difference of velocity value between A and B variants occurs at Plan 2, which corresponds to the maximum capacity flow of the turbines. This significant change in velocity is due to the operation of the power plant, which uses a significant portion of the flow in the riverbed.

For the existing condition (Variant A), the water depth was found to be higher at the right bank of the river. The highest depths are regularly reached in the concave bend of the riverchannel. The Variant A results of the velocity field distribution indicate that for flows less than 55.93 $m^3.s^{-1}$ (Plan 4), velocities are at their highest at the inflow to the existing raft sluice. In contrast, for flows greater than 55.93 $m^3. s^{-1}$, higher velocities are found on the right bank near the HPP inflow channel.

For the proposed Variant B, the depths on the right bank and in the concave bend of the channel are again significantly higher than on the left bank. At the minimum residual flow, the highest velocities are reached at the fish passage exit and then around the entrance of the sports sluice. However, once the HPP is switched on, the greater velocities are found at the inflow channel of the HPP. At this point it is important to observe the speeds in areas of critical distance, i.e. at the exit of the fish passage. Fortunately, it has been verified by the 2D model that the maximum velocity requirements are met, and the fish should be able to safely leave the fish passage at the tailwater area and continue their migration upwards. At Q_1 flow, the velocity at the sports sluice reaches 1 $m.s^{-1}$.

From the observation of the velocity field distribution for all the plans, it was found that there is a strong current towards the right bank in the Mazourov weir tailwater area. This current is directed to the right of the sports sluice. If paddlers are not cautious enough to direct their boats to the sports sluice in time, it is possible that the current will pull them towards the powerhouse inflow channel. To avoid accidents and prevent this from happening, it is recommended to use warning signs at a sufficient distance upstream of the weir and to install warning buoys on the right bank.

3.3.3 Interpretation of Individual Plans

The main reason for simulating minimal residual flow in the riverbed as Plan 1 was to see the change of streamlines and velocity field. In Variant A, most of the flow is directed to the sluice and the rest flows relatively evenly over the weir structure. However, this is not the case for the proposed Variant B. The results of Variant B show that at the minimum residual flow in the river, most of the water flows into the sports sluice, then into the fish passage and only a small proportion overflows the weir crest. The results from HEC-RAS confirm the calculations in the table 9. The velocities around the exit of the fish passage reach maximum speeds of 0.5 $m.s^{-1}$, thus meeting the Standard according to which the fish passage was designed.

The flow rate for Plan 2 was selected because it is the highest flow rate in the channel during the operation of the HPP that does not increase the water in the headwater (upstream) area. At flow rate 14.69 $m^3.s^{-1}$, the water level stands at 307.81 MASL for Variant B. As is the case of Plan 1, there are visible changes in the direction of the streamlines in plan 2. In variant A, the streamlines are primarily directed into the spillway and then overflow the lowest parts of the weir. Velocities range between 0.2 and 0.3 $m.s^{-1}$ over almost the entire width of the weir, excluding the sluice. However, for the new weir scenario, Variant B, a different claim applies. At this moment, 12 $m^3.s^{-1}$ is heading to the power plant, which is a major proportion of the total riverflow. Only the minimum residual flow remains in the rest of the river profile. This claim is supported by the results from HEC-RAS. In figures with the modelled results, it can be seen that the largest flow is at the right bank and is directed to the inlet channel. The highest velocities are found at the apex of the right bank bend near the inflow channel. At the very edge of the power plant inflow, the velocity field must be the same at every point so that the turbines operate under optimum conditions. The results show that these conditions are met, as the velocities are around 0.7 m.s-1. A fish passage is located next to the HPP. In order not to endanger the exit from the fish passage by high velocities, it is recommended to terminate it as close as possible to the weir edge.

Plans 3 and 4 mainly show the difference between the flow rates when the plant is switched on and switched off. This is also the case for the previous Plan 2. In all 3 cases (plans 1, 2, 3), the maximum capacity flow passes through the HPP, but the flow through the remaining river profile differs. If the power plant is shut down and not operating, high speeds are not reached at the right bank. On the contrary, the highest velocities are observed around the river axis where the sluice is located. For the remaining weir width, the velocities are within a narrow range of 0.27-0.4 $m.s^{-1}$ for Plan 3 and 0.6 - 0.8 $m.s^{-1}$ for Plan 4. A completely different state of flow and velocities is observed for Variant B. For Plan 3, the highest velocities are found in the inflow channel area in the range of 0.6 - 1.0 $m.s^{-1}$. Higher velocities are also found at the exit of the fish passage, so it is important to terminate it as close to the weir as possible. However, Plan 4 shows a reduction in velocities

in the concave bend. The highest velocities at the weir occur at the weir overflow crest located between the fish passage and the sports sluice, where velocities reach approximately 0.8 $m.s^{-1}$. A notable difference between Plans 3 and 4 of Variant B can be further observed in the convex bend of the left bank. There is a slight increase in depths and a significant increase in velocities in this area as a result of higher flows. It is interesting to note that variant A achieves higher velocities at the left bank than Variant B. This is due to the function of the power plant, which in this calculation Plan 3 significantly reduces the flow in the rest of the river.

The purpose of simulating Plan 5 was to determine the spill rate at a n-year flow. The flow rate Q_1 - 121 $m^3.s^{-1}$ was selected. The aim was to determine how the reconstruction of the weir would affect the passage of flood flows. In the current state (Variant A), the water passes over the entire width of the weir. The depths are high, especially on the right bank and in the naturally formed inflow to the power plant, which is not yet standing there. As far as the velocity field distribution is concerned, the highest velocities are again at the top of the concave bend of the right bank. On the left bank, the flow reaches smaller velocities. It was found that at Q_1 there is no dangerous spillage of water outside the riverbed. The results for Variant B are influenced by the HPP, or in other words by the fact that no flow passes through the HPP inflow channel. Therefore, water overflows only in the rest of the weir body. However, the values of velocities are generally smaller for Variant B and the velocity field is almost evenly distributed. Regarding the spill of water outside the Sázava River channel, for both Variants A and B it is possible to observe 'flooded' areas outside the river channel on both banks of the river. In reality, these flooded areas are terrain depressions, and their flooding will only occur if surface water enters them. As there is no spillage from the Sázava River channel at Q_1 flow, no flooding of these depressions will occur.

The 2D model in the HEC RAS software was used to verify the functionality of the proposed hydraulic objects. It was verified that the velocities at the fish passage outlet meet the prescribed values in the standards. It was also verified that the location of the individual objects is suitable and meets the conditions for future realisation.

4 CONSTRUCTION DESIGN PROPOSAL of HPP

In addition to the development of 2D model in HEC-RAS for the proposed reconstruction of the weir, the thesis assignment includes hydraulic design proposal of the small hydropower plant up to the level of documentation for the building permit. This design proposal of small hydropower plant covers water management design proposal, construction design proposal and drawings appropriate to the corresponding level of documentation.

Water management design proposal of small HPP is descripted in the chapter 2.4.5 in detail. The chapter discusses for example the turbine type with parameters of the technology (maximum and minimum turbine capacity), turbine output, energy production.

16 individual drawings are attached to the thesis as well including 4 layouts and 12 drawings of separate hydraulic structures.

In this chapter, the construction design proposal of small hydropower plant and its adjacent parts are explored.

4.1 General Information about the Design

The investor of the design of a small hydropower plant (later only small HPP) is a private owner of the Mazourov weir and the adjacent right bank land. The purpose of this design proposal is to use the 1.23 m gradient to generate electricity. The land on which the hydropower plant is located is situated in the non-urbanised part of the area and is adjacent to the industrial part of the village, where the Soběšín Sawmill Ltd is based. The proposed design consists of new structures which connections to the technical infrastructure (electricity) is expected to be solved directly on the construction site via electric power pole with transformer. A distribution substation has already been built on the site of interest, which will be connected to the local electricity pole via an underground cable.

The designed power plant is expected to operate as a flow-through plant. Flow-through power plants use the normal river current at the weirs. Flow-through hydroelectric power plants generally operate continuously and use either the entire flow or only part of the original flow. The key parameters determining the amount of usable energy of a watercourse are the gradient and the flow of water through the power station. In general, the higher the gradient, the higher the potential energy of the water and the higher the power output of the power plant, and the more water that flows through the power plant, the more energy it gives up to the hydro turbine [14].

The water that will be used for the green energy production will be later transported back to the Sázava riverbed through the open outlet channel. The water will be returned to the river in the same condition as before.

4.2 Construction Design Proposal of a Small HPP

4.2.1 The Machine House

The power plant consists of a machine house, an inflow channel, an outlet channel and a bypass channel. The engine house is a detached building housing two sets of Kaplan PIT turbine units. The entrance to the engine room is located at the level of Q_{100}, i.e. 311,29 MASL. Furthermore, on the above-ground floor, there is an entrance handling platform with low and high-voltage electrical switchboards and the technical facilities of the engine room. The underground floor with the floor at 309.30 MASL accommodates all the technological equipment, which is the generator, the hydraulic unit of the turbine and the hydraulic unit of the cleaning machines.

The external width of the separate engine room building is 12.2 m, and the length in the direction of water flow is 15.9 m. The height of the building above the modified terrain is 4.0 m, and the depth below the modified terrain is 9.16 m (lowest level of the foundation joint). The lowest level of the foundation joint corresponds to 301,55 MASL.

The foundation and floor of the engine room is made of a reinforced concrete slab made of C 30/37 XC4 XF3 waterproof reinforced concrete. The thickness of the slab is 500 mm. During the concreting process, the anchoring elements for the suction cup and machinery are first concreted in the locations specified by the technology supplier. The foundation slab also includes a 500x500x500 seepage sump with a fitted sump pump. The foundation slab is connected to the 500 mm thick underground walls, also made of C 30/37 XC4 XF3 waterproof reinforced concrete. The north- west wall will include an opening for the supply pipe for both turbine sets, after the installation of the pipe it will be concreted. All joints of reinforced concrete structures will be watertight. In the southeastern wall, the steel body of the soakaway will be connected to a reinforced concrete channel with a maximum variable height of 2.4 m and a width of 3.5 m. This channel is connected in the face of the wall to the reinforced concrete waste channel, which serves to connect to the existing channel of the Sázava River. The maximum height of the waste channel is 5.1 m and the maximum width is 19.0 m.

The engine room is equipped with two sluice gates at the inlet of the supply pipe to the building and two sluice gates at the outlet of the engine room before the connection to the waste channel.

The floor at 311,29 MASL is accessible via an outward opening double door with a width of 2,0 m and a height of 2,0 m. The south-east wall is fitted with two single-pane double-glazed windows, the outer pane is made of safety glass. The floor of the above-ground floor at the level of Q_{100} 311.29 MASL consists of a 300 mm thick reinforced concrete platform, which is inserted into the perimeter walls on three sides, the free side towards the engine room is monolithic. The above- ground perimeter load-bearing walls are above the terrain and made of blocks. The total compositional height of the above-ground part of the perimeter wall is 3.0 m. The lintels of the openings are designed with prefabricated reinforced concrete lintels.

The interior staircase of the engine room is made of two steel arms - the first arm accessing the platform at 309.30 m above sea level, the second arm leads from the floor at 309.30 m above sea level to the platform at 307.35 m above sea level.

Two HEB 200 mounting beams are woven transversely into the outer walls, on which a sliding mounting beam of the HEB 240 profile, also 9.8 m in length, is perpendicularly placed for the suspension of the manual assembly hoist. The roofing is made of a sloping surface with a maximum height of 1.0 m with rainwater drainage into a gutter located at the edge of the roof. The roof slope is 11,5 %.

The building of the engine room and combing plant is made of monolithic reinforced concrete C30/37 XC4 XF3, water seepage less than 4 cm. The part of the engine room building above the Q_{100} level mark (311.29 MASL) will be bricked.

The interior of the engine room is heated by generators. In the event of a shutdown, an electric heater can be connected. There is 1 intake ventilation grille and 1 exhaust ventilation grille in the wall of the engine room. According to consultation with the manufacturer, the ventilation of the generators can be led out through a separate air duct.

4.2.2 The Inlet Channel

The inlet to the power plant is designed with an open reinforced concrete trough. The embankment includes the following in the course of the river: a burrow wall with coarse screens with a spacing of 20 cm and a footbridge with a railing, fine combs with spacing of 40 mm with an automatic conveyor that transports the combs to the bypass channel and a hydraulic comb cleaning machine. There are 2 hydraulic pressure sensors on the inlet walls, one in front of the fine screens and one behind the fine screens. There is also a wall pump in the area behind the fine combs to drain excess water into the bypass channel. The reinforced concrete platform on which the cleaning machine and the sluice gate are located is situated at an altitude of 309,47 MASL.

The inlet structure is designed as a reinforced concrete wall with foundation. The entire wall is in the shape of L. This wall will be covered with boulders to the required slope.

4.2.3 The Outflow Channel

The outflow channel, which serves to connect to the existing channel of the Sázava River, is made of water-building reinforced concrete C 30/37 XC4 XF3 with a thickness of 400 mm. The outlet from the engine room corresponds to the dimension 303.82 and using the outflow channel with a gently rising bottom it reaches the dimension of the Sázava river bottom at the connection point for a length of approx. 16.0 m.

The connection of the engine room to the drainage channel is provided with two sluice gates, which are operated mechanically by the operator. These gates can be accessed directly, i.e. via the stairs to the right of the entrance to the engine room. The staircase gives access to the steel footbridge. The steel service footbridge provides access to the control of the sluice gates and the bypass channel.

4.2.4 The Bypass Channel

On the southeast side of the engine room, close to the existing weir, there is a bypass channel which serves to flush coarse dirt from the combs on the bore wall and scrapes from fine combs conveyed by an automatic conveyor. The inlet to the bypass channel is equipped with a manual sluice gate, behind which a gridded basket is placed as a sorting device. The scraps from the fine combs are moved by the conveyor into the basket, the coarse dirt is caught on the grates where it is regularly sorted by the operator. The bypass channel flows into the outflow channel, which returns the water to the existing channel of the Sázava River. The bypass flushing channel is located between the small hydropower plant building and the fish passage. The right wall of the canal consists of a 600 mm thick reinforced concrete wall of the HPP, while the left wall of the canal is shared with the fish passage, again 600 mm thick. The height of the left wall of the channel and the right wall of the fish passage is derived from the height of the water level at one-year flow Q_1. The height dimension is 308.58 MASL in the upstream and 308.19 MASL in the downstream. The width of the channel is 1,0 m and the length of the channel axis is 25.5 m. The bottom elevation at the upstream end is 307.27 MASL, the bottom of the outlet is 307.37 MASL The channel overcomes a gradient of 1.9 m using a bottom slope of 7.5 %. The entrance to the canal is equipped with a sluice gate that will be in operation for most of the year, thus not taking water from the river profile. It will only be opened if flushing is necessary.

The resistance of the small hydropower plant is ensured by the compressive strength of the concrete, the tensile strength of the reinforcement and the strength of the soil.

The small hydropower plant is a permanent structure that does not ensure barrier-free use. The plant will operate independently in automatic mode, with occasional control.

In the building of the engine room there are cabinets with electrical switchboards, thanks to which the building will be connected to power grid by a pole with a transformer. The pole is located on the owner's (investor’s) property.

When the construction is complete, the ground will be restored to a satisfactory and safe condition for the use of the surrounding buildings on the site. Soil from the construction excavation will be used to level the uneven terrain on the construction site. Unpaved areas affected by construction will be graded and grassed. A new paved access road must be constructed to provide access to the site, site facilities and subsequent connection of the building to the road.

The construction of the power plant will require partial disconnection of the riverbed by armoured support. The engine house foundation pit will have a pumping sump from where water will be pumped into the river. The foundation pit of the combs will be pumped into the embankment; the facility will be constructed with the embankment drained. During construction, surface water will be diverted away from the site of the excavation. The excavation shall be kept free of water during installation. If drains are used, they must be abandoned upon completion of the work. Surface water runoff is not affected, rainwater is discharged into the river.

The construction will not have a negative impact on the environment, and no emissions will be generated during its operation. The construction of the building is to generate green energy. The construction only affects trees and vegetation on the banks of the river at the site of the engine house. The existing bank vegetation consists of grasses and shrubs.

CONCLUSION

The master thesis was prepared for the purpose of designing a layout solution for the reconstruction of the Mazourov weir on the Sázava River. To verify the location of the individual proposed objects (small hydropower plant, fish passage, sports sluice), a 2D model was created in the HEC-RAS software. In HEC-RAS, four suitable geometries were created with the corresponding boundary conditions applied. A total of 10 computational processes (plans) were performed and the results were used to interpret the obtained outputs.

The proposed reconstruction works firstly include raising the weir crest from the existing state (307.40 -307.94 MASL) to 307.80 MASL. It is recommended to carry out these construction works in stages, so that the water can always pass over a part of the weir that is not being worked on. In addition to raising the weir crest, the newly proposed design includes construction of individual hydraulic structures (HPP, fish passage, sports sluice). Basic parameters of the hydraulic structures were designed, their capacity was calculated, and the proposed general cross sections are attached as well.

One of the most crucial parts in the design of the structures was to decide on the level of the overflow edges of individual structures. The elevation of the spillway edges of the individual structures significantly affects the Q-H capacity curve of the entire weir. Finally, the proposed design corresponds to the weir crest located at 307.80 MASL, the bottom of the inlet to the sports spillway located at 307.52 MASL and the bottom of the fish passage outlet located at 307.27 MASL.

Furthermore, a flow-through small hydropower plant with two sets of Kaplan PIT turbines was designed. The small hydropower plant proposal includes an inflow channel bringing water to the plant and an outflow channel connecting the structure to the existing riverbed of Sázava River. It was determined that a small hydropower plant would operate in the flow range of 5.35 $m^3.s^{-1}$ to 55.93 $m^3.s^{-1}$ in the Sázava River. The estimated annual production of the proposed small hydropower plant is 466 MWh.

A reinforced concrete slotted fish passage has been proposed that will be in operation for at least 355 days per year. To ensure sufficient length of the fish passage, its structure is taken form of a zigzag, and is situated along the engine house of the small hydropower plant. The entrance to the fish passage is located as close as possible to the outlet channel of the power plant. The outlet of the fish passage is located directly on the edge of the weir.

A new 2.5-metre-wide sports sluice has been designed in place of the existing 6.1-metre-wide sports sluice. The proposed structure is longer than the existing structure and provides safe passage for boaters for a minimum of 355 days per year. Thanks to the significant narrowing of the sports culvert,

the flow through the hydraulic structure at a flow rate in the river of Q_{355d} (minimal residual flow) was reduced while maintaining sufficient depths for navigation.

The 2D model in the HEC RAS software was used to verify the locations and functionality of the proposed hydraulic objects. Thanks to the created 2D model, information on the velocity field distribution was obtained both in the whole modelled area of the riverbed and especially in the proximity of individual designed hydraulic structures. It was verified that the velocities at the fish passage outlet meet the prescribed values in the standards. Furthermore, the values of maximum depths of the modelled area and streamlines became a valuable output. And finally, the 2D model was used to verify that the proposed placement of the small hydropower plant, the fish passage and the sports sluice is suitable and meets the requirements for a reliable and trouble-free function.

The thesis is suitable as a basis for the next steps of the project documentation. Before applying for a building permit, however, a more comprehensive elaboration of the individual structural parts must be carried out.

Table of Figures

Table of Equations

List of Tables

List of Attachments

Bibliography

[1] A VOITH AND SIEMENS COMPANY. Bulb/Pit/S-Turbines and Generators. *VOITH* [online]. [cit. 2024-01-06]. Available from: https://voith.com/corp-en/Voith_t3366e_Bulb_Pit_S-turbines_screen.pdf

[2] BRUNNER, Gary W. US ARMY CORPS OF ENGINEERS, INSTITUT FOR WATER RESOURCES. *HEC-RAS, River Analysis System, 2D Modeling User's Manual: Version 5.0* [online]. 2016 [cit. 2023-10-10]. Available from: https://www.hec.usace.army.mil/confluence/rasdocs/rasum/latest

[3] ČÁBELKA, Jaroslav a Pavel GABRIEL. *Matematické a fyzikální modelování v hydrotechnice*. Prague: Československé akademie věd, 1987.

[4] FOŠUMPAUR, Pavel. *Využití generátoru srážek v teorii nádrží a vodohospodářských soustav*. Prague, 2010. Habilitation thesis. CTU.

[5] GABRIEL, Pavel, František ČIHÁK a Petr KALANDA. *Malé vodní elektrárny*. 1998. First: CTU, 1998. ISBN 80-01-0112-1.

[6] HAVLÍK, Aleš a Tomáš PICEK. *Přepady* [Lecture]. Prague: CTU, Department of Hydraulics and Hydrology, 2021.

[7] HAVLÍK, Aleš a Tomáš PICEK. *Vodní skok, tlumení kinetické energie, řešení průběhu hladin v otevřených korytech* [Lecture]. Prague: CTU, Department of Hydraulics and Hydrology, 2021.

[8] MATOUŠEK, Václav. *Pohyb reálné kapaliny: Matematické modelování a Navier-Stokesova rovnice* [Lecture]. Prague: CTU, Department of Hydraulics and Hydrology, 2022.

[9] MATOUŠEK, Václav. *Pohyb reálné kapaliny: Neustálené proudění v otevřených korytech* [Lecture]. Prague: CTU, Department of Hydraulics and Hydrology, 2022.

[10] MATOUŠEK, Václav. *Pohyb reálné kapaliny: Základy fyzikálního modelování* [Lecture]. Prague: CTU, Department of Hydraulics and Hydrology, 2022.

[11] MEDŘICKÝ, Vladimír a Petr VALENTA. *Hydrotechnické stavby 1: Navrhování jezů*. Prague: CTU, 2009. ISBN 978-80-01-04309-7.

[12] VALENTA, Petr. *Dvourozměrné numerické modelování proudění vody v otevřených korytech a inundačních územích*. Prague, 2005. Habilitation thesis. CTU.

[13] MINISTRY OF AGRICULTURE OF THE CZECH REPUBLIC. *Zprůchodňování migračních bariér rybími přechody*. Second. Prague: Ministry of Agriculture of the Czech Republic, 2011, 27 s. Available from: https://eagri.cz/public/web/file/104412/TNV_75_2321.pdf

[14] CEZ GROUP. *Svět Energie - Vzdělávací portál ČEZ: Vodní elektrárny* [online]. 2020 [cit. 2023-10-12]. Available from: https://www.svetenergie.cz/

[15] HYDROLOGIC ENGINEERING CENTER, US ARMY CORPS OF ENGINEERS, *HEC-RAS* [online]. [cit. 2023-10-10]. Available from: https://www.hec.usace.army.mil/software/hec-ras/

[16] WATER MANAGEMENT DEVELOPMENT AND CONSTRUCTION JOINT STOCK COMPANY (VRV). *Matematické modelování* [online]. [cit. 2023-10-09]. Available from: https://www.vrv.cz/sluzby-matematicke-modelovani-uniky

[17] THE CZECH HYDROMETEOROLOGICAL INSTITUTE, FLOOD FORECASTING SERVICE. *Evidenční list hlásného profilu č.152: Station category: B* [PDF]. Hydrosoft Veleslavín s.r.o. 2023.

[18] POVODÍ VLTAVY, STATE ENTERPRISE. *Studie proveditelnosti zprůchodnění migračních překážek na vodních tocích v povodí Vltavy: 4. Katalog příčných překážek - Sázava*. Prague: Water Management Development and Construction joint stock Company (VRV).

[19] POVODÍ VLTAVY, STATE ENTERPRISE. *Studie proveditelnosti zprůchodnění migračních překážek na vodních tocích v povodí Vltavy: 3. Hodnocení - Sázava*. Prague: Water Management Development and Construction joint stock Company (VRV).

[20] POVODÍ VLTAVY, STATE ENTERPRISE. *Plán dílčího povodí Dolní Vltavy: V. Ochrana před povodněmi a vodní režim krajiny*. Prague: Povodí Vltavy, State Enterprise, 2016. Available from: https://www.pvl.cz/portal/pdp/VH/V_Ochrana_pred_povodnemi/1_Text/HVL_V_TEXT.pdf

[21] AOPK ČR AND CTU. *Standard Rybí přechody*. Prague, 2015, 35 s. Available from: https://nature.cz/documents/20121/1199906/02006_Rybi_prechody.pdf/f704daf0-29f1-89b4-a6ee-f4bef4a09143?t=1652776207374